Fall 2015

# Marine Microzooplankton are Indirectly Affected by Ocean Acidification Through Direct Effects on Their Phytoplankton Prey

Kasey Kendall
*Western Washington University*, kendalk3@students.wwu.edu

# MARINE MICROZOOPLANKTON ARE INDIRECTLY AFFECTED BY OCEAN ACIDIFICATION THROUGH DIRECT EFFECTS ON THEIR PHYTOPLANKTON PREY

By

Kasey Kendall

Accepted in Partial Completion
of the Requirements for the Degree
Master of Science

Kathleen L. Kitto, Dean of the Graduate School

ADVISORY COMMITTEE

Chair, Dr. Brooke Love

Co-Chair, Dr. Suzanne Strom

Dr. M. Brady Olson

**MASTER'S THESIS**

In presenting this thesis in partial fulfillment of the requirements for a master's degree at Western Washington University, I grant to Western Washington University the non-exclusive royalty-free right to archive, reproduce, distribute, and display the thesis in any and all forms, including electronic format, via any digital library mechanisms maintained by WWU.

I represent and warrant this is my original work, and does not infringe or violate any rights of others. I warrant that I have obtained written permissions from the owner of any third party copyrighted material included in these files.

I acknowledge that I retain ownership rights to the copyright of this work, including but not limited to the right to use all or part of this work in future works, such as articles or books.

Library users are granted permission for individual, research, and non-commercial reproduction of this work for educational purposes only. Any further digital posting of this document requires specific permission from the author.

Any copying or publication of this thesis for commercial purposes, or for financial gain, is not allowed without my written permission.

Kasey Kendall
9 Nov 2015

# MARINE MICROZOOPLANKTON ARE INDIRECTLY AFFECTED BY OCEAN ACIDIFICATION THROUGH DIRECT EFFECTS ON THEIR PHYTOPLANKTON PREY

A Thesis
Presented to
The Faculty of
Western Washington University

In Partial Fulfillment
Of the Requirements for the Degree
Master of Science

By
Kasey Kendall
December 2015

## ABSTRACT

To date there is little evidence to suggest that marine microzooplankton are directly affected by ocean acidification (OA), and few studies have explored indirect effects of OA on microzooplankton. Microzooplankton grazing behavior is acutely sensitive to prey cell size, physiology, and nutritional state, which may all be influenced by OA in phytoplankton. Therefore, microzooplankton may be indirectly affected by OA through their prey. Due to undersaturation of $CO_2$ for the carboxylating enzyme, RuBisCO, increasing availability of $CO_2$ through acidification could influence phytoplankton cellular energy budgets. This could, in turn, affect algal cellular processes, physiological states, and the nutritional value for their primary consumers, the microzooplankton. In this study I tested whether there are indirect effects of ocean acidification on three microzooplankton species, representing two ecologically significant functional groups of microzooplankton, tintinnid ciliates (*Favella taraikaensis* and *Eutintinnus* sp.) and heterotrophic dinoflagellates (*Oxyrrhis marina*). To achieve this I first characterized the direct effects of OA on the physiology and biochemistry of their phytoplankton prey. Two phytoplankton, *Emiliania huxleyi* CCMP 2668 and *Rhodomonas* sp. CCMP 755, were cultured semi-continuously under three $pCO_2$ treatments in media equilibrated at 400ppmv, 750ppmv, and 1000ppmv $pCO_2$ (Ambient, Moderate, and High, respectively). After acclimation for 10 days, I quantitatively assessed cell size, C:N, growth rate, photosynthetic capacity, cellular carbohydrate and chlorophyll *a* concentrations. Phytoplankton cell size increased significantly under Moderate and High treatments, while there were no consistent changes in phytoplankton biochemistry with elevated $pCO_2$. To test for indirect effects on microzooplankton, the grazers were fed a diet of $pCO_2$-acclimated cells for durations of time ranging from minutes to hours. Epifluorescent microscopy was used to quantify ingestion at pre-determined time intervals. All three microzooplankton species showed increased short-term ingestion rates, and had a higher percentage of the population feeding on *E. huxleyi* grown in elevated $pCO_2$.

Multiple Linear Regression models for each grazer revealed that increased prey cell size was the sole predictive factor for the increased short-term grazing rates. I showed that OA indirectly affects microzooplankton through direct effects on the size of their phytoplankton prey. This indirect pathway for OA effects to microzooplankton has the potential for widespread impacts within marine food webs.

## TABLE OF CONTENTS

# LIST OF FIGURES

# LIST OF TABLES

# INTRODUCTION

Microzooplankton are the primary consumers of marine phytoplankton (Landry and Hassett 1982; Sherr et al. 1992, Sherr and Sherr 1994; Jeong et al. 2010), on average consuming 60-75% of phytoplankton production, compared to 21-34% consumed by mesoplankton (Landry and Calbet 2004). Communities of microzooplankton, defined as zooplankton between 20 – 200 μm in length (Sieburth et al. 1978), are primarily composed of ciliates and heterotrophic dinoflagellates (Sherr and Sherr 2007). Because microzooplankton consume such a large fraction of primary production, they significantly contribute to biogeochemical cycling. Microzooplankton grazing influences nutrient cycling in the surface waters and the flux of organic matter from the euphotic zone to the deep sea (Sherr and Sherr 1994; 2002).

Because microzooplankton are such critical players in marine nutrient and carbon cycling, considerable research over the last few decades has focused on their grazing behavior, namely the mechanisms that govern their prey selection (reviewed by Tillman 2004). Evidence shows that microzooplankton are acutely sensitive to their prey's cell size (Jonsson 1986; Verity and Villareal 1986, Boenigk 2001, Calbet et al. 2001), physiology (Verity 1988; Anderson and Pondaven 2003; Barofsky et al. 2010), and nutritional state (Meunier et al. 2011; Montagnes et al. 2011). It is therefore vital to understand the environmental variables that alter phytoplankton size, nutritional quality, and chemical signature.

Phytoplankton physiology and biochemistry are influenced by a number of key environmental factors, primarily light (energy) availability, nutrient concentration, and temperature (reviewed by Boyd et al. 2010). These factors exert 'bottom-up' control over phytoplankton growth and physiology, in contrast to the 'top-down' control that microzooplankton exert over phytoplankton biomass. Ocean acidification (OA) is a changing set of environmental conditions that is exerting increasing influence on phytoplankton production and physiology through 'bottom-up' control.

Ocean acidification occurs when rising $pCO_2$ alters oceanic carbonate chemistry. As $CO_2$ dissolves into the surface ocean, hydrogen ions ($H^+$) are released when carbonic acid ($H_2CO_3$) dissociates to form bicarbonate ($HCO_3^-$). Bicarbonate can further dissociate into a second hydrogen ion ($H^+$) and carbonate ($CO_3^{2-}$). The complete equilibrium reactions of $CO_2$ in water are:

$$CO_2\ (g) + H_2O\ (aq) \leftrightarrow H_2CO_3 \leftrightarrow HCO_3^-(aq) + H^+(aq) \leftrightarrow CO_3^{2-}(aq) + 2H^+(aq)$$

The excess $H^+$ generated by the dissociation of carbonic acid is driving the reduction in ocean pH, while the changing balance of the dissolved inorganic carbon species (increased $CO_2$, increased $HCO_3^-$ and decreased $CO_3^{2-}$) is reducing aragonite and calcite saturation states, and changing the availability of each constituent of the carbonate series (Feely et al. 2004). Reducing saturation state decreases the thermodynamic potential for a mineral to form. In the case of OA, the minerals in question are aragonite and calcite, the two dominant forms of calcium carbonate mineralization.

Atmospheric $CO_2$ has risen from a pre-industrial concentration of 280 ppmv to a present day concentration of 400 ppmv, and is expected to increase to approximately 1000 ppmv by the year 2100 (IPCC 2007). This increase is largely driven by anthropogenic emission of $CO_2$ overwhelming the earth's natural $CO_2$ sinks (Canadell et al. 2007, Le Quere et al. 2009). Since atmospheric $CO_2$ is in equilibrium with dissolved oceanic $CO_2$ ($pCO_2$), the $pCO_2$ of the oceans is also rising (Chen 1993). The world's oceans are currently absorbing approximately 30% of global carbon dioxide emissions each year (Sabine et al. 2004, Le Quere et al. 2009). As $CO_2$ concentration rises in the ocean over the course of the next century, the average surface ocean pH is expected to drop from the current pH of 8.2 to as low as 7.6 by year 2100 (Haugan and Drange 1996, Caldeira and Wickett 2003).

As atmospheric and oceanic $CO_2$ concentrations continue to rise, there is a growing need to understand how marine organisms will respond to OA (Kroeker et al. 2010), with particular concern for calcifying organisms (Beaufort et al. 2011). As aragonite and calcite saturation states decrease, dissolution of $CaCO_3$ becomes thermodynamically more favorable. Because of this, calcification

becomes energetically more costly and reduced saturation state can have detrimental effects on calcifying organisms (Orr et al. 2005, Feely et al. 2004). However, recent studies show that calcifying organisms that photosynthesize have varied responses to elevated $pCO_2$ (Fabry 2008), not all of which are negative reactions.

The coccolithophore *Emiliania huxleyi* is an ecologically important calcifying phytoplankton that forms large blooms (Moore et al. 2012) and is responsible for major export of inorganic carbon from the surface ocean to the seafloor (Riebesell et al. 2007, Frada et al. 2012). Short-term experiments (2-20 days) in which *E. huxleyi* was cultured under elevated $pCO_2$ reveal strain-specific calcification responses to elevated $pCO_2$ (Iglesias-Rodriguez et al. 2008). Some studies show that calcification of *E. huxleyi*, as measured by particulate inorganic carbon per cell (PIC $cell^{-1}$), increases with elevated $pCO_2$ (Iglesias-Rodriguez et al. 2008; Fiorini et al. 2011; Bach et al. 2013), while contrasting studies show PIC $cell^{-1}$ decreases with increasing $pCO_2$ (Zondervan et al. 2002; De Bodt et al. 2010; Hoppe et al. 2011; Lefebvre et al. 2012; Rokitta and Rost 2012). Lohbeck et al. (2012) demonstrated during experiments spanning hundreds of generations (>1 year) that *E. huxleyi* populations have high genetic variability that allow populations to quickly adapt to elevated $pCO_2$ conditions.

Aside from the potential to alter calcification in select phytoplankton, ocean acidification could have a positive effect on phytoplankton carbon fixation through increased availability of $CO_2$. The phytoplankton carboxylating enzyme ribulose bisphosphate carboxylase oxygenase (RuBisCo) is constrained to using only $CO_2$ as its carbon source for carbon fixation. Phytoplankton are $CO_2$ limited under current ocean conditions, due to RuBisCo being less than half saturated with respect to $pCO_2$ (Giordano et al. 2005; Low-Decarie et al. 2014). To alleviate $CO_2$ limitation, many phytoplankton employ carbon concentrating mechanisms (CCMs) to enhance the activity of RuBisCo and promote photosynthesis (Giordano et al. 2005; Reinfelder 2011). Evidence suggests that *E. huxleyi* is also $CO_2$

limited and employs a CCM to enhance photosynthesis and growth (Beardall and Raven, 2013; Bach et al. 2013). Coccolith formation can serve as a carbon concentrating mechanism in *E. huxleyi*. The generation of hydrogen ions during calcification increases intracellular $CO_2$ as the pH inside the cell shifts the carbonate equilibrium toward $CO_2$ formation (Reinfelder 2011; Beardall and Raven 2013). As $pCO_2$ concentration rises in the oceans and, presumably, $CO_2$ limitation is alleviated, there may be reduced dependence on the use, development, and maintenance of CCMs (i.e. calcification), potentially resulting in shunting of cellular energy away from calcification toward other cellular processes (Rokitta and Rost 2012).

If indeed phytoplankton cellular energy budgets are reallocated in a $pCO_2$- enriched ocean, a resultant change in phytoplankton biochemistry and physiology may be expected (Beardall and Raven 2004). The evidence to support this is conflicting. Some studies have shown depressed growth rates in *E. huxleyi* under high $pCO_2$ (Iglesias-Rodriguez et al. 2008; Hoppe et al. 2011; Borchard and Engel 2012; Van de Waal et al. 2013), while others have shown elevated (Fiorini et al. 2011; Lohbeck et al. 2012) or no change in growth rate (Zondervan et al. 2002; De Bodt et al. 2010; Arnold et al. 2012). In some studies, reduced calcification in *E. huxleyi* is correlated with reduced photosynthesis (Hoppe et al. 2011), and therefore reduced total energy available to the cell. However, there is also evidence showing increased photosynthesis in some strains of *E. huxleyi* (Jin et al. 2013). In many experiments *E. huxleyi* cellular particulate organic carbon (POC) increased with elevated $pCO_2$ (Zondervan et al. 2002; Iglesias-Rodriguez et al. 2008; De Bodt et al. 2010; Rokitta and Rost 2012), but others report decreased POC (Fiorini et al. 2010; Hoppe et al. 2011). Borchard and Engel (2012) showed that in *E. huxleyi* (PML B 92/11), a portion of the increased POC was attributed to an increase in cellular carbohydrate content. In some strains of *E. huxleyi*, elevated $pCO_2$ also affected cellular morphology. For example De Bodt et al. (2010) showed that cell size decreased under high $pCO_2$ in strain AC481. Others, however, showed that cell size did not significantly change under elevated $pCO_2$ (Riebesell et

al. 2007; Arnold et al. 2012). Wuori (2012) and Iglesias-Rodriguez et al. (2008), however, showed that several strains of *E. huxleyi* increased in cell size with increasing $pCO_2$ (Wuori: CCMP 374, 2668; Iglesias-Rodriguez et al.: unknown strain).

Ocean acidification does not seem to directly affect microzooplankton grazing. Olson et al. (unpub.) showed that microzooplankton pre-acclimated to elevated $pCO_2$ and fed non-acclimated prey did not alter their grazing rate. A more likely way that OA affects microzooplankton is through $pCO_2$-induced effects on the biochemistry, physiology, and morphology of their phytoplankton prey. A change in the feeding ecology of microzooplankton through indirect effects of OA may have cascading effects on food webs.

This study was designed to test whether planktonic food webs will be affected in an acidifying ocean. Will microzooplankton grazing be indirectly affected by ocean acidification through direct effects of elevated $pCO_2$ on their phytoplankton prey? More specifically, I tested the following hypotheses: 1) Ocean acidification will directly influence the physiology and biochemistry of two ecologically significant phytoplankton species, *E. huxleyi* and *Rhodomonas* sp., and 2) Microzooplankton short-term grazing will be indirectly affected by ocean acidification-induced changes in their phytoplankton prey.

To test the first hypothesis, a series of phytoplankton physiological and biochemical metrics were characterized across three different $pCO_2$ levels for the phytoplankton species *E. huxleyi* and *Rhodomonas* sp. The specific metrics characterized were population growth rate, individual cell size, cellular chlorophyll *a*, cellular particulate C and N, carbohydrate content, and photosynthetic rates. The second hypothesis was tested through a series of short-term grazing experiments. Short-term ingestion rates were measured for three microzooplankton grazers, the tintinnid ciliates *Eutintinnus sp.* and *Favella taraikaensis*, and the heterotrophic dinoflagellate *Oxyrrhis marina*, all feeding on *E. huxleyi* cultures that were pre-acclimated to elevated $pCO_2$ conditions.

## METHODS

### Experimental Overview

To quantitatively assess the indirect effects of ocean acidification (OA) on microzooplankton through OA-induced changes to their prey, I first characterized the effects of OA on the biochemistry, physiology, and morphology of two ecologically significant phytoplankton species, *Emiliania huxleyi* and *Rhodomonas* sp. The phytoplankton were cultured semi-continuously under three $pCO_2$ treatments (described below) in a series of experiments. *E. huxleyi* CCMP 2668 is a coccolithophorid that is a bloom-forming, calcifying prymnesiophyte (Frada et al. 2012). *E. huxleyi* 2668 was obtained from the National Center for Marine Algae and Microbiota (NCMA, formerly CCMP) and was originally isolated from the Gulf of Maine in 2002. The second phytoplankton species characterized in this study was a cryptophyte, *Rhodomonas* sp. CCMP 755. *Rhodomonas* sp. 775 was obtained from NCMA and was originally isolated from Long Island Sound in 1956. Three microzooplankton species were chosen to test how potential changes in prey state may affect their grazing rates. The specific microzooplankton used in this study were selected because they are known to feed on *E. huxleyi* in maintenance culture at Shannon Point Marine Center. They include two ciliates, *Eutintinnus* sp. and *Favella taraikaensis*, and a dinoflagellate, *Oxyrrhis marina*. The ciliate *Eutintinnus* sp. (SPMC 144) was collected from Burrow's Bay, WA in 2010, while *F. taraikaensis* (SPMC 150) was collected from East Sound, Orcas Island, WA in 2011. The dinoflagellate *O. marina* (SPMC 107) was collected from the North Puget Sound and has been maintained in culture at Shannon Point since 1993.

Three characterization experiments were focused on *E. huxleyi*, and one on *Rhodomonas* sp. The first experiment (OA1) with *E. huxleyi* included characterization of cellular particulate carbon and nitrogen, cell size, and growth rate at several time points during the course of a 10 day

experiment, with a single short-term grazing experiment with *Eutintinnus* sp. on the final day of the experiment. The second *E. huxleyi* experiment (OA2) also included characterization of particulate carbon and nitrogen, growth rate, and cell size during the course of the experiment, and concluded with two short-term ingestion experiments with *Favella taraikaensis* (OA2a) on day 8 of the experiment and *Oxyrrhis marina* (OA2b) on day 10. Experimental details can be found in Table 1. The final experiment (OA3) with *E. huxleyi* included characterization of cellular particulate carbon and nitrogen, chlorophyll *a* (chl *a*), total cellular carbohydrate concentration, growth rate, and cell size throughout the experiment, and ended with an assessment of photosynthetic capacity on the last day. Experiment OA4 with *Rhodomonas* sp. also included characterization of cellular particulate carbon and nitrogen, chl *a*, total carbohydrate content, growth rate, and cell size during the course of 10 dilution days, with analysis of photosynthetic capacity on the final day of the experiment.

### $CO_2$ Culturing System Overview

The ocean acidification laboratory at SPMC is a unique alternative to traditional methods of acidifying water, e.g. flow through and direct bubbling systems. Experimental cultures are inoculated into media that was previously pre-equilibrated to $pCO_2$ treatment concentrations through direct bubbling with the corresponding treatment air. Cultures are placed into atmosphere-controlled chambers that are supplied with treatment air, where equilibration of the treatment air into the media helps to maintain seawater carbonate chemistry (Figure 1).

The three treatment levels (Ambient, Moderate, and High) correspond to three $pCO_2$ concentrations. The Ambient level (400ppmv) was determined as the modern day global average atmospheric $CO_2$ concentration (www.esrl.noaa.gov). The Moderate (750 ppmv) and High (1000 ppmv) media levels correspond to optimistic and pessimistic scenarios of $CO_2$ concentrations by the year 2100 as described by the Intergovernmental Panel on Climate Change (IPCC 2007).

Table 1. Description of each experiment, including species used, duration, and the physiological and biochemical attributes assessed. * indicates that the experiments were conducted with the upgraded $CO_2$ system described below. GR: growth rate ($\mu$, $d^{-1}$); CS: cell size ($\mu m^3$); TPC: total particulate carbon; PON: particulate organic nitrogen; CARB: carbohydrate (pg $cell^{-1}$); PI curves: photosynthesis vs. irradiance response curves ($\alpha$, $P_{max}$); IR: short-term ingestion rate (cells $grazer^{-1}$); PF: percent population feeding.

| Species | Experiment | Duration | Final Day | Attributes Assessed |
|---|---|---|---|---|
| *Emiliania huxleyi* | OA1 | 10 dilution days | *Eutintinnus* sp. feeding exp. Day 10 | GR, CS, TPC, PON, IR, PF |
| | OA2a | 10 dilution days | *Favella taraikaensis* feeding exp. Day 8 | GR, CS, TPC, PON, IR, PF |
| | OA2b | | *Oxyrrhis marina* feeding exp. Day 10 | GR, CS, TPC, PON, IR, PF |
| | OA3* | 10 dilution days | PI curves Day 10 | GR, CS, TPC, PON, CARB, Chl *a*, PI curves |
| *Rhodomonas* sp. | OA4* | 10 dilution days | PI curves Day 10 | GR, CS, TPC, PON, CARB, Chl *a*, PI curves |

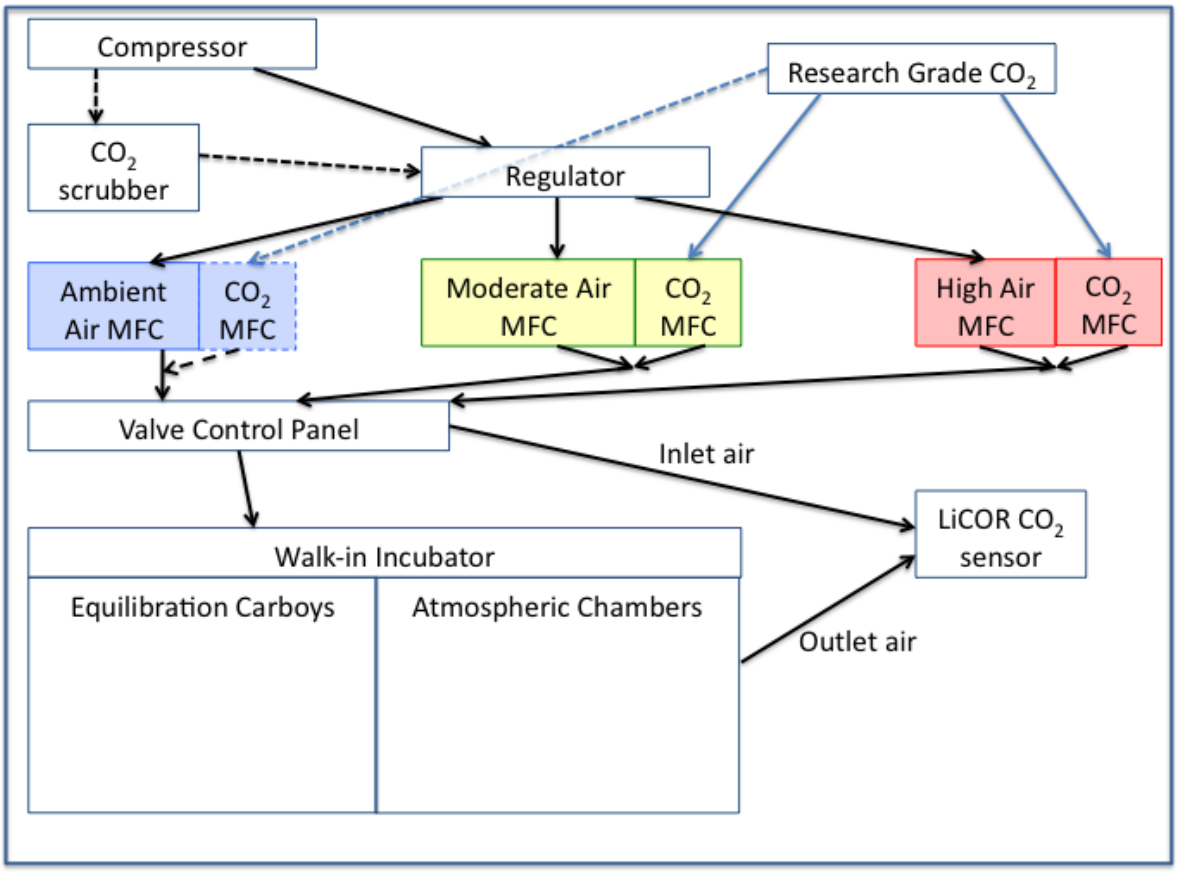


Figure 1. Diagram of SPMC's ocean acidification culturing facility. Dotted lines indicate upgrades to the system that are described below and that are only applicable to OA3 and OA4. MFCs are Sierra® mass flow controllers.

For the first two experiments (OA1, OA2a, and OA2b) ambient air was drawn from outside SPMC (Figure 1). This was necessary to reduce fluctuation in experimental $CO_2$ concentrations that would result from the large daily fluctuations in $CO_2$ that occur within the facility as a result of human activity.

Outside air was compressed with two 1.6 HP, 15G DeWALT Oil-free Electric Air Compressors that were plumbed in series to maintain continuous air flow at 25 psi to downstream Sierra® mass flow controllers (MFCs). The compressed ambient air (400ppmv ± 25ppmv) was enriched with research grade $CO_2$ using MFCs to create the Moderate and High $CO_2$ treatments. The MFCs allow for precise control of $CO_2$ and ambient air flow, with the $CO_2$ and air mixing at a point just downstream of the MFCs. After gas mixing, the respective treatment gasses are plumbed into a switchboard of valves that control the volume of airflow into the pre-equilibration jugs, atmospheric chambers, and an inline LiCOR® $CO_2$ sensor (Figure 1). The LiCOR $CO_2$ sensor ensures that the real-time $CO_2$ concentrations in the mixed air are on target with desired treatment levels. The pre-equilibration carboys and atmospheric chambers are vented to allow the incoming gas to escape and prevent pressurization of chambers and carboys. The venting gas can also be routed through the LiCOR $CO_2$ sensor to monitor the concentration of $CO_2$ in the air leaving the chambers and carboys. These measures are necessary to ensure that drawdown of $CO_2$ by photosynthesizing phytoplankton cultures does not outpace $CO_2$ equilibration, and as a check to ensure media is in equilibrium with the treatment gas.

Treatment media (5-10L) were pre-equilibrated in 20L carboys housed inside an environmental chamber held at 15°C and without light. Treatment air delivered into the media is forced through a small air stone. The air stone disperses the treatment gas into small bubbles that maximize gas exchange with the media. The addition of pressurized air to the carboys creates a slightly positive pressure gradient above the media, further allowing the treatment air to equilibrate

with the media before venting out of the carboy. The media are assumed to be fully equilibrated to the treatment air when the inlet and outlet $CO_2$ concentrations match, typically taking 24 - 48 hrs. Media were pre-equilibrated within to 50 ppmv of target concentrations (Table 2).

The atmospheric chambers containing experimental flasks are housed in a walk-in incubator maintained at 15°C and under a 14:10 day/night cycle. The chambers are continuously supplied with appropriate treatment air and serve to create a $CO_2$ atmosphere that equals the pre-equilibrated media $pCO_2$. As treatment air flows into the boxes, gas exchange with the culture media helps to maintain the $CO_2$ concentration in the culture as the photosynthetic activity of the cultures is also drawing down $CO_2$.

## System Upgrades

After experiments OA1 and OA2a/b upgrades were made to the system. A single Powerex oil-less rotary scroll compressor replaced the 2 Dewalt Oil-free Electric Air Compressors. A $CO_2$ scrubber was installed that strips compressed air of $CO_2$. Addition of the $CO_2$ scrubber eliminated the natural variation in local atmospheric $CO_2$ concentrations and allowed for greater control over the $CO_2$ concentrations in the three treatments. The air downstream of the $CO_2$ scrubber was treated as described above, with the addition of MFCs to regulate the addition of research grade $CO_2$ to the Ambient treatment to return the compressed air to 400 ppmv.

## Semi-continuous Culturing

In each semi-continuous experiment, the phytoplankton were cultured under the three $pCO_2$ treatments listed above under a light level of 250 µmol $m^{-2}$ $sec^{-1}$ for *E. huxleyi* experiments and 60 µmol $m^{-2}$ $sec^{-1}$ for the *Rhodomonas* sp. experiment.

Table 2. Realized $pCO_2$ concentrations in the pre-equilibrated media averaged across experiments for Ambient, Moderate, and High treatments (± 1 SD). 'Culture after 24 hours' represents daily $pCO_2$ concentrations after 24 hours of culture growth, with replicate values averaged across all days on all experiments (± 1 SD).

| Treatment | Media | Culture after 24 hrs |
|---|---|---|
| **Ambient** | 385 ± 45 | 368 ± 42 |
| **Moderate** | 710 ± 48 | 672 ± 44 |
| **High** | 943 ± 39 | 882 ± 41 |

Each treatment included three replicates, and replicate bottles in each treatment contained 500 mL of culture volume in a 1L square polycarbonate bottle. Wuori (2012) showed that this surface area:volume was optimal for maintaining carbonate chemistry in experimental bottles. *Emiliania huxleyi* and *Rhodomonas* sp. cultures were inoculated at very low cell densities (2500 cells/mL) and allowed to grow exponentially for four days prior to semi-continuous culturing in order to reach the target densities described below. Daily dilutions began on the morning of day 4 after inoculation. Each treatment culture was amended with pre-equilibrated media (Table 2). Dilution volumes were set by first determining the cell density above which carbonate chemistry within experimental bottles could no longer be near-regulated by air-sea gas exchange. Wuori (2012) showed that when *E. huxleyi* cell densities rise above 100,000 cells $mL^{-1}$, the drawdown of $CO_2$ through photosynthetic activity in the cultures significantly alters carbonate chemistry. Preliminary experiments determined *Rhodomonas* sp. alters carbonate chemistry when cell densities rise above 90,000 cells $mL^{-1}$. In order to maintain these cell densities, cultures were diluted to 25,000 cells $mL^{-1}$ for *E. huxleyi* and 40,000 cells for *Rhodomonas* sp., as calculated from growth rates during preliminary experiments. Daily cell counts were used to calculate the volume of culture that needed to be removed to achieve target dilution cell densities.

In preparation for phytoplankton cell counts, cultures were gently mixed prior to sampling. Cell counts for *E. huxleyi* were conducted on a BD FACSCalibur flow cytometer. *E. huxleyi* cells were quantified by side scatter and red fluorescence (FL3) parameters. Cell concentration was determined by the ratio between cells and beads counted. 100 µL of 2.0 µm Yellow-Green Latex bead solution (Flow Check intermediate intensity level 1 fluorescence in nanopure water) were added to each subsample of *E. huxleyi*. The original bead concentration was determined by manual counts via epifluorescent microscopy using UV light. Duplicate samples for manual cell counts were taken at the same time as flow cytometry counts, and were fixed in Alkaline Lugol's for later analysis. Manual

cell counts for both phytoplankton species were done using a Sedgewick Rafter Chamber or a Hemocytometer depending on cell density.

Additionally, daily morning sampling included removing a small volume from each treatment replicate for pH measurement for *E. huxleyi* and DIC measurement for *Rhodomonas* sp.. The total volume removed each morning prior to dilution was accounted for in calculating the dilution volumes, and the amount of culture removed for dilution (minus the volume already taken for pH and DIC) was the volume of culture available for analysis of physiological and biochemical attributes. Since this volume limited the number of analyses that could be sampled for each day, the analyses were distributed throughout a semi-continuous experiment in a way that fully utilized the volume of culture removed. Total alkalinity was sampled every other day, and on the other days samples for C:N, Chl *a*, and carbohydrates were taken.

**Carbonate Chemistry Measurements**

During the experiments involving *E. huxleyi*, (OA1, OA2a/b, and OA3), values of pH and total alkalinity (TA) were used to calculate $pCO_2$ of each treatment using CO2sys (Pierrot et al. 2006). Since pre-existing culture was amended with fresh pre-equilibrated media every day, the $pCO_2$ measured each morning was a reflection of 24 hours of growth and represented the lowest $pCO_2$ each day (Table 2). pH was analyzed spectrophotometrically with m-cresol dye on a Agilent 8453A UV-VIS Diode Array Spectrophotometer using a modified version of Best Practices for Ocean $CO_2$ Measurements SOP 6b (2007). The samples for pH were first filtered through 25mm glass fiber filters (GF/F) to remove any *E. huxleyi* cells and loose coccoliths. This was necessary because preliminary experiments demonstrated that filtering reduced optical scatter, leading to improved accuracy of pH measurements. Samples were warmed to 25 °C in a water bath and run within three hours of collection.

One hundred mL of culture removed for daily dilutions were used for TA measurement during *E. huxleyi* experiments. This volume was filtered through 25mm GF/F into 125mL glass bottles. The filtrate was immediately fixed with mercuric chloride and stored until analysis. Samples were analyzed using open cell titration in a jacketed beaker with a Metrohm Titrando titrator. Dickson's Certified Reference material was used for quality control according to the Best Practices for Ocean $CO_2$ Measurements SOP 6b (2007). TA was calculated using a modified Gran titration method as described by Millero et al. (1993). On alternating days of *Rhodomonas* sp. experiment OA4, 100 mL samples for alkalinity were poisoned with mercuric chloride and stored in 125 mL glass bottles at 6°C for later analysis. Because *Rhodomonas* sp. does not calcify, dissolution of carbonate was not a concern and filtration was not required. The poisoned samples were analyzed for TA as described above. Samples for DIC were taken in the final days of OA4 by first filtering 5 mL of culture into small vials with no headspace. The vials were kept at 6°C until analysis. The samples were analyzed ≤ 2 weeks after initial sampling using an Apollo SciTech DIC Analyzer AS-C3 which incorporates the LI-7000 $CO_2/H_2O$ Analyzer. TA and DIC values were used to calculate $pCO_2$ using CO2sys. Spectrophotometric pH was not determined for *Rhodomonas* cultures because preliminary experiments showed that dissolved compounds were released by the cell that absorbed light at the same wavelengths as the m-cresol purple dye that was used as the pH indicator (Figure A1).

## PHYTOPLANKTON CHARACTERIZATION

### Cell Size

Cells were taken from each $pCO_2$ replicate on alternating days during all *E. huxleyi* experiments for analysis of cell size. Live cells were mounted on a microscope slide and 200 cells from each treatment were imaged using RSImage software under 400X magnification on an Olympus CHA microscope. Since *E. huxleyi* cells are rough spheres, the volume of the spherical cell was calculated using:

$$V(\mu m^3) = \frac{4}{3}\pi r^3$$

where the radius, *r*, was calculated as:

$$r(\mu m) = \sqrt{\frac{A}{\pi}}$$

with area, *A*, determined from 2-D images using ImageJ software.

Because *Rhodomonas* sp. is mobile, images were taken of cells first fixed in 2% Acid Lugol's. Images were taken as described above. The length (*l*) and width (*w*) of the ellipsoid *Rhodomonas* sp. cells were used to calculate cell volume according to:

$$V(\mu m^3) = \frac{4}{3}\pi\left(\left(\frac{1}{2}\right)l \times \left(\frac{1}{2}w\right)^2\right)$$

Cells were imaged on each day of the experiment, with 50 cells from each replicate assessed.

### Particulate Carbon and Nitrogen

For experiments OA1, OA2a, OA2b, and OA3, 200 mL samples were split into 100 mL samples for total particulate carbon (TPC) and total particular organic carbon (POC) on even days

(D4, D6, D8 and D10). The two 100 mL samples were each filtered onto 21mm muffled GF/F filters with gentle vacuum pressure. One filter was used for TPC and the other for POC. Samples for TPC were placed in tin capsules and samples for POC were placed in silver capsules. The POC samples in silver capsules were first dried at 60°C for 24 hrs before being fumed with concentrated sulfuric acid for 24 hours to remove the PIC contained in *E. huxleyi*'s coccoliths. The silver capsules and filters were subsequently dried again at 60°C for 24 hrs. After final drying, the silver capsules and filters were folded into pellets. The silver pellets are also wrapped in tin and folded into pellets a second time to ensure that they combust with the same signature as the set of tin only pellets. The second set of filters of *E. huxleyi* samples in tin capsules were dried for 24 hrs at 60°C, and folded into pellets for analysis. After folding, the pellets were stored in a desiccator until analysis. For analysis, pellets were combusted in a CE Elantech Flash EA 1112 elemental analyzer. Standard curves were made using known weights of Acetanilide wrapped in tin capsules. Media blanks, filter blanks, and capsule blanks were included with each filter set as controls for background noise (i.e. concentration of dissolved organic carbon in the media and filters). The samples within the tin capsules yield TPC and total particulate nitrogen (PON). The acid-fumed samples within silver capsules yield POC and PON. Cellular PIC was obtained by subtracting POC values from the TPC values. PIC:PON and POC:PON ratios were calculated by dividing cellular PIC or POC by PON. PIC, POC, and PON were also normalized to cell size.

POC and PON of *Rhodomonas* sp. was sampled on even days (D4, D6, D8, and D10) and analyzed in the same manner as with *E. huxleyi*, with the exception that only one set of filters was necessary. The filters were placed in tin capsules and dried for 24 hrs. at 60°C, after which they were folded into pellets and stored in a desiccator until later analysis. Two sample days (D4 and D6) were analyzed at SPMC using a CE Elantech FLASH EA 1112 elemental analyzer with Acetanilide standards. Of these, one sample set was lost due to instrument malfunction (D6). Two sample days

(D8 and D10) were sent off for analysis by the University of California-Davis Stable Isotope Facility on a PDZ Europa ANCA-GSL elemental analyzer. POC:PON ratios were calculated from this analysis in the same manner as for *E. huxleyi* and the carbon and nitrogen data were also normalized to cell size.

### Chlorophyll *a*

Samples for Chl *a* were taken on alternating days (D4, D6, D8, and D10) of *E. huxleyi* experiment OA3 and *Rhodomonas* sp. experiment OA4. Ten mL of culture was filtered through 25mm GF/F to collect cells. The filters were placed in 6mL of 90% v/v acetone and allowed to extract for 24 hours at -20°C. After extraction, the samples were analyzed on a Turner 10-AU or Turner Trilogy fluorometer. Cellular Chl *a* was calculated using the acidification method of Parsons et al. (1984). Cellular Chl *a* concentrations were also normalized to cell size.

### Carbohydrates

Carbohydrate content of *E. huxleyi* and *Rhodomonas* sp. during experiments OA3 and OA4 for *E. huxleyi* and *Rhodomonas* sp., respectively, was assessed on alternating days (D4, D6, D8, and D10) by filtering 20mL of culture through 25mm muffled GF/F under gentle vacuum pressure. The filters were gently folded into muffled aluminum foil squares and stored at -40°C until analysis. Extraction of carbohydrates was done according DuBois et al. (1956). Briefly, filters were placed in 8 mL muffled glass vials containing 1mL of 80% sulfuric acid for 20 hrs. The vials were placed in a sonicating water bath for 30 min prior to the 20 hr extraction at room temperature. When extraction was complete, 6mL of ice-cold DI water was added to the extract and 1.6mL of the diluted extract was moved to clean, pre-muffled glass vials. Then 4 mL concentrated sulfuric acid and 0.8 mL 10% phenol were added to the vials in quick succession and the vials were capped and inverted. The

samples were allowed to fully react (≥ 30 min) before they were analyzed spectrophotometrically on a Spec20D+ spectrophotometer at 490nm. Carbohydrate content of the samples was calculated via a standard curve using known fructose concentrations.

## Algal Photosynthesis

On the final day of OA3 and OA4 (D10), the photosynthetic response of *E. huxleyi* and *Rhodomonas* sp. was assessed through photosynthesis vs.irradiance response (PE) using the $^{14}C$ method (Steeman-Nielsen 1952) and SPMC's photosynthetron. For each treatment replicate, 200 µL of $NaH^{14}CO_3$ was added to 8 mL of culture (~80,000 cells/mL). Then 0.5mL of the culture containing $NaH^{14}CO_3$ was placed in each of 12 7mL glass scintillation vials. The vials from each replicate and a dark control were then incubated in the photosynthetron in a 20 ºC water bath for 30 min under 11 irradiance levels ranging between 10 and 1200 µmol photons $m^{-2}$ $sec^{-1}$ for *E. huxleyi* and between 10 and 800 µmol photons $m^{-2}$ $sec^{-1}$ for *Rhodomonas* sp. After incubation, any remaining $NaH^{14}CO_3$ was acidified with 300 µL 1N HCl and the vials vented in the fume hood for 24 hours. After 24 hours the remaining acid was neutralized with 300 µL 1N NaOH and 5mL of scintillation fluid was added to each vial. The radioactivity in the vials was counted using a Packard 1900 TR Scintillation Counter. Photosynthetic rates from each vial were used to construct PE curves. SigmaPlot 9.0 was used to analyze the PE curves as defined by the function:

$$P = P_m * tanh\left(\alpha * \frac{\varepsilon d}{P_m}\right)$$

where $P$ is photosynthetic rate, $P_m$ is the photosynthetic max ($P_{max}$), $\varepsilon d$ is irradiance, and $\alpha$ is the photosynthetic efficiency. SigmaPlot 9.0 was also used to determine the maximum photosynthetic rate ($P_{max}$) and photosynthetic efficiency (α) of each culture replicate.

**Micro-zooplankton Short-term Ingestion experiments**

Using epifluorescent microscopy, it is possible to visualize photosynthetic prey cells inside microzooplankton grazer food vacuoles. Microzooplankton appear green under blue-light excitation, while their photosynthetic prey appear red or orange, depending on the prey cell's photopigment signature. Using this method, I was able to quantify microzooplankton grazing in *Eutintinnus* sp., *Favella taraikaensis*, and *Oxyrrhis marina* feeding on *E. huxleyi* that were adapted to elevated $pCO_2$.

The accuracy with which this method quantifies grazing is dependent on how much non-experimental prey remains in the microzooplankton food vacuoles prior to experiments. Any residual fluorescing prey remaining in the food vacuoles interferes with visual identification of ingested treatment prey, which is a requirement for accurate assessment of microzooplankton ingestion rate. In order to alleviate this complication, microzooplankton grazers are starved prior to each feeding experiment. Extended starvation, however, can induce behavioral feeding changes in microzooplankton. As a result, great care must be taken to ensure that food vacuoles are cleared, and the microzooplankton remain able and active grazers. For this study, the length of starvation required to empty microzooplankton food vacuoles was determined through preliminary starvation experiments. Additional experiments determined the optimal starvation duration whereby the microzooplankton return promptly to an active feeding state upon addition of a food source. To remove maintenance prey and commence starvation, the ciliates were gently sieved to remove prey. This also served to concentrate the population in preparation for experiments. Since *O. marina* at high densities will totally clear its maintenance food, and can withstand long-term starvation without deleterious effects, sieving was not necessary for concentration. The cultures were maintained at SPMC in 0.2 µm filtered and autoclaved seawater amended with trace metals and were allowed to graze down any residual maintenance food for eight days prior to experiments. An Optimal Diet control was included in each grazing experiment to ensure that the grazers had rebounded from

starvation and/or sieving. Consistent feeding rates on the optimal diet demonstrated that the grazers were unaffected by the pre-experiment starvation and sieving. If grazing on the Optimal Diet is normal, then any changes in grazing rates seen in the treatment bottles is likely due to treatment effects. Optimal Diet controls were *Heterocapsa rotundata, H. triquetra, Duneliella tertiolecta* for *Eutintinnus* sp., *F. taraikaensis,* and *O. marina* respectively.

An additional requirement for this method to be effective is that the grazer food vacuoles do not fill to a point that counting ingested cells becomes unreliable within the time span of the experiment. At this point, not only is it difficult and time-prohibitive to quantify continued ingestion of prey cells, but overlap of cells causes increased counting error and feeding rate cannot be estimated from a change in fullness over time. Feeding trials were performed for each grazer to determine optimal sampling intervals. Sampling intervals were based on the time it takes the grazer to fill their food vacuoles to capacity and the delay in grazing that occurs when prey are first introduced to a starved grazer. Based on this information, the ciliates, *Eutintinnus* sp. and *F. taraikaensis*, were sampled at 15, 30, and 45 minutes, while *O. marina* was sampled at 30, 60, and 90 minutes. The larger time spacing during *O. marina* experiments was required because *O. marina* ingests prey slower than the larger ciliates.

For each of the short-term ingestion experiments (Table 3), grazers were added to 12 Ambient media bottles, each with a final grazer density of 20 grazers $mL^{-1}$ for both ciliate species, and 150 grazers $mL^{-1}$ of *O. marina.* The 12 replicate bottles were split into 4 different feeding treatments with 3 replicates each treatment. Treatment diets consisted of the Optimal Diet (Table 3), and *E. huxleyi* pre-acclimated to Ambient, Moderate, or High $pCO_2$. The *E. huxleyi* used in these experiments were obtained after 8-10 days of semi-continuous culture in their respective $pCO_2$ treatments. *E. huxleyi* from OA1 and OA2 were offered as prey to microzooplankton grazers in experiments OA1, OA2a, and OA2b.

Table 3. Organization of short-term ingestion experiments for each microzooplankton species. Each grazing experiment included an Optimal Diet and *E. huxleyi* acclimated to Ambient, Moderate, and High $pCO_2$.

| Microzooplankton | Experiment | Dilution Day | Sampling Time Points (min) |
|---|---|---|---|
| *Eutintinnus* sp. | OA1 | 10 | 15, 30, 45 |
| *Favella taraikaensis* | OA2a | 8 | 15, 30, 45 |
| *Oxyrrhis marina* | OA2b | 10 | 30, 60, 90 |

The three microzooplankton species chosen for this study, *Eutintinnus* sp. (~80 µm), *F. taraikaensis* (~150 µm), and *O. marina* (~25 µm), were not pre-acclimated to $pCO_2$ treatments because previous experiments (Olson et al. unpub. data) showed that feeding rates of microzooplankton acclimated to elevated $pCO_2$ and fed an un-acclimated prey were unaffected by $pCO_2$ treatment.

Once grazers were added to 125 ml experimental bottles, initial samples without addition of *E. huxleyi* or optimal diet prey were taken to control for any prey still remaining in food vacuoles after starvation. Quantification of short-term grazing started when each respective grazer was provided a saturating carbon concentration (~400 µg C $L^{-1}$) of $pCO_2$-acclimated *E. huxleyi*. Based on estimates of total particulate carbon content of *E. huxleyi* 2668 from previous experiments, saturating C concentration was determined to be 13,600 cells $mL^{-1}$. Optimal diet concentrations were 8380 cells $mL^{-1}$ for *H. rotundata* (> 400 µg C $L^{-1}$) and *H. triquetra* (~300 µg C $L^{-1}$), and 6160 cells $mL^{-1}$ for *D. tertiolecta* (~ 300 µg C $L^{-1}$) as calculated by approximate cell volume of each species and published C:volume ratios (Menden-Deuer and Lessard 2000). In two cases, the optimal diet concentrations were not saturating, but the cell concentrations were sufficient to establish that the grazers were able to recover quickly from pre-experimental starvation and begin ingesting optimal prey quickly. Once prey was added to the first experimental bottle, the addition of prey to each subsequent bottle was staggered by 30 seconds. This time-gap was necessary to allow for precise time-sampling of all treatment bottles.

Time-point sampling consisted of taking a 20 mL sample from each experimental bottle and dispensing it into a 20ml serum vial that was previously filled with 1 mL 10% Glutaraldehyde (0.5% final concentration) and 0.2 mL of 10 µg $mL^{-1}$ 4',6-diamidino-2-phenylindole (DAPI) nucleic acid stain (0.1µg $mL^{-1}$ final concentration). Serum vials containing grazer samples were stored at 6°C for 24 h. This time duration allowed the DAPI stain to fully penetrate the nucleus before slides were made so that individual prey cells are easier to differentiate. After 24 h, each sample was filtered onto

polycarbonate (PC) filters under gentle vacuum filtration. PC filters of 20 μm and 10 μm pore size were used for the ciliates and *O. marina*, respectively. After filtration, the filters were placed on microscope slides, submerged in immersion oil, and covered with a microscope cover slide. Slides were stored at -20°C until analysis.

For analysis, the slides were examined under 1000x oil immersion using an epifluroescent microscope under blue-light excitation. The first 100 microzooplankton on each slide were assessed, and individual prey cells were counted in each grazer food vacuole. Quantifying cells within food vacuoles at each time point allowed me to quantify ingestion of *E. huxleyi* and optimal diet prey cells. Non-feeding microzooplankton were included in the counts to accurately assess population ingestion rates and also allowed for calculation of percent population feeding. Ingestion rates were calculated based on the number of cells ingested between time points ($T_0 - T_1$, $T_1 - T_2$, $T_2 - T_3$), divided by the time interval (in minutes). Percent population feeding was calculated by dividing the number of feeding grazers by the total number of grazers assessed in the sample.

**Statistical Analysis**

One-way ANOVAs (IBM SPSS Statistics 20 software) were used to assess differences in cell size, PIC:POC, POC:PON, Chl *a*, carbohydrates, and photosynthetic parameters across treatments on the final day of each semi-continuous experiment. Values for Chl *a*, carbohydrates, grazing rates, and photosynthetic capacity on the final day of each experiment were further normalized to cell size, and one-way ANOVAs were used to assess differences in each parameter. In addition to analysis of growth rate averaged by treatment across the length of each experiment, phytoplankton growth rates were analyzed with one-way ANOVA on the final day of each experiment. The first timepoint of each grazing experiment was measured to assess the immediate grazing response of starving grazers feeding on *E. huxleyi* grown in elevated $pCO_2$. The first timepoint allowed me to assess the initial

grazing impact of elevated $pCO_2$. Further, significant overlap of cells within grazer food vacuoles decrease counting accuracy and eliminate timepoint three from statistical analysis. Cell ingestion rates, biovolume-normalized ingestion rates, and percent population feeding at the $T_1$ timepoint were analyzed using one-way ANOVA.

Multiple linear regression (MLR) models were used to explore the predictive biochemical and physiological factors that accounted for the increased short-term ingestion rates observed on High $CO_2$-acclimated *E. huxleyi* cells for all three grazer species. MLR model variables included cell size, POC cell$^{-1}$, PON cell$^{-1}$, PIC cell$^{-1}$, Chl *a* cell$^{-1}$, and carbohydrate cell$^{-1}$. The model eliminates stepwise those variables that are not significant predictors of initial ingestion rates, using a p value of 0.1 to exit and a p value of 0.05 to enter the model.

## RESULTS

### *Rhodomonas* sp. results may be found in the Appendix

### *Emiliania huxleyi* BIOCHEMISTRY AND PHYSIOLOGY

### Growth Rate

*Emiliania huxleyi* intrinsic growth rate ($d^{-1}$) was variable over the duration of each semi-continuous experiment, with no consistent differences in growth rate between treatments on the final day of each experiment (Table 4). However, on the final day of OA1 there was a significant difference between the Ambient (1.58 ± 0.26) and High (0.93 ± 0.49) treatments ($p = 0.041$, $\alpha = 0.05$, Table 4). The time-averaged growth rate during OA1 was 1.4 ± 0.28 for Ambient cells, 1.26 ± 0.21 for Moderate cells, and 1.20 ± 0.32 for High cells, with no significant difference between treatments ($p = 0.071$, $\alpha = 0.05$, Table 4). Average growth rate during OA2 was 1.02 ± 0.02 in the Ambient treatment, 0.99 ± 0.02 in the Moderate treatment, and 1.00 ± 0.03 in the High treatment, with no significant treatment effect (0.974, $\alpha = 0.05$, Table 4). Similarly, average *E. huxleyi* growth rates for OA3 were 0.99 ± 0.04 for Ambient cells, 1.02 ± 0.01 for Moderate cells, and 0.98 ± 0.02 for High cells, with no treatment effect ($p = 0.259$, $\alpha = 0.05$, Table 4).

### Cell Size

A significant treatment effect of elevated $pCO_2$ on cell size was observed on the final day of each semi-continuous culture experiment (Figure 2; $p < 0.001$ for OA1, OA2a, and OA2b, $p = 0.013$ for OA3), and all three treatments were significantly different from each other in all three grazing experiments (Table 5; OA1, OA2a, OA2b).

Table 4. *Emiliania huxleyi* growth rate on the final day of each semi-continuous experiment and the average combined growth rate over the course of each experiment across $pCO_2$ treatments ($d^{-1}$ ± 1 SD). Bold indicates significant difference across $pCO_2$ treatment (ANOVA; $\alpha$ = 0.05); treatments with the same letters (a, b, c) are not significantly different.

| Experiment | Final Day | | | | Experiment Average | | | |
|---|---|---|---|---|---|---|---|---|
| | Ambient | Moderate | High | p value | Ambient | Moderate | High | p value |
| OA1 | **1.58 ± 0.26$_a$** | **1.35 ± 0.25$_{a,b}$** | **0.93 ± 0.49$_b$** | **0.041** | 1.40 ± 0.28 | 1.26 ± 0.21 | 1.20 ± 0.32 | 0.071 |
| OA2a | 1.11 ± 0.05 | 1.12 ± 0.02 | 1.13 ± 0.06 | 0.937 | -- | -- | -- | -- |
| OA2b | 1.11 ± 0.04 | 1.12 ± 0.03 | 1.13 ± 0.05 | 0.940 | 1.02 ± 0.02 | 0.99 ± 0.02 | 1.00 ± 0.03 | 0.974 |
| OA3 | 0.97 ± 0.05 | 1.06 ± 0.06 | 0.96 ± 0.02 | 0.095 | 0.99 ± 0.04 | 1.02 ± 0.01 | 0.98 ± 0.02 | 0.259 |

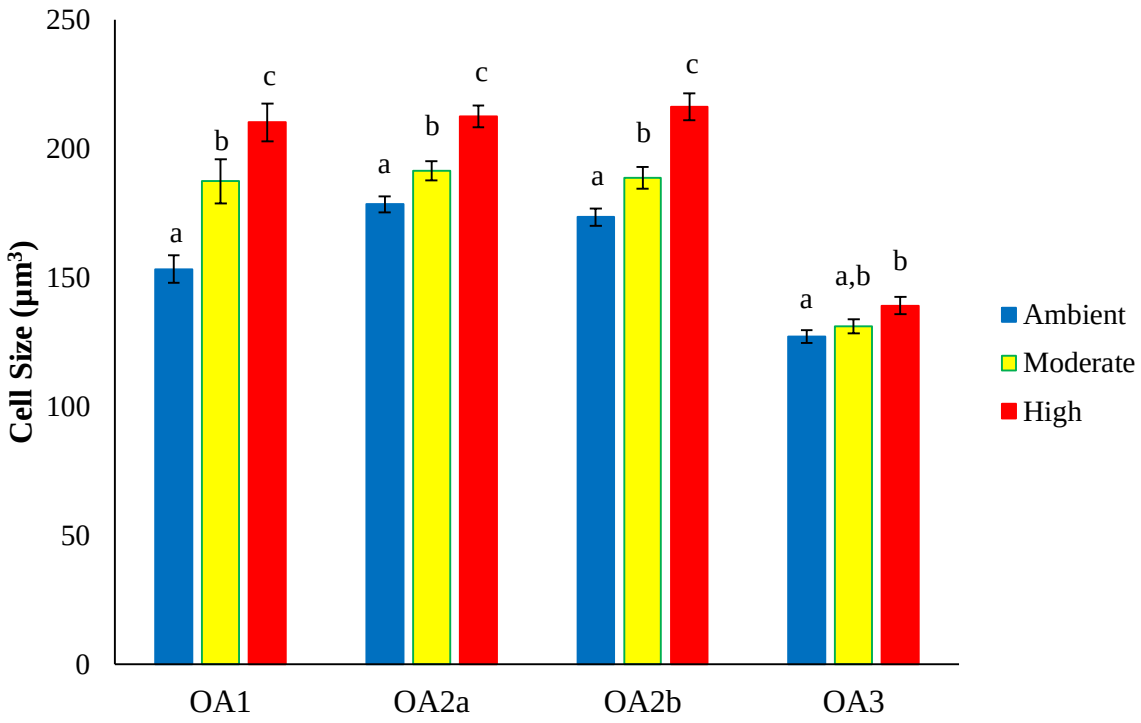


Figure 2. *Emiliania huxleyi* cell size across $pCO_2$ treatment on the final day of each semi-continuous experiment ($\mu m^3 \pm 1$ SD). Values were obtained from samples taken during grazing experiments (OA1, OA2a, OA2b) and assessment of photosynthesis (OA3). Letters over bars show significant differences across treatments within each experiment; bars with shared letters represent treatments that were not statistically different (Tukey's post hoc analysis). Refer to Table 5 for data and p values.

Table 5. Average *Emiliania huxleyi* cell size on the final day of each semi-continuous experiment ($\mu m^3 \pm 1$ SD). Bold font indicates a significant treatment effect (ANOVA, $\alpha = 0.05$), and letters (a, b, c) denote treatments which are significantly different from each other (Tukey's post hoc test).

| | **Ambient** | **Moderate** | **High** | **p value** |
|---|---|---|---|---|
| OA1 | **$153.24 \pm 39.88_a$** | **$187.27 \pm 61.30_b$** | **$210.09 \pm 52.84_c$** | **<0.001** |
| OA2a | **$178.37 \pm 44.01_a$** | **$191.41 \pm 53.68_b$** | **$212.54 \pm 59.87_c$** | **<0.001** |
| OA2b | **$173.36 \pm 46.23_a$** | **$188.63 \pm 59.68_b$** | **$216.13 \pm 74.7_c$** | **<0.001** |
| OA3 | **$127.20 \pm 5.56_a$** | **$131.07 \pm 1.32_{a,b}$** | **$139.10 \pm 7.87_b$** | **0.013** |

Cell size ($\mu m^3$) increased in a stepwise fashion, where cell size in the Moderate treatment (187, 191, and 189 $\mu m^3$ for OA1, OA2a, and OA2b respectively) was higher than in the Ambient treatment (153, 178, 173, and 127 $\mu m^3$ for OA1 – OA3 respectively) and cell size in the High treatment (210, 213, 216, and 139 $\mu m^3$ for OA1 – OA3 respectively) was higher than both the Ambient for OA1 – OA3 and the Moderate in OA1, OA2a, and OA2b.

**Particulate Cellular Carbon and Nitrogen**

While significant effects of elevated $pCO_2$ were seen in *E. huxleyi* particulate organic carbon content (pg C $cell^{-1}$), the trends were not consistent (Table 6, Figure 3). In experiments OA1 and OA2a, POC $cell^{-1}$ was greater in cells grown under elevated $pCO_2$. During OA1 there was a significant treatment effect ($p = 0.003$, $\alpha = 0.05$), with Tukey's post hoc analysis revealing that the High $pCO_2$ treatment had more POC $cell^{-1}$ ($22.24 \pm 2.83$) than the Ambient and Moderate treatments ($16.92 \pm 0.16$ and $14.05 \pm 0.38$, respectively). During OA2a, there was also a significant treatment effect ($p < 0.001$, $\alpha = 0.05$). In this experiment the Moderate and High treatments did not differ, but both were significantly different from the Ambient treatment, with more pg POC $cell^{-1}$ in High and Moderate ($19.66 \pm 0.42$ and $19.04 \pm 0.62$, respectively) than in the Ambient treatment ($15.55 \pm 0.29$). There was no significant treatment effect seen during OA2b ($p = 0.459$) or OA3 ($p = 0.969$).

No statistical difference in particulate inorganic carbon content per cell was observed between $pCO_2$ treatments in any experiment (Table 6, Figure 4). However, there was a significant treatment effect in *E. huxleyi* PIC:POC in experiment OA2a (Table 6, Figure 5). In OA2a, PIC:POC decreased in cultures grown under elevated $pCO_2$ ($p = 0.007$; $\alpha = 0.05$), with Moderate ($0.48 \pm 0.04$) and High ($0.54 \pm 0.27$) significantly lower than the Ambient treatment ($0.67 \pm 0.06$).

Table 6. *Emiliania huxleyi* particulate carbon and nitrogen (PIC, POC, and PON) expressed as pg cell$^{-1}$ ± 1 SD on the final day of each experiment Bold font indicates a significant treatment effect (ANOVA, $\alpha = 0.05$), and letters (a, b) denote treatments which are significantly different from each other (Tukey's post hoc test).

| Parameter | Experiment | Ambient | Moderate | High | p-value |
|---|---|---|---|---|---|
| PIC(pg cell$^{-1}$) | OA1 | 9.21 ± 1.96 | 8.94 ± 0.93 | 11.04 ± 3.16 | 0.492 |
| | OA2a | 10.36 ± 0.85 | 9.38 ± 0.87 | 10.24 ± 0.19 | 0.261 |
| | OA2b | 4.17 ± 3.72 | 6.03 ± 0.33 | 5.16 ± 1.36 | 0.589 |
| | OA3 | 5.01 ± 1.57 | 4.64 ± 0.82 | 4.52 ± 0.45 | 0.844 |
| POC (pg cell$^{-1}$) | **OA1** | **14.05 ± 0.38$_a$** | **16.92 ± 0.16$_a$** | **22.24 ± 2.83$_b$** | **0.003** |
| | **OA2a** | **15.55 ± 0.29$_a$** | **19.66 ± 0.42$_b$** | **19.04 ± 0.62$_b$** | **<0.000** |
| | OA2b | 22.37 ± 2.75 | 22.13 ± 0.22 | 23.96 ± 1.53 | 0.459 |
| | OA3 | 12.10 ± 0.23 | 12.42 ± 1.20 | 12.32 ± 2.49 | 0.969 |
| PIC:POC | OA1 | 0.65 ± 0.12 | 0.53 ± 0.06 | 0.51 ± 0.21 | 0.474 |
| | **OA2a** | **0.67 ± 0.06$_a$** | **0.48 ± 0.04$_b$** | **0.54 ± 0.27$_b$** | **0.007** |
| | OA2b | 0.19 ± 0.19 | 0.27 ± 0.02 | 0.22 ± 0.07 | 0.663 |
| | OA3 | 0.41 ± 0.12 | 0.37 ± 0.06 | 0.38 ± 0.10 | 0.874 |
| PON(pg cell$^{-1}$) | **OA1** | **1.62 ± 0.19$_a$** | **1.55 ± 0.33$_a$** | **2.57 ± 0.15$_b$** | **0.003** |
| | OA2a | 1.80 ± 0.09 | 1.90 ± 0.09 | 1.85 ± 0.04 | 0.377 |
| | OA2b | 1.85 ± 0.16 | 1.77 ± 0.16 | 1.93 ± 0.16 | 0.495 |
| | OA3 | 2.40 ± 0.12 | 2.50 ± 0.22 | 2.47 ± 0.48 | 0.926 |
| POC:PON | OA1 | 10.57 ± 2.35 | 15.26 ± 5.08 | 13.32 ± 5.31 | 0.477 |
| | **OA2a** | **8.64 ± 0.56$_a$** | **10.37 ± 0.36$_b$** | **10.27 ± 0.53$_b$** | **0.009** |
| | OA2b | 12.80 ± 3.44 | 12.56 ± 1.17 | 12.42 ± 0.96 | 0.974 |
| | OA3 | 5.04 ± 0.23 | 4.96 ± 0.17 | 4.98 ± 0.04 | 0.835 |

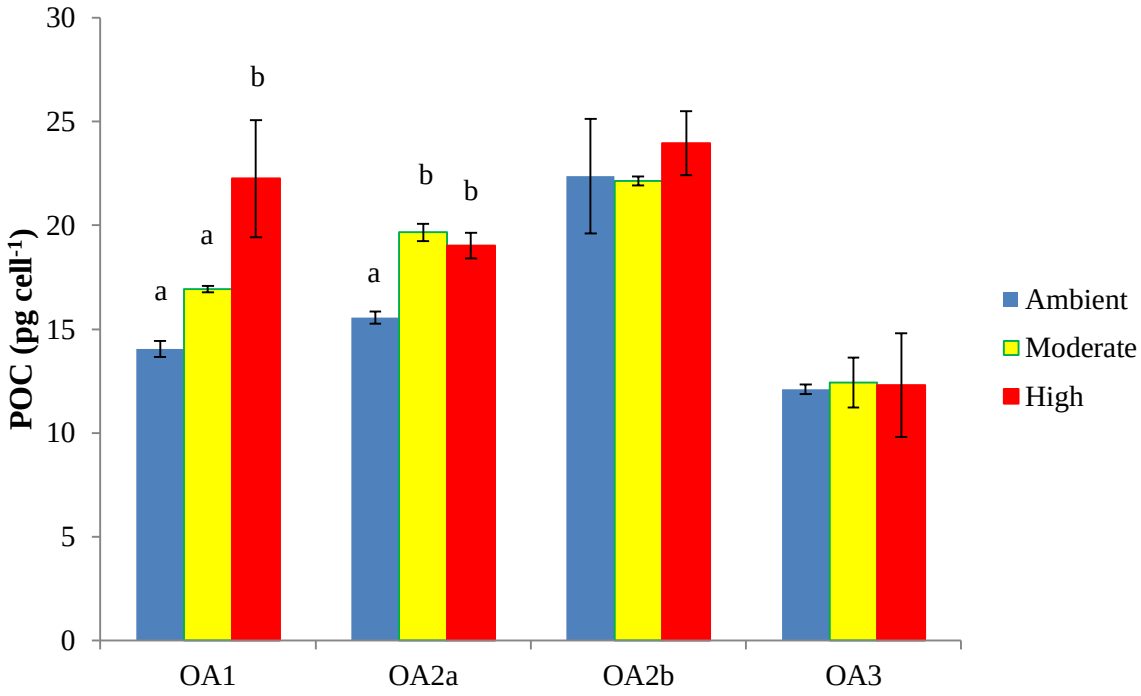


Figure 3. *Emiliania huxleyi* particulate organic carbon (pg POC cell$^{-1}$) taken from samples obtained on the last day of semi-continuous culture during grazing experiments (OA1, OA2a, OA2b) and assessment of photosynthesis (OA3). Letters over bars denote significant differences across treatments within each experiment; bars with shared letters represent treatments that were not statistically different (Tukey's post hoc analysis). Refer to Table 6 for data and p values. Error bars represent ± 1 SD.

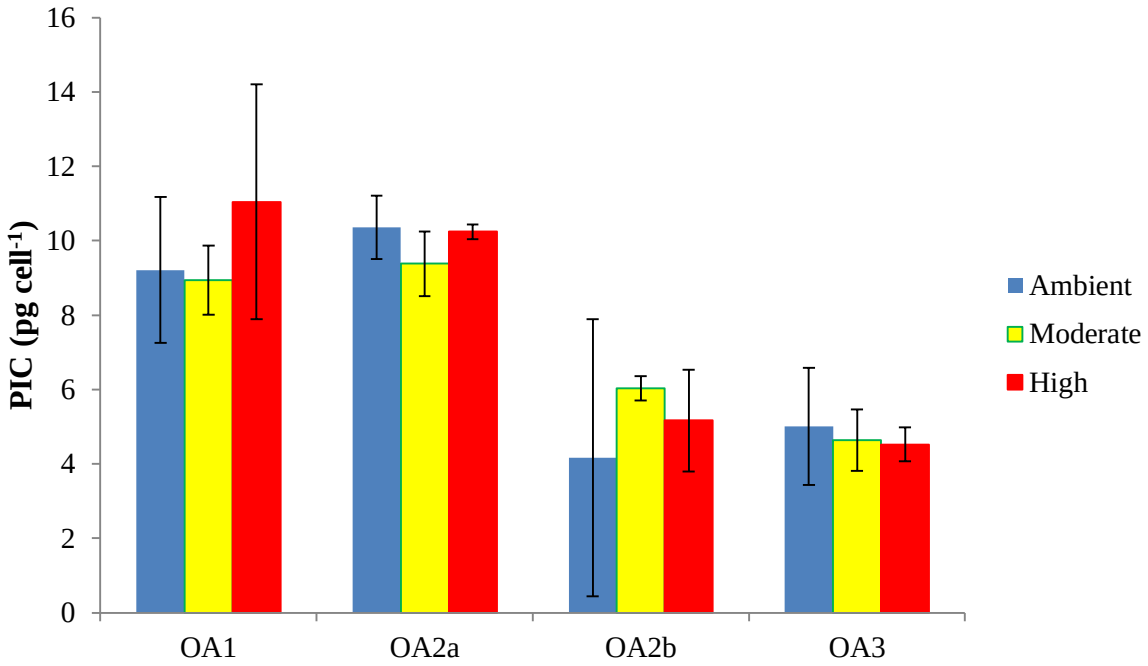


Figure 4. *Emiliania huxleyi* particulate inorganic carbon (pg PIC cell$^{-1}$) taken from samples obtained on the last day of semi-continuous culture during grazing experiments (OA1, OA2a, OA2b) and assessment of photosynthesis (OA3). Error bars represent ± 1 SD.

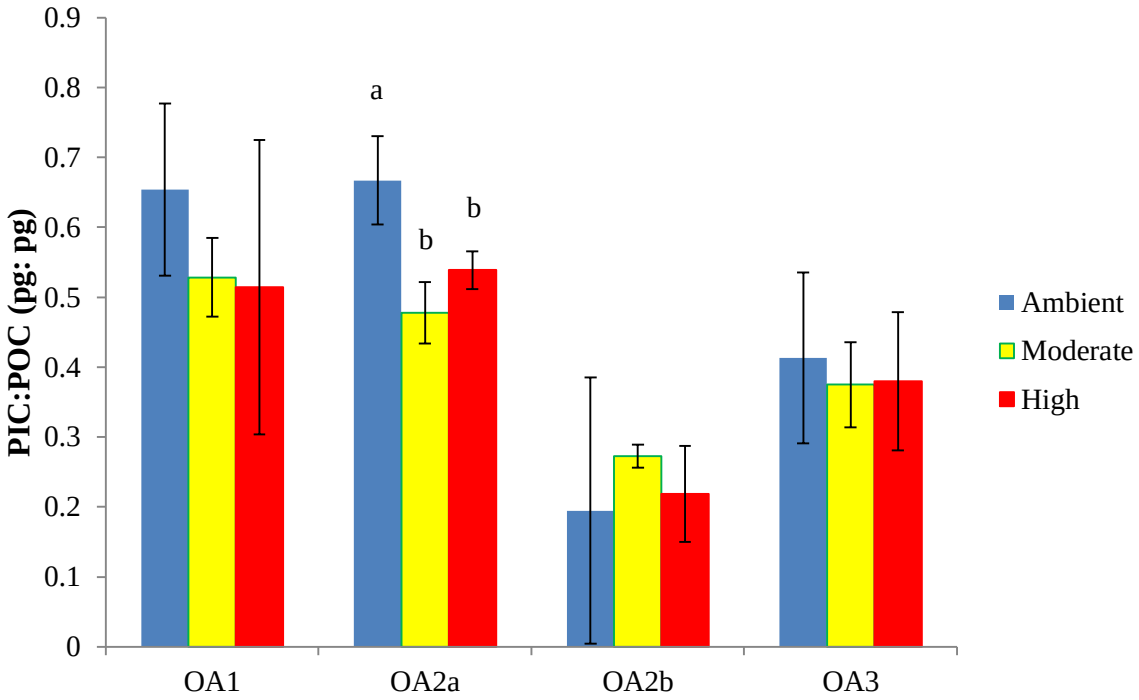


Figure 5. *Emiliania huxleyi* ratio of particulate inorganic to organic carbon (pg PIC: pg POC) from samples taken on the last day of semi-continuous culture during grazing experiments (OA1, OA2a, OA2b) and assessment of photosynthesis (OA3). Letters over bars denote significant treatment differences within each experiment; bars with shared letters represent treatments that are not statistically different (Tukey's post hoc analysis). Refer to Table 6 for data and p values. Error bars represent ± 1 SD.

*E. huxleyi* particulate organic nitrogen content (pg PON $cell^{-1}$) did not differ across $pCO_2$ treatments, with the exception of experiment OA1 (Table 6, Figure 6), where a significant increase in PON $cell^{-1}$ was observed in elevated $pCO_2$ ($p = 0.003$, $\alpha = 0.05$). The High $pCO_2$ treatment ($2.57 \pm 0.15$) was significantly greater than the Ambient and Moderate treatments ($1.62 \pm 0.19$ and $1.55 \pm 0.33$, respectively). Despite a significant increase in *E. huxleyi* POC $cell^{-1}$ in experiments OA1 and OA2a, a significant treatment effect on POC:PON per cell was observed only in OA2a (Table 6, Figure 7). POC:PON was significantly higher in elevated $pCO_2$ ($p = 0.009$; ANOVA, $\alpha = 0.05$), where the Moderate ($10.37 \pm 0.36$) and High ($10.27 \pm 0.53$) treatments were significantly greater than the Ambient ($8.64 \pm 0.56$) $pCO_2$ treatment (Tukey's post hoc analysis). In experiment OA1 both POC $cell^{-1}$ and PON $cell^{-1}$ were elevated in the high $pCO_2$ treatment, resulting in no significant difference in POC:PON.

When *E. huxleyi* POC $cell^{-1}$ and PON $cell^{-1}$ were normalized to cell biovolume ($\mu m^3$), only experiment OA2a showed a significant difference in cellular POC $\mu m^{-3}$ and PON $\mu m^{-3}$ (Table 7). In OA2a, *E. huxleyi* carbon density (fg POC $\mu m^{-3}$) was significantly greater in the Moderate $pCO_2$ treatment ($10 \pm 2.0$; $p < 0.001$; $\alpha = 0.05$) compared to the Ambient ($87 \pm 2.0$) and High ($90 \pm 3.0$) $pCO_2$ treatments (Tukey's post hoc analysis). The density of PIC (fg PIC $\mu m^{-3}$) in OA2a was significantly lower under elevated $pCO_2$ ($p = 0.035$; $\alpha = 0.05$). In that experiment, the High treatment ($48 \pm 1.0$) was significantly lower than the Ambient treatment ($58 \pm 5.0$), but Moderate ($49 \pm 5.0$) was not different from Ambient or High $pCO_2$ treatments (Tukey's post hoc analysis). Nitrogen density (fg PON $\mu m^{-3}$) decreased significantly in OA2a with increasing $pCO_2$ ($p = 0.017$; $\alpha = 0.05$). No change was observed between Ambient ($10 \pm 0.5$) and Moderate ($10 \pm 0.5$) treatments, but significantly lower PON $\mu m^{-3}$ was observed in the High ($9 \pm 0.2$) $pCO_2$ treatment (Tukey's post hoc analysis).

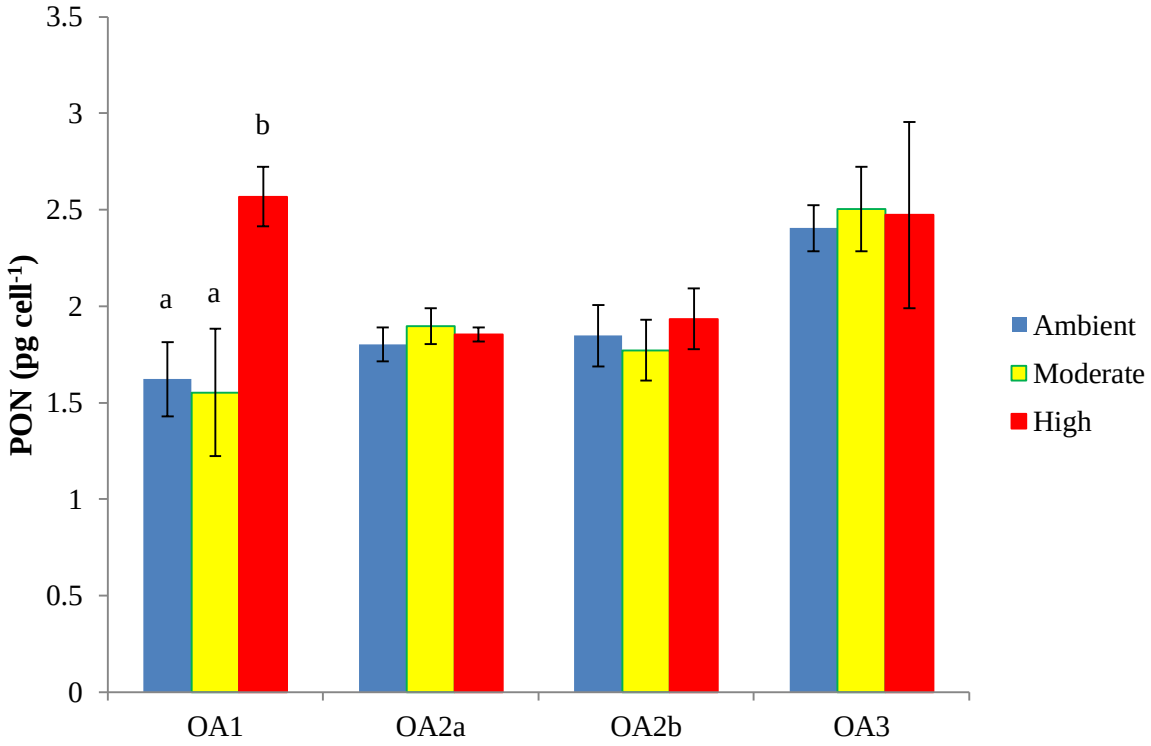


Figure 6. *Emiliania huxleyi* particulate organic nitrogen (pg PON cell$^{-1}$) from samples obtained on the last day of semi-continuous culture during grazing experiments (OA1, OA2a, OA2b) and assessment of photosynthesis (OA3). Letters over bars show significant differences across treatments within each experiment; bars with shared letters represent treatments that were not statistically different (Tukey's post hoc analysis). Refer to Table 6 for data and p values. Error bars represent ± 1 SD.

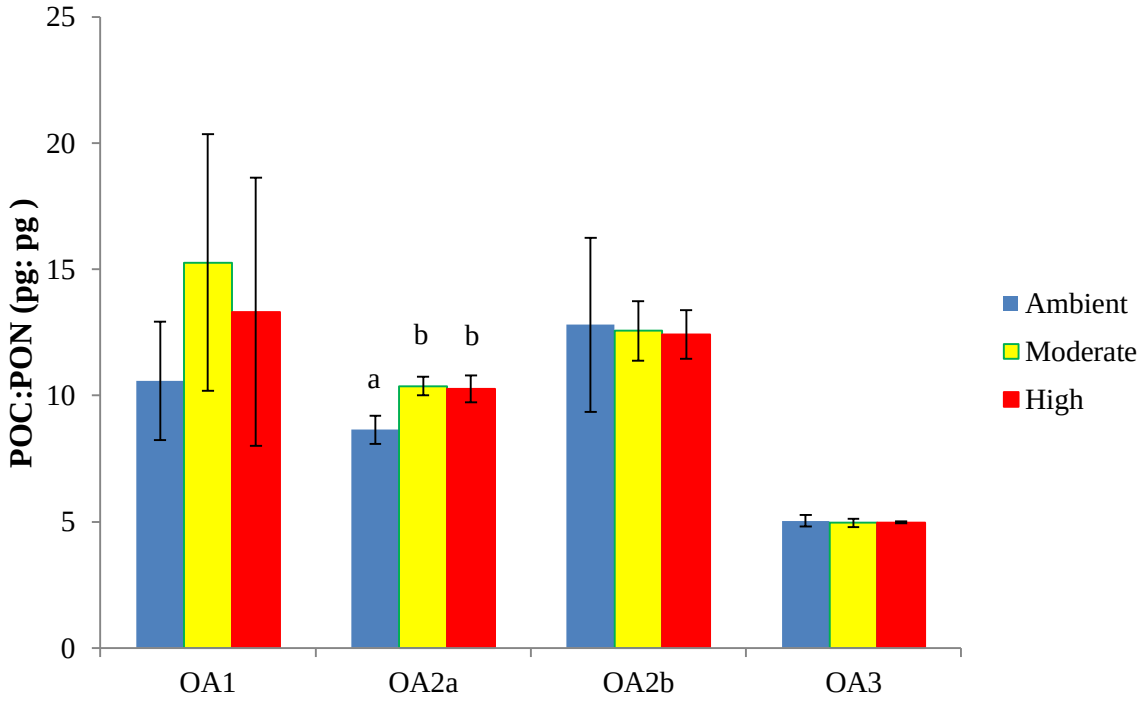


Figure 7. *Emiliania huxleyi* particulate organic carbon to nitrogen ratio (pg POC: pg PON) from samples taken on the last day of semi-continuous culture during grazing experiments (OA1, OA2a, OA2b) and assessment of photosynthesis (OA3). Letters over bars show significant differences across treatments within each experiment; bars with shared letters represent treatments that were not statistically different (Tukey's post hoc analysis). Refer to Table 6 for data and p values. Error bars represent ± 1 SD.

Table 7. *Emiliania huxleyi* PIC, POC and PON (fg $\mu m^{-3}$ ± 1SD). Bold font indicates a significant treatment effect (ANOVA, $\alpha = 0.05$), and letters (a, b) denote treatments which are significantly different from each other (Tukey's post hoc test).

| Parameter | Experiment | Ambient | Moderate | High | p-value |
|---|---|---|---|---|---|
| PIC (fg $\mu m^{-3}$) | OA1 | 60 ± 13 | 48 ± 5.0 | 53 ± 15 | 0.474 |
| | **OA2a** | **58 ± 5.0$_a$** | **49 ± 5.0$_{a,b}$** | **48 ± 1.0$_b$** | **0.035** |
| | OA2b | 24 ± 21 | 32 ± 2.0 | 24 ± 6.0 | 0.608 |
| | OA3 | 39 ± 11 | 35 ± 6.0 | 33 ± 4.0 | 0.602 |
| POC(fg $\mu m^{-3}$) | OA1 | 92 ± 3.0 | 90 ± 1.0 | 110 ± 13 | 0.097 |
| | **OA2a** | **87 ± 2.0$_a$** | **103 ± 2.0$_b$** | **90 ± 3.0$_a$** | **<0.000** |
| | OA2b | 129 ± 16 | 117 ± 1.0 | 111 ± 7.0 | 0.160 |
| | OA3 | 95 ± 2.0 | 95 ± 8.0 | 88 ± 13 | 0.579 |
| PIC:POC | OA1 | 0.65 ± 0.12 | 0.53 ± 0.06 | 0.51 ± 0.21 | 0.474 |
| | **OA2a** | **0.67 ± 0.06$_a$** | **0.48 ± 0.04$_b$** | **0.54 ± 0.03$_b$** | **0.007** |
| | OA2b | 0.13 ± 0.18 | 0.27 ± 0.03 | 0.22 ± 0.07 | 0.663 |
| | OA3 | 0.41 ± 0.12 | 0.37 ± 0.06 | 0.38 ± 0.099 | 0.874 |
| PON (fg $\mu m^{-3}$) | OA1 | 11 ± 1.0 | 8 ± 2.0 | 12 ± 1.0 | 0.029 |
| | **OA2a** | **10 ± 0.5$_a$** | **10 ± 0.5$_a$** | **9 ± 0.2$_b$** | **0.017** |
| | OA2b | 11 ± 0.9 | 18 ± 2.0 | 13 ± 4.0 | 0.103 |
| | OA3 | 19 ± 1.0 | 19 ± 1.0 | 18 ± 2.0 | 0.592 |
| POC:PON | OA1 | 8.72 ± 0.87 | 11.26 ± 2.48 | 8.72 ± 1.57 | 0.210 |
| | **OA2a** | **8.64 ± 0.56$_a$** | **10.37 ± 0.36$_b$** | **10.28 ± 0.53$_b$** | **0.009** |
| | OA2b | 12.25 ± 2.61 | 12.56 ± 1.17 | 12.42 ± 0.96 | 0.977 |
| | OA3 | 5.04 ± 0.23 | 4.96 ± 0.17 | 4.98 ± 0.04 | 0.835 |

## Chlorophyll a

No significant difference in pg Chl *a* $cell^{-1}$ was observed across $pCO_2$ treatments ($p = 0.614$, $\alpha = 0.05$) on the final day of OA3 (Figure 8). The mean cellular Chl *a* was 0.24 ± 0.02, 0.21 ± 0.08, and 0.23 ± 0.02 for the Ambient, Moderate, and High treatments, respectively. Normalizing Chl *a* to cell biovolume ($\mu m^3$) also showed no significant difference across $pCO_2$ treatments. The mean Chl *a* concentration on the final day of OA3 was 2.0 ± 0.2, 2.0 ± 0.6, and 2.0 ± 0.04 fg Chl *a* $\mu m^{-3}$ in the Ambient, Moderate, and High treatments, respectively (Figure 9, $p = 0.438$, $\alpha = 0.05$).

## Carbohydrates

No $pCO_2$ treatment effect was observed in *E. huxleyi* carbohydrate content during OA3. The mean *E. huxleyi* cellular carbohydrate content on the final day of OA3 was 0.78 ± 0.18, 1.89 ± 2.00, and 0.475 ± 0.439 pg fructose equivalents $cell^{-1}$ in the Ambient, Moderate, and High treatments, respectively ($p = 0.530$ $\alpha = 0.05$; Figure 10). Normalizing carbohydrate content to cell biovolume ($\mu m^3$) also showed no significant treatment effect ($p = 0.534$, $\alpha = 0.05$; Figure 11). The mean carbohydrate concentration on the final day of OA3 was 6.3 ± 2.0, 14.6 ± 15, and 3.5 ± 3.0 fg fructose equivalents $\mu m^{-3}$ in the Ambient, Moderate, and High treatments, respectively.

## Photosynthetic Capacity

Analysis of *E. huxleyi* photosynthesis vs. irradiance response (PE) curves (Figure 12) on the final day of OA3 revealed no photosynthetic treatment effect to elevated $pCO_2$. *E. huxleyi* photosynthetic efficiency (α, alpha) normalized to Chl *a* ranged from 0.010 ± 0.001 in the High treatment, 0.015 ± 0.005 in the Moderate, to 0.014 ± 0.003 in the Ambient treatment (mg C $hr^{-1}$ (mg Chl $a^{-}1$) (µmol photons $m^{-2}$ $s^{-1}$)$^{-1}$) with no significant treatment effect (Figure 13, $p = 0.155$, $\alpha = 0.05$).

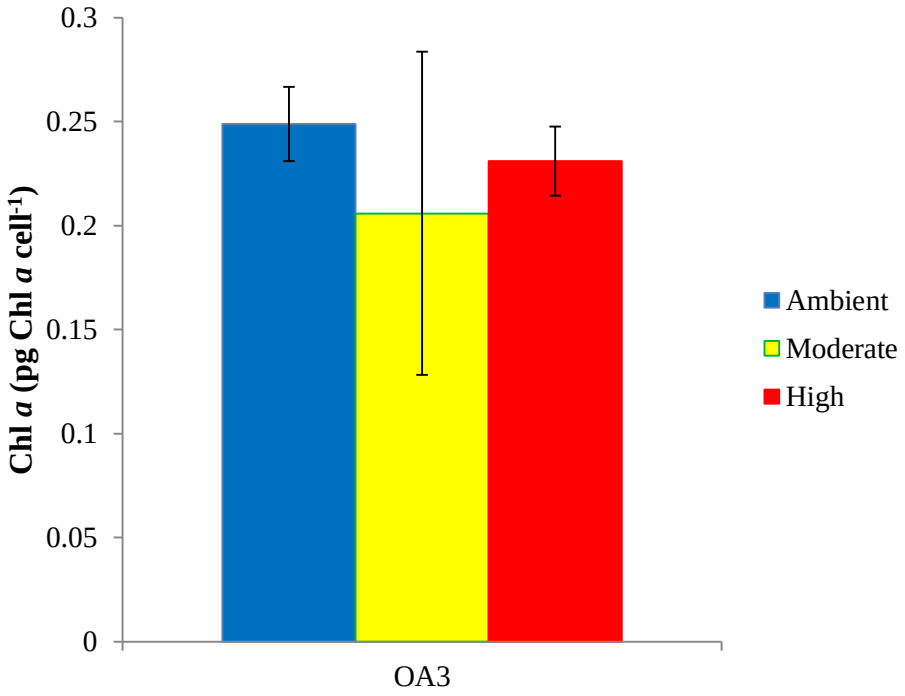


Figure 8. *Emiliania huxleyi* chlorophyll *a* (pg Chl *a* cell$^{-1}$) on the last day of semi-continuous experiment OA3. Error bars represent ± 1 SD.

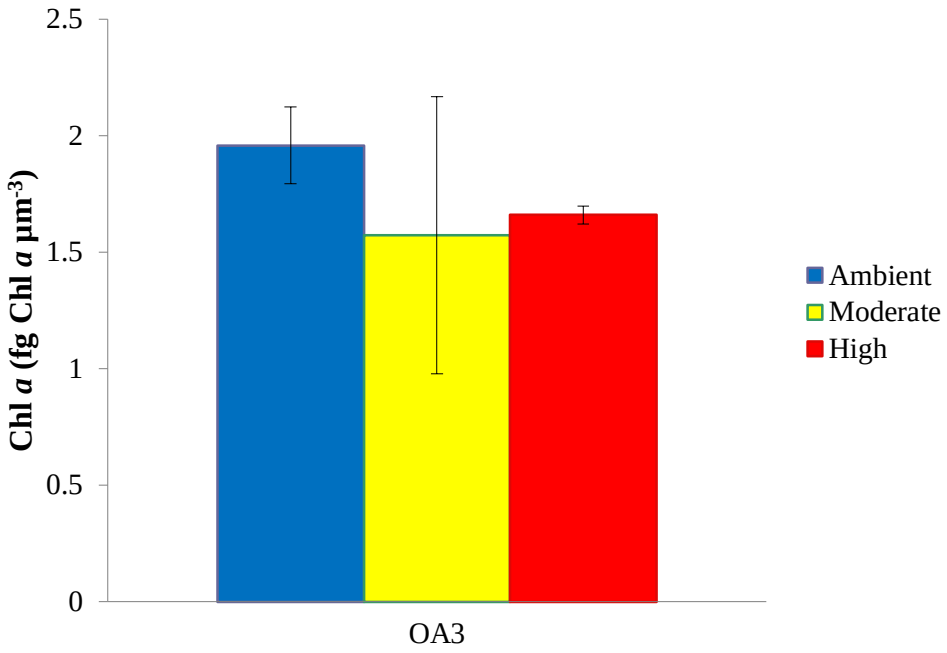


Figure 9. *Emiliania huxleyi* chlorophyll *a* normalized to cell biovolume (fg Chl a $\mu m^{-3}$) on the last day of semi-continuous experiment OA3. Error bars represent ± 1 SD.

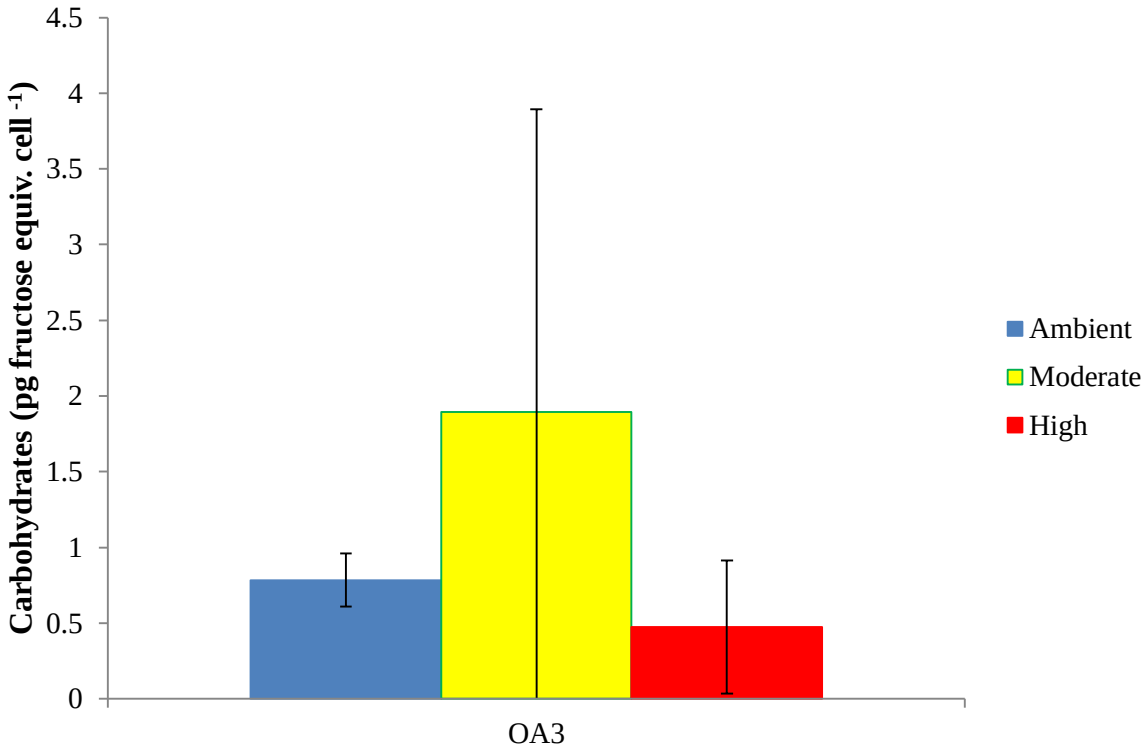


Figure 10. *Emiliania huxleyi* total carbohydrate content (pg fructose equiv. cell$^{-1}$) on the final day of semi-continuous experiment OA3. Error bars represent ± 1 SD.

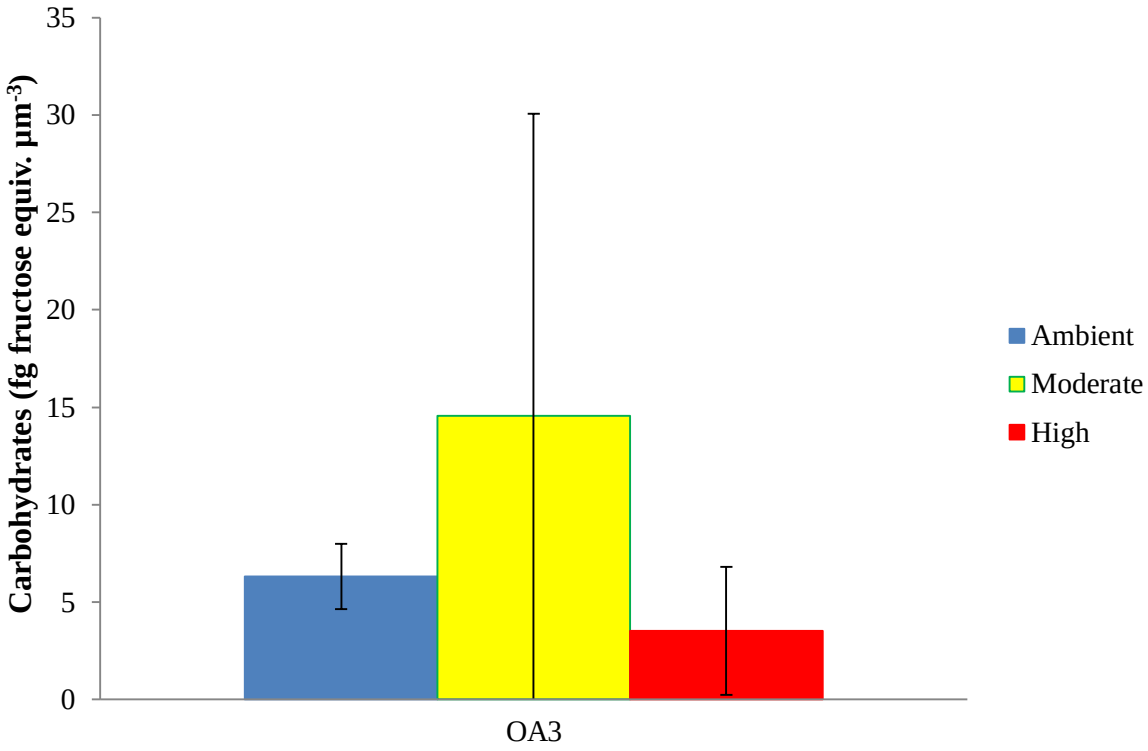


Figure 11. *Emiliania huxleyi* total carbohydrate content normalized to cell biovolume (fg fructose equiv. $\mu m^{-3}$) on the final day of semi-continuous experiment OA3. Error bars represent ± 1 SD.

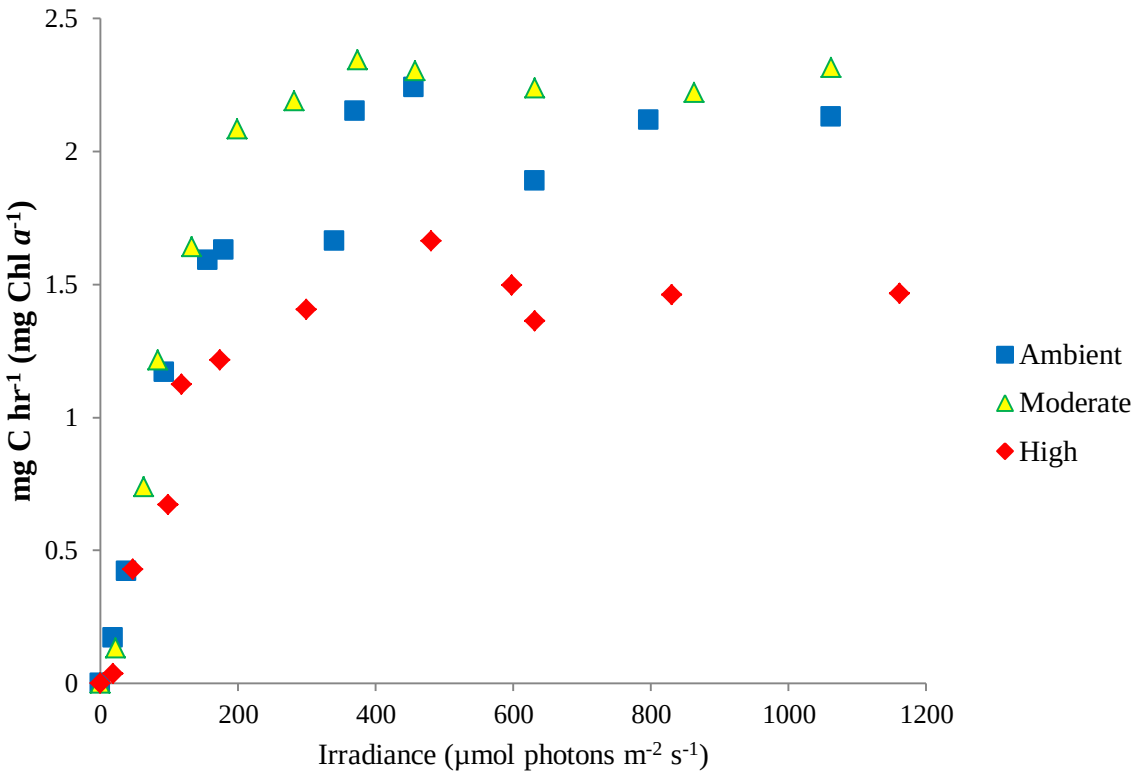


Figure 12. Treatment averaged photosynthesis vs. irradiance response (PE) curves for *E. huxleyi* on the final day of OA3.

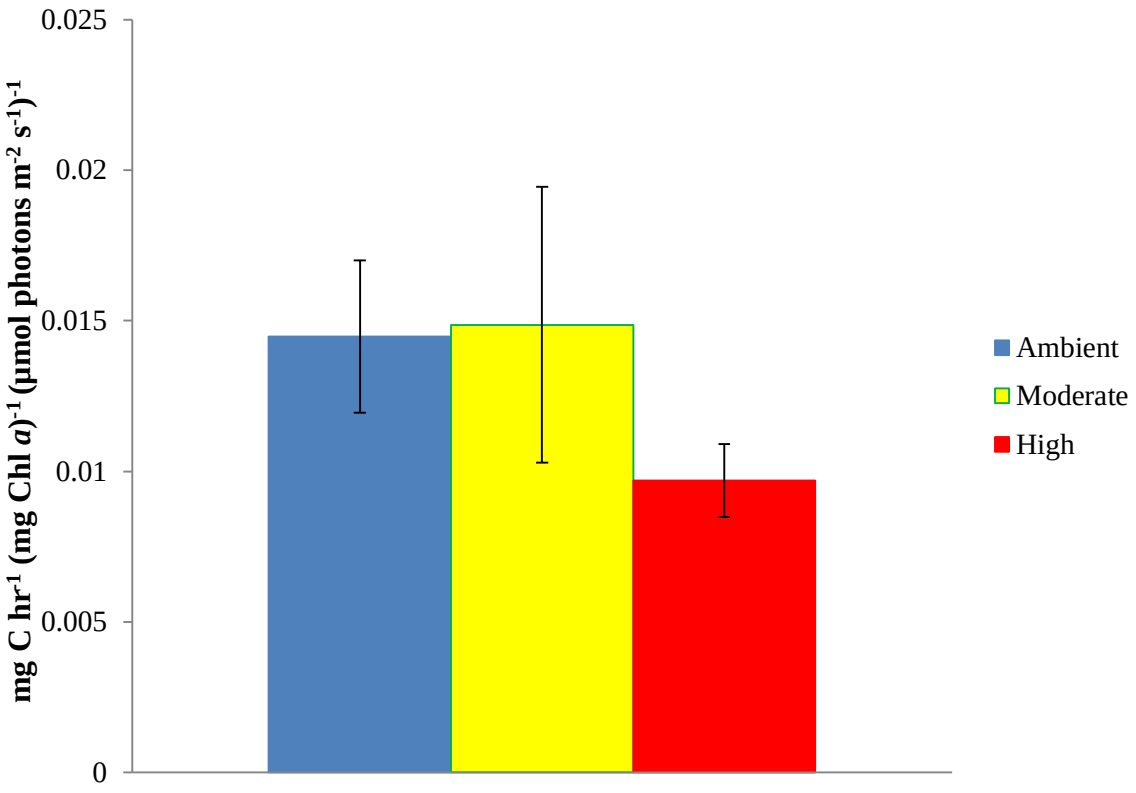


Figure 13. *Emiliania huxleyi* α normalized to cellular Chl *a* (mg C $hr^{-1}$ (mg Chl *a*)$^{-1}$ (µmol photons $m^{-2}$ $s^{-1}$)$^{-1}$) analyzed on the final day of semi-continuous experiment OA3. Error bars represent ± 1 SD.

There was also no treatment effect on the Chl *a* normalized maximum photosynthetic rate ($P_{max}$) for *E. huxleyi*. Chlorophyll *a* normalized $P_{max}$ ranged from 2.101 ± 0.693 in the Ambient treatment, 2.277 ± 0.566 in the Moderate, and 1.491 ± 0.397 in the High treatment (mg C (mg Chl *a*)$^{-1}$ hr$^{-1}$) with no significant treatment effect (Figure 14; $p = 0.277$; $\alpha = 0.05$).

## MICROZOOPLANKTON GRAZING

### Cell Ingestion Rate

The number of cells ingested by each microzooplankton grazer was quantified at the three time points. This allowed for ingestion rates to be calculated at $T_1$ and $T_2$. By the third time point, quantification of *E. huxleyi* within the grazers' food vacuoles had become difficult for a portion of the population, indicating that food vacuoles were beginning to fill. Additionally, optimal diet ingestion rates are similar to those seen in preliminary experiments, meaning that the grazers were unaffected by pre-experiment starvation and sieving (Table 8). Short-term ingestion rates for all three microzooplankton grazers were significantly higher on *E. huxleyi* grown in elevated $pCO_2$ (Table 8). *Eutintinnus* sp. ingestion rate at $T_1$ (15 min) was significantly greater on *E. huxleyi* cells grown in the High $pCO_2$ treatment (0.26 ± 0.04 cells grazer$^{-1}$ min$^{-1}$) compared to ingestion on cells grown in Ambient (0.18 ± 0.03 cells grazer$^{-1}$ min$^{-1}$) and Moderate (0.18 ± 0.03 cells grazer$^{-1}$ min$^{-1}$) treatments (Figure 15; $p = 0.037$; ANOVA, $\alpha = 0.05$; Tukey's post hoc analysis). *F. taraikaensis* ingestion rates at $T_1$ (15 min) were also significantly higher on *E. huxleyi* cells grown in High $pCO_2$ (0.35 ± 0.05 cells grazer$^{-1}$ min$^{-1}$) compared to the Ambient (0.22 ± 0.01 cells grazer$^{-1}$ min$^{-1}$) treatment, while ingestion rates on cells grown in the Moderate (0.27 ± 0.06 cells grazer$^{-1}$ min$^{-1}$) were not significantly different from Ambient or High treatments (Figure 16; $p = 0.034$; ANOVA, $\alpha = 0.05$; Tukey's post hoc analysis). Similarly, there was a significant stepwise increase in ingestion rates at $T_1$ (30 min) for *O. marina* from the Ambient to High $pCO_2$ treatments.

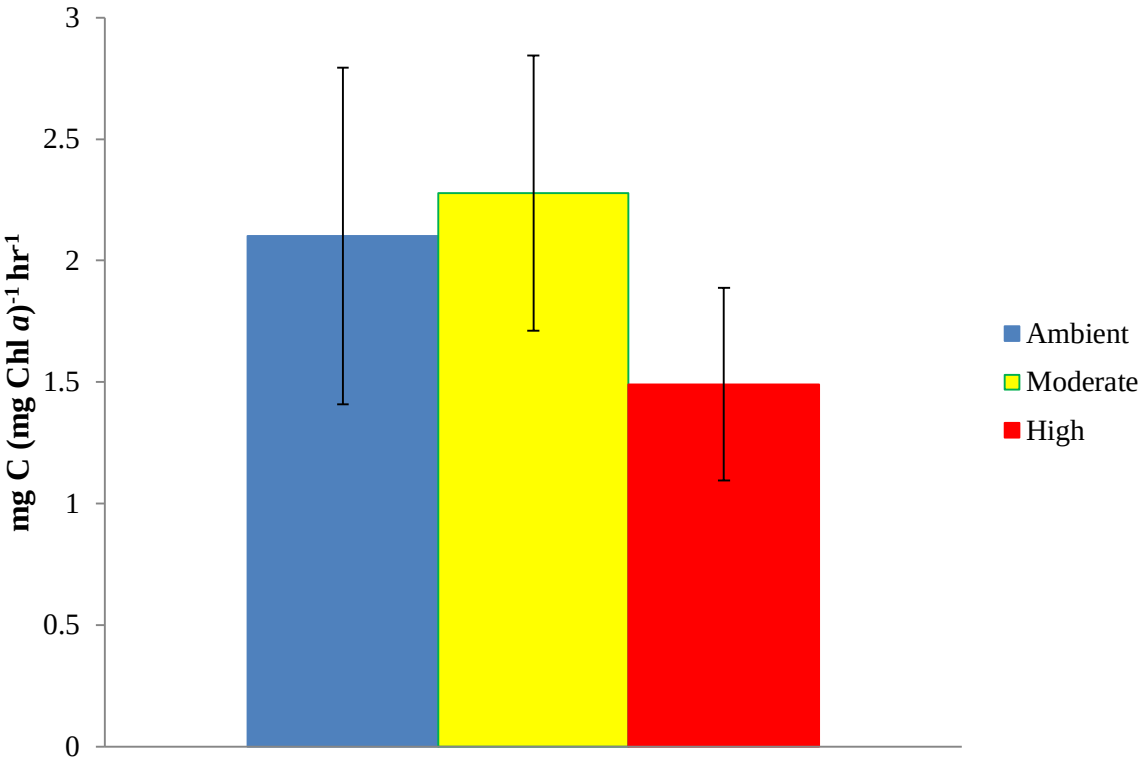


Figure 14. *Emiliania huxleyi* $P_{max}$ normalized to cellular chlorophyll *a* (mg C (mg chl $a^{-1}$) $hr^{-1}$) analyzed on the final day of semi-continuous experiment OA3. Error bars represent ± 1 SD.

Table 8. Microzooplankton ingestion rates (cells grazer$^{-1}$ min$^{-1}$ ± 1 SD) on *E. huxleyi* grown in Ambient, Moderate, and High $pCO_2$ treatment conditions. Bold font indicates a significant treatment effect (ANOVA, $\alpha = 0.05$), and letters (a, b, c) denote treatments which are significantly different from each other (shared letters indicate no significant difference; Tukey's post hoc analysis, excludes Optimal Diet).

| Grazer | Time Point | Ambient | Moderate | High | Optimal Diet | p value |
|---|---|---|---|---|---|---|
| *Eutintinnus sp.* | **T1 (15 min)** | **0.18 ± 0.03$_a$** | **0.18 ± 0.03$_a$** | **0.26 ± 0.04$_b$** | 0.19 ± 0.05 | **0.037** |
| | T2 (30 min) | 0.11 ± 0.06 | 0.27 ± 0.05 | 0.28 ± 0.15 | 0.09 ± 0.08 | |
| | T3 (45 min) | 0.07 ± 0.04 | 0.07 ± 0.11 | 0.10 ± 0.08 | 0.09 ± 0.02 | |
| *Favella taraikaensis* | **T1 (15 min)** | **0.22 ± 0.01$_a$** | **0.27 ± 0.06$_{a,b}$** | **0.35 ± 0.05$_b$** | 0.23 ± 0.02 | **0.034** |
| | T2 (30 min) | 0.24 ± 0.02 | 0.10 ± 0.05 | 0.09 ± 0.07 | 0.05 ± 0.09 | |
| | T3 (45 min) | 0.10 ± 0.03 | 0.12 ± 0.001 | 0.01 ± 0.06 | -- | |
| *Oxyrrhis marina* | **T1 (30 min)** | **0.05 ± 0.01$_a$** | **0.07 ± 0.002$_b$** | **0.08 ± 0.003$_c$** | 0.04 ± 0.002 | **<0.001** |
| | T2 (60 min) | 0.05 ± 0.002 | 0.05 ± 0.009 | 0.05 ± 0.009 | 0.12 ± 0.09 | |
| | T3 (90 min) | 0.04 ± 0.01 | 0.04 ± 0.013 | 0.04 ± 0.003 | -- | |

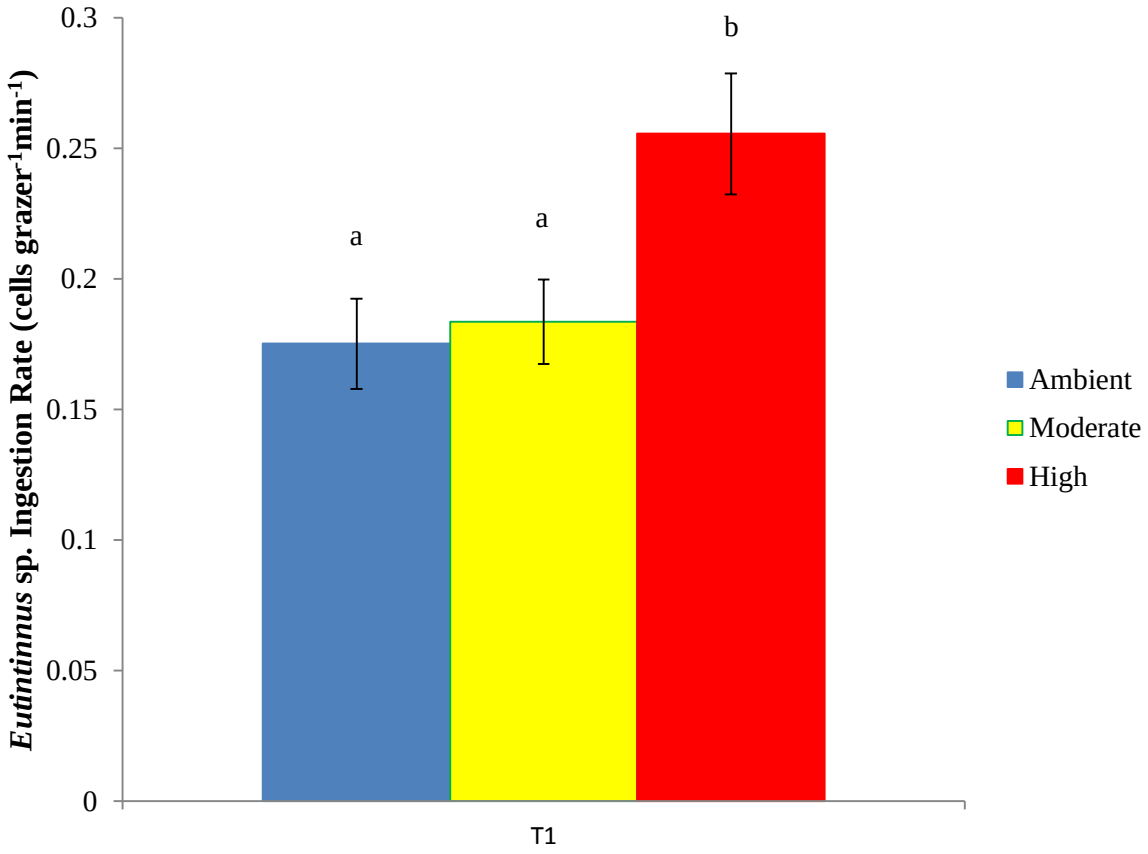


Figure 15. *Eutintinnus* sp. ingestion rate (cells grazer$^{-1}$ min$^{-1}$) on *Emiliania huxleyi* at time point $T_1$ (15 min). *E. huxleyi* was pre-acclimated to Ambient, Moderate, and High treatments. Letters over bars show significant differences across treatments within each experiment; bars with shared letters represent treatments that were not statistically different (Tukey's post hoc analysis). Refer to Table 8 for data and p values. Error bars represent ± 1 SD.

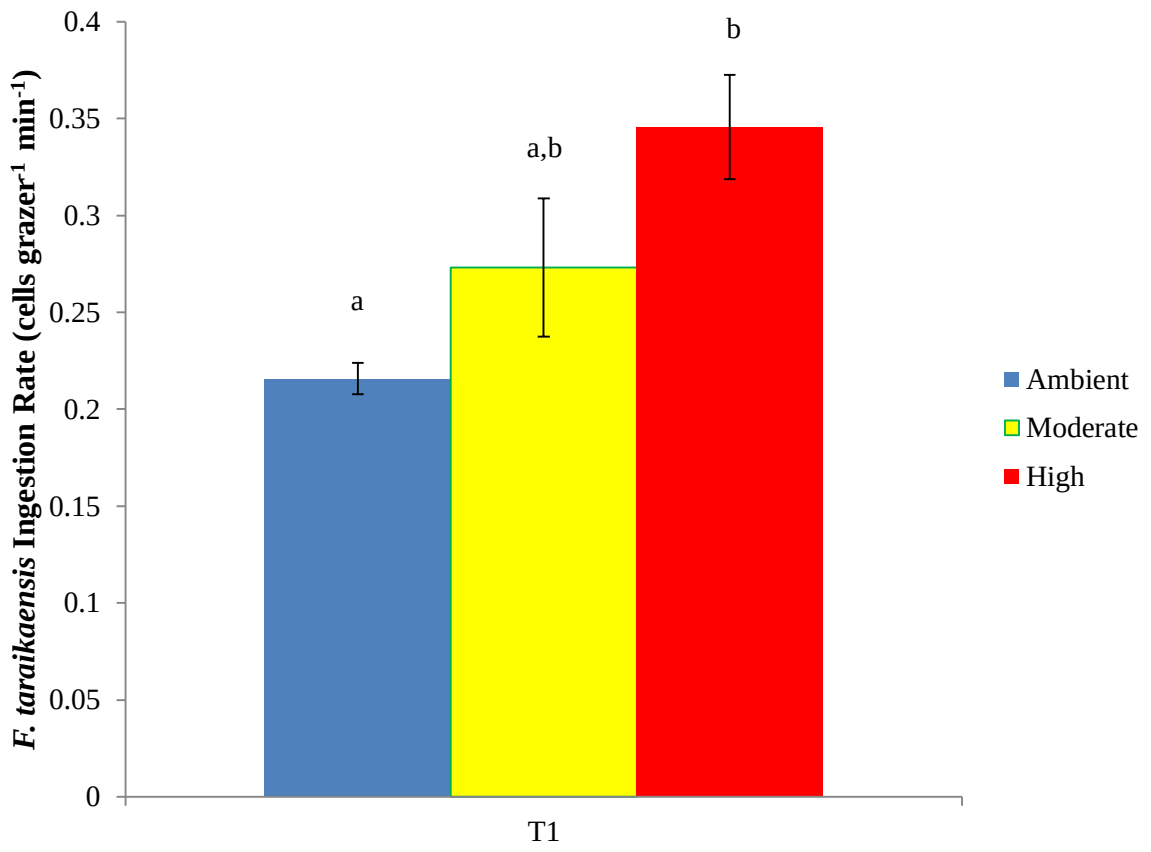


Figure 16. *Favella taraikaensis* ingestion rate (cells grazer$^{-1}$ min$^{-1}$) on *Emiliania huxleyi* at time point $T_1$ (15 min). *E. huxleyi* was pre-acclimated to Ambient, Moderate, and High treatments. Letters over bars show significant differences across treatments within each experiment; bars with shared letters represent treatments that were not statistically different (Tukey's post hoc analysis). Refer to Table 8 for data and p values. Error bars represent ± 1 SD.

Ingestion rates were 0.05 ± 0.01, 0.07 ± 0.002, and 0.08 ± 0.003 cells grazer$^{-1}$ min$^{-1}$ for Ambient, Moderate, and High treatments, respectively, with each treatment being significantly greater than the preceding treatment (Figure 17; $p < 0.001$; ANOVA, $\alpha = 0.05$; Tukey's post hoc analysis).

**Biovolume Ingestion Rate**

Ingestion rates for each grazer were normalized to *E. huxleyi* cell biovolume. Normalizing ingestion rates to biovolume ingested allows for assessment of the potential impact of cell biovolume on the initial ingestion rate of the grazers. It also allows me to distinguish between the volume of *E. huxleyi* ingested vs. the number of cells ingested. Short-term biovolume ingestion rates for all three microzooplankton were higher at $T_1$ on *E. huxleyi* grown under elevated $pCO_2$ conditions (Table 9). *Eutintinnus* sp. biovolume ingestion rate at $T_1$ (15 min) was significantly higher on *E. huxleyi* grown in the High (53.7 ± 8.43 µm$^3$ grazer$^{-1}$ min$^{-1}$) treatment than in the Ambient (26.8 ± 4.57 µm$^3$ grazer$^{-1}$ min$^{-1}$) or Moderate (34.4 ± 5.26 µm$^3$ grazer$^{-1}$ min$^{-1}$) treatments (Figure 18; $p = 0.005$, $\alpha = 0.05$). *F. taraikaensis* biovolume ingestion rates at $T_1$ (15 min) were significantly higher on cells grown in the High (73.44 ± 9.86 µm$^3$ grazer$^{-1}$ min$^{-1}$) treatment compared to ingestion rates on cells grown in the Ambient (38.5 ± 2.46 µm$^3$ grazer$^{-1}$ min$^{-1}$) treatment (Figure 19; $p = 0.009$; $\alpha = 0.05$). However, biovolume ingestion rates in the Moderate treatment (52.28 ± 11.79 µm$^3$ grazer$^{-1}$ min$^{-1}$) were not significantly different from Ambient or High treatments (Tukey's post hoc analysis). *O. marina* biovolume ingestion rates at $T_1$ (30 min) also showed a significant stepwise increase from cells grown in Ambient (8.94 ± 0.39 µm$^3$ grazer$^{-1}$ min$^{-1}$), to Moderate (12.91 ± 0.35 µm$^3$ grazer$^{-1}$ min$^{-1}$), to High $pCO_2$ treatments (16.89 ± 0.55 µm$^3$ grazer$^{-1}$ min$^{-1}$) (Figure 20; $p < 0.001$, $\alpha = 0.05$; Tukey's post hoc analysis).

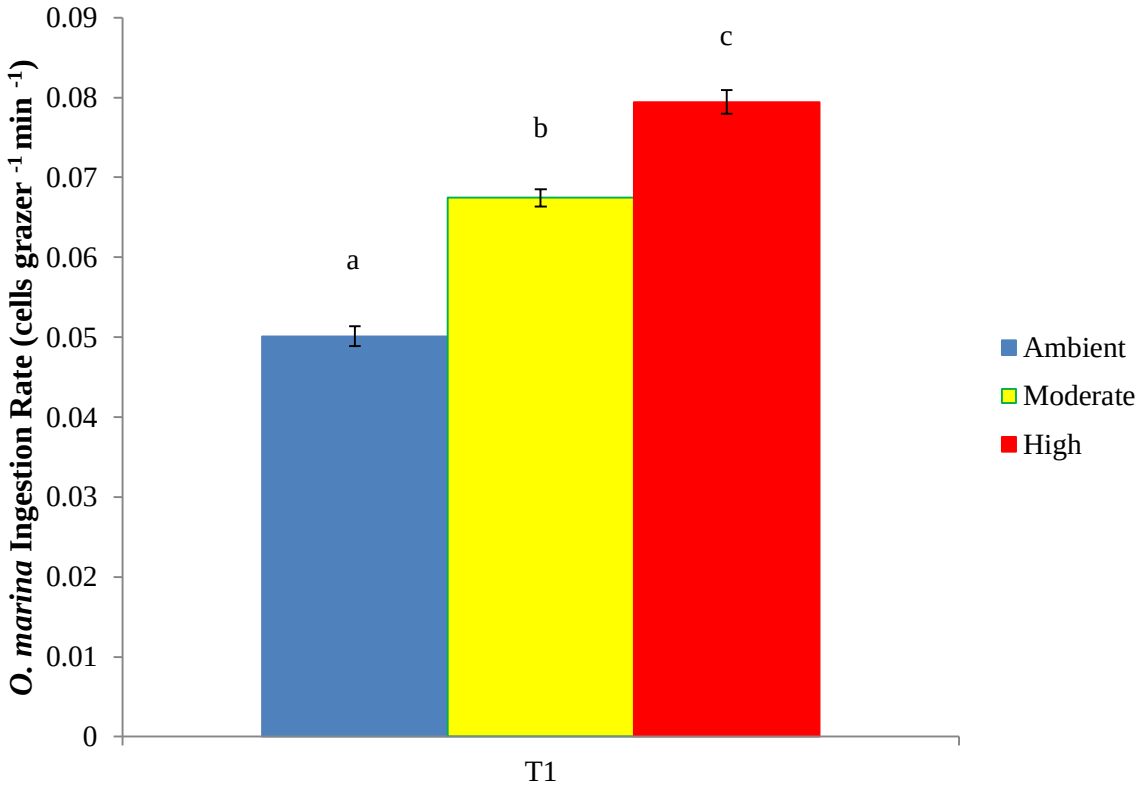


Figure 17. *Oxyrrhis marina* ingestion rate (cells grazer$^{-1}$ min$^{-1}$) on *Emiliania huxleyi* at time point $T_1$ (30 min). Letters over bars show significant differences across treatments within each experiment; bars with shared letters represent treatments that were not statistically different (Tukey's post hoc analysis). Refer to Table 8 for data and p values. Error bars represent ± 1 SD.

Table 9. Microzooplankton biovolume ingestion rates ($\mu m^3$ $grazer^{-1}$ $min^{-1}$ ± 1 SD) on *E. huxleyi* grown in Ambient, Moderate, and High $pCO_2$ treatment conditions. Bold and font indicates a significant treatment effect (ANOVA, $\alpha = 0.05$), and letters (a, b, c) denote treatments which are significantly different from each other (shared letters indicate no significant difference; Tukey's post hoc analysis).

| Grazer | Time Point | Ambient | Moderate | High | p value |
|---|---|---|---|---|---|
| *Eutintinnus* sp. | **T1 (15 min)** | **$26.8 \pm 4.57_a$** | **$34.4 \pm 5.26_a$** | **$53.7 \pm 8.43_b$** | **0.005** |
| | T2 (30 min) | 17.0 ± 9.59 | 50.3 ± 4.25 | 59.2 ± 31.3 | |
| | T3 (45 min) | 11.1 ± 6.13 | 12.9 ± 21.55 | 20.4 ± 15.99 | |
| *Favella taraikaensis* | **T1 (15 min)** | **$38.5 \pm 2.46_a$** | **$52.28 \pm 11.79_{ab}$** | **$73.44 \pm 9.86_b$** | **0.009** |
| | T2 (30 min) | 42.9 ± 3.90 | 19.91 ± 10.25 | 19.22 ± 15.38 | |
| | T3 (45 min) | 17.92 ± 4.79 | 23.08 ± 0.09 | 21.07 ± 13.49 | |
| *Oxyrrhis marina* | **T1 (30 min)** | **$8.94 \pm 0.39_a$** | **$12.91 \pm 0.35_b$** | **$16.89 \pm 0.55_c$** | **<0.001** |
| | T2 (60 min) | 8.77 ± 0.55 | 9.57 ± 1.76 | 10.18 ± 1.84 | |
| | T3 (90 min) | 7.17 ± 1.81 | 8.23 ± 2.47 | 8.24 ± 0.67 | |

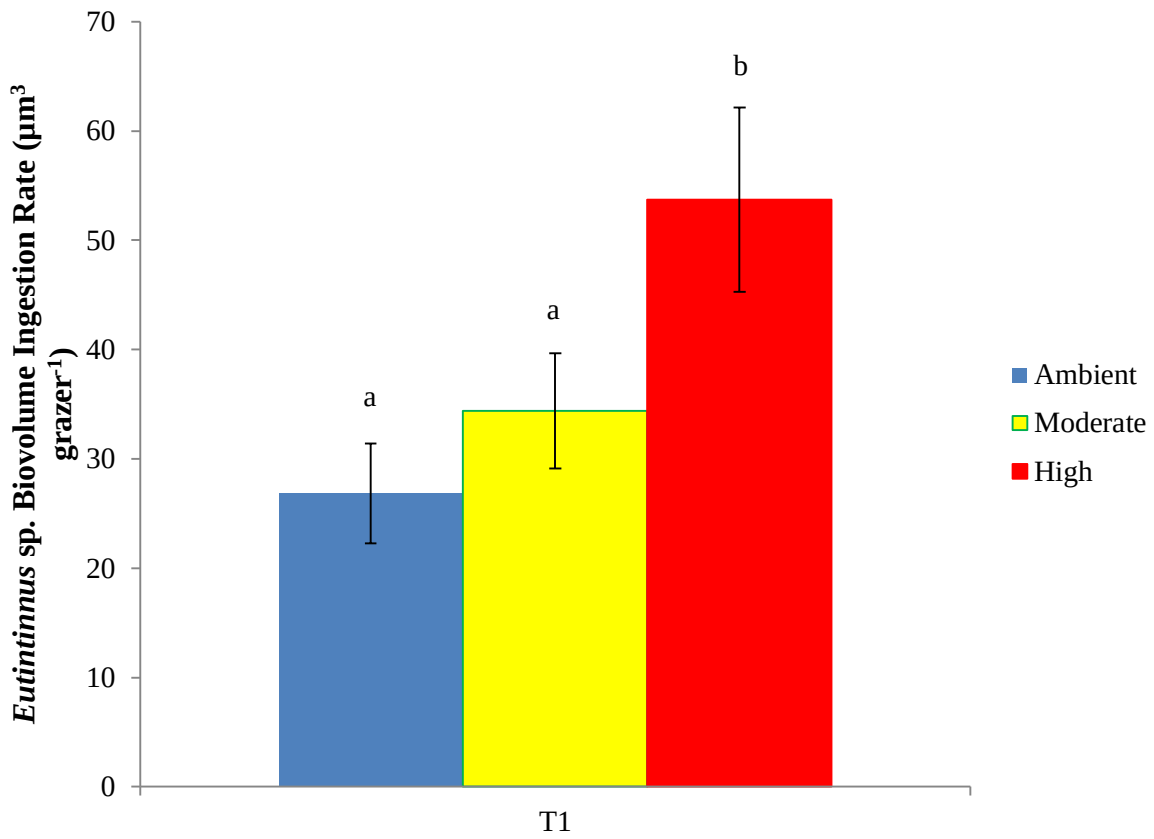


Figure 18. *Eutintinnus* sp. biovolume ingestion rate ($\mu m^3$ $grazer^{-1}$ $min^{-1}$) on *E. huxleyi* at time point $T_1$ (15 min). *E. huxleyi* was pre-acclimated to Ambient, Moderate, and High $pCO_2$ treatments. Letters over bars indicate significant differences across treatments within each experiment; bars with shared letters represent treatments that were not statistically different (Tukey's post hoc analysis). Refer to Table 9 for data and p values. Error bars represent ± 1 SD.

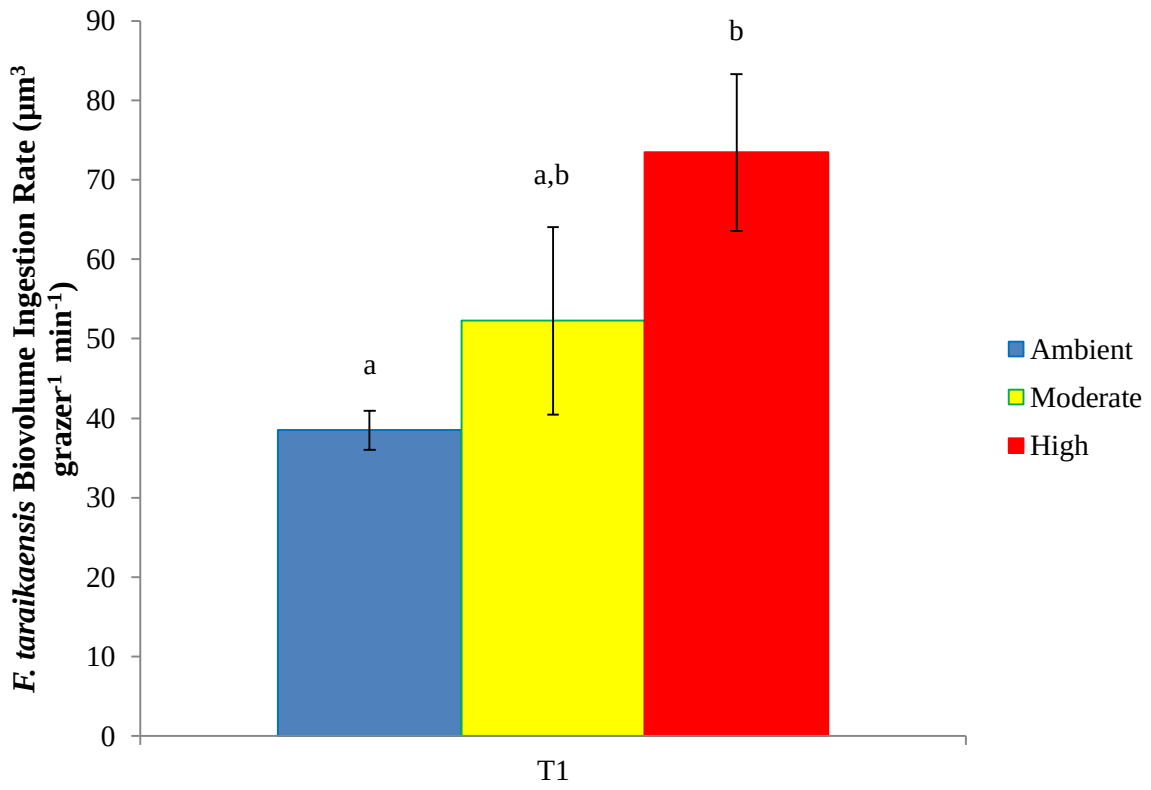


Figure 19. *Favella taraikaensis* biovolume ingestion rate (µm$^3$ grazer$^{-1}$ min$^{-1}$) on *E. huxleyi* at time point $T_1$ (15 min). *E. huxleyi* was pre-acclimated to Ambient, Moderate, and High $pCO_2$ treatments. Letters over bars indicate significant differences across treatments within each experiment; bars with shared letters represent treatments that were not statistically different (Tukey's post hoc analysis). Refer to Table 9 for data and p values. Error bars represent ± 1 SD.

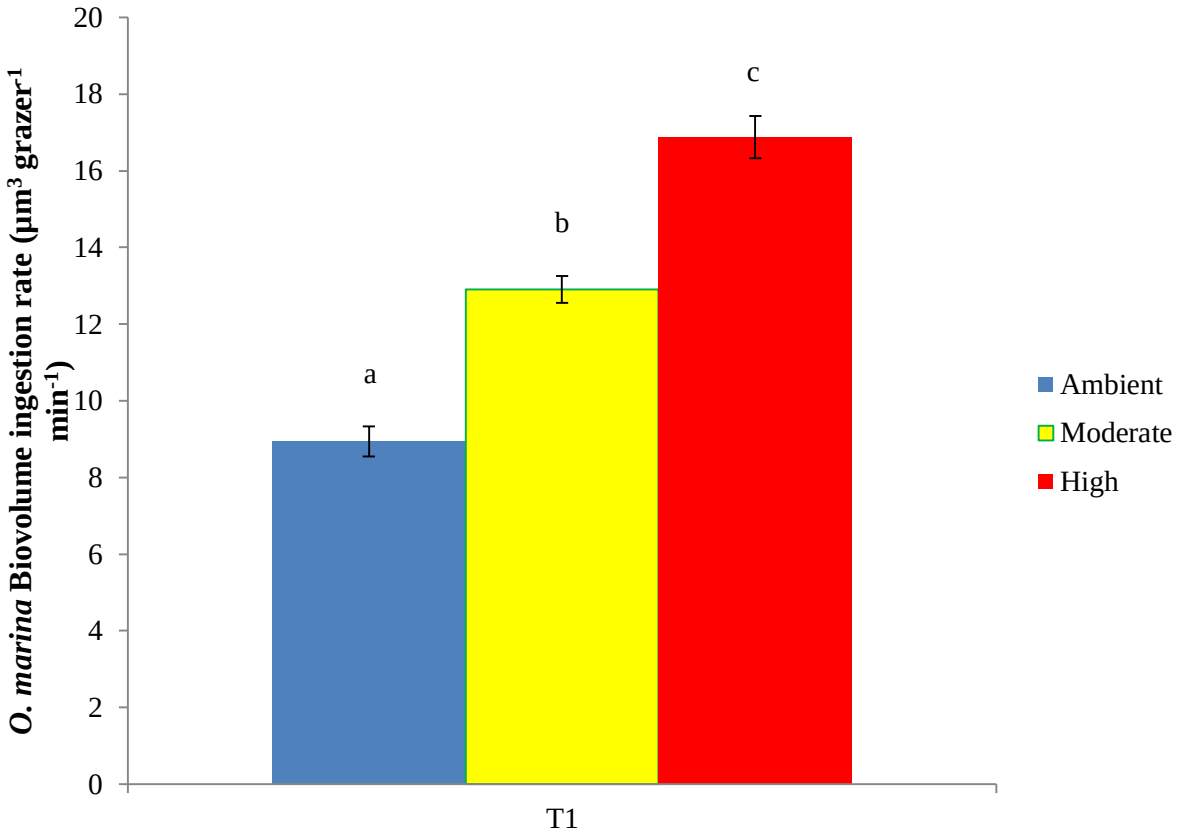


Figure 20. *Oxyrrhis marina* biovolume ingestion rate ($\mu m^3$ $grazer^{-1}$ $min^{-1}$) on *E. huxleyi* at time point $T_1$ (30 min). *E. huxleyi* was pre-acclimated to Ambient, Moderate, and High $pCO_2$ treatments. Letters over bars indicate significant differences across treatments within each experiment; bars with shared letters represent treatments that were not statistically different (Tukey's post hoc analysis). Refer to Table 9 for data and p values. Error bars represent ± 1 SD.

## Percent Population Feeding

For all three grazers, the portion of the population feeding on treatment conditions was similar to the portion feeding in optimal diet controls. This suggests that the grazers were unaffected by pre-experiment starvation and the changes seen in grazing rates on *E. huxleyi* is due to a treatment effect. The portion of the microzooplankton population feeding was significantly affected by *E. huxleyi* $pCO_2$ treatment conditions (Table 10). *Eutintinnus* sp. showed a step-wise increase in percent population feeding at $T_1$ with increasing $pCO_2$. The percentage of the *Eutintinnus* sp. population feeding on High treatment *E. huxleyi* (69 ± 2%) was higher than on Moderate *E. huxleyi* (59 ± 9%), which was also higher than percent population feeding on Ambient grown *E. huxleyi* (53 ± 3%) (Figure 21; $p = 0.042$; $\alpha = 0.05$). *F. taraikaensis* percent population feeding at $T_1$ was greater on cells grown in the High treatment (76 ± 2%) than in the Moderate (63 ± 1%) and Ambient (58 ± 6%) treatments (Figure 22; $p = 0.002$; $\alpha = 0.05$). *O. marina* also showed higher percent population feeding on *E. huxleyi* grown in elevated $pCO_2$ at $T_1$ (Figure 23). At $T_1$, percent feeding was not significantly different between the Moderate (82 ± 1.5%) and High (84 ± 1%) treatments, while both the Moderate and High treatments showed significantly higher percent population feeding than in the Ambient treatment (71 ± 0%) ($p < 0.001$; $\alpha = 0.05$).

## Multiple Linear Regression Model

The *E.huxleyi* OA responses examined here were used in a Multiple Linear Regression Model (MLR) to explore which factors explained the variation in microzooplankton short-term ingestion rates. Initial model variables included cell size ($\mu m^3$), POC $cell^{-1}$, PON $cell^{-1}$, PIC $cell^{-1}$, Chl *a* $cell^{-1}$, and carbohydrate $cell^{-1}$. The MLRs, paired with Pearson Correlation Matrices, showed that cell size was the variable that contributed the most to the variation in microzooplankton grazing. Cell size explained 98%, 67%, and 91% of the variation for *Eutintinnus* sp., *F. taraikaensis*, and *O. marina*, respectively. The regression equations for each grazer can be found in Table 11, and Figures 24-26.

Table 10. Microzooplankton percent population feeding on *E. huxleyi* grown in Ambient, Moderate, and High $pCO_2$ treatment conditions. Bold font indicates a significant treatment effect (ANOVA, $\alpha = 0.05$), and letters (a, b, c) denote treatments which are significantly different from each other (shared letters indicate no significant difference; Tukey's post hoc analysis).

| Grazer | Time Point | Ambient | Moderate | High | Optimal Diet | p value |
|---|---|---|---|---|---|---|
| *Eutintinnus sp.* | **T1 (15 min)** | **$53 \pm 3_a$** | **$59 \pm 9_{a,b}$** | **$69 \pm 2_b$** | 62 ± 3 | **0.042** |
| | T2 (30 min) | 59 ± 8 | 76 ± 11 | 84 ± 12 | 63 ± 6 | |
| | T3 (45 min) | 62 ± 2 | 79 ± 8 | 85 ± 5 | 77 ± 6 | |
| *Favella taraikaensis* | **T1 (15 min)** | **$58 \pm 6_a$** | **$63 \pm 1_a$** | **$76 \pm 2_b$** | 71 ± 6 | **0.002** |
| | T2 (30 min) | 68 ± 3 | 66 ± 2 | 76 ± 4 | 75 ± 4 | |
| | T3 (45 min) | 76 ± 3 | 73 ± 7 | 75 ± 3 | 80 ± 6 | |
| *Oxyrrhis marina* | **T1 (15 min)** | **$71 \pm 0_a$** | **$82 \pm 1.5_b$** | **$84 \pm 1_b$** | 69 ± 4 | **<0.001** |
| | T2 (30 min) | 89 ± 1 | 93 ± 2 | 95 ± 2 | 75 ± 4 | |
| | T3 (45 min) | 96 ± 1 | 100 ± 0 | 99 ± 0 | 80 ± 6 | |

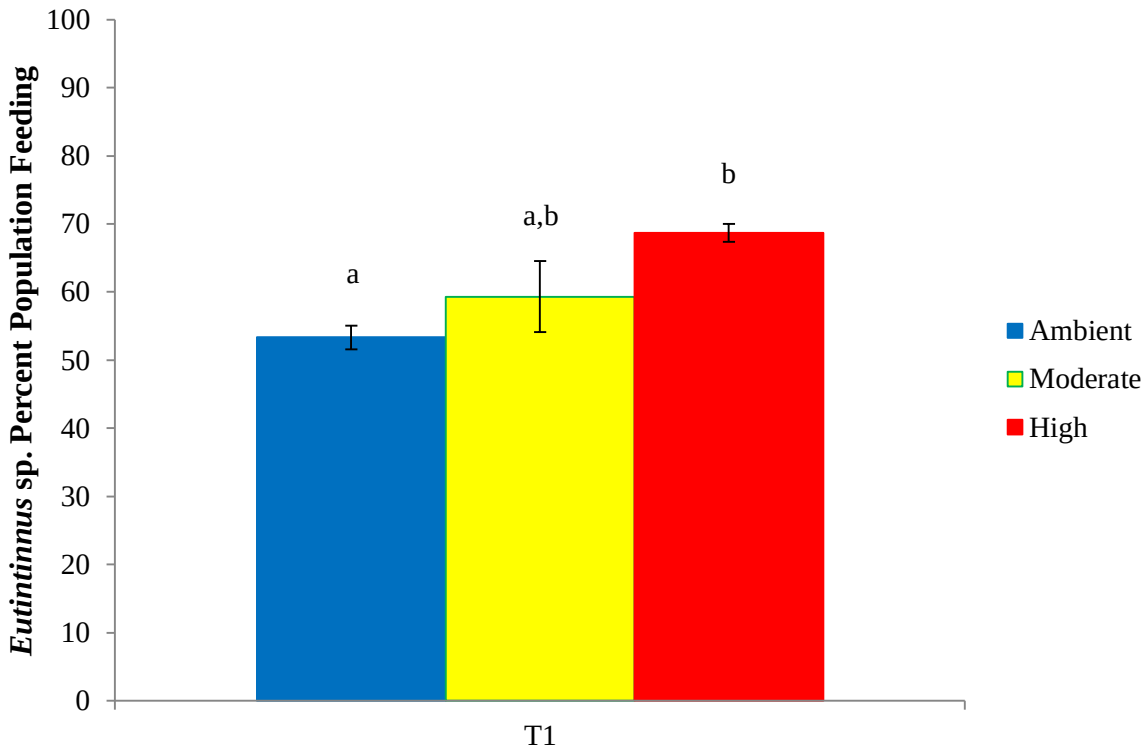


Figure 21. *Eutintinnus* sp. percent population feeding on *E. huxleyi* at time point $T_1$ (15 min). *E. huxleyi* was pre-acclimated to Ambient, Moderate, and High $pCO_2$ treatments. Letters over bars indicate significant differences across treatments within each experiment; bars with shared letters represent treatments that were not statistically different (Tukey's post hoc analysis). Refer to Table 10 for data and p values. Error bars represent ± 1 SD.

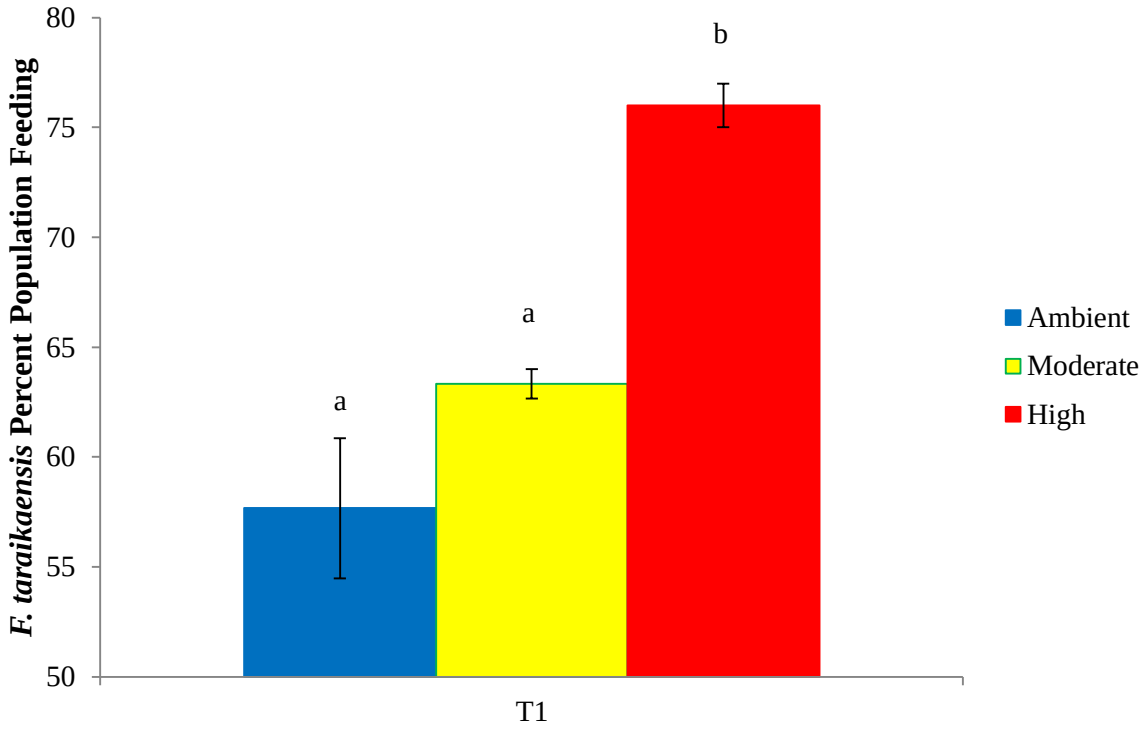


Figure 22. *Favella taraikaensis* percent population feeding on *E. huxleyi* at time point $T_1$ (15 min). *E. huxleyi* was pre-acclimated to Ambient, Moderate, and High $pCO_2$ treatments. Letters over bars show significant differences across treatments within each experiment; bars with shared letters represent treatments that were not statistically different (Tukey's post hoc analysis). Refer to Table 10 for data and p values. Error bars represent ± 1 SD.

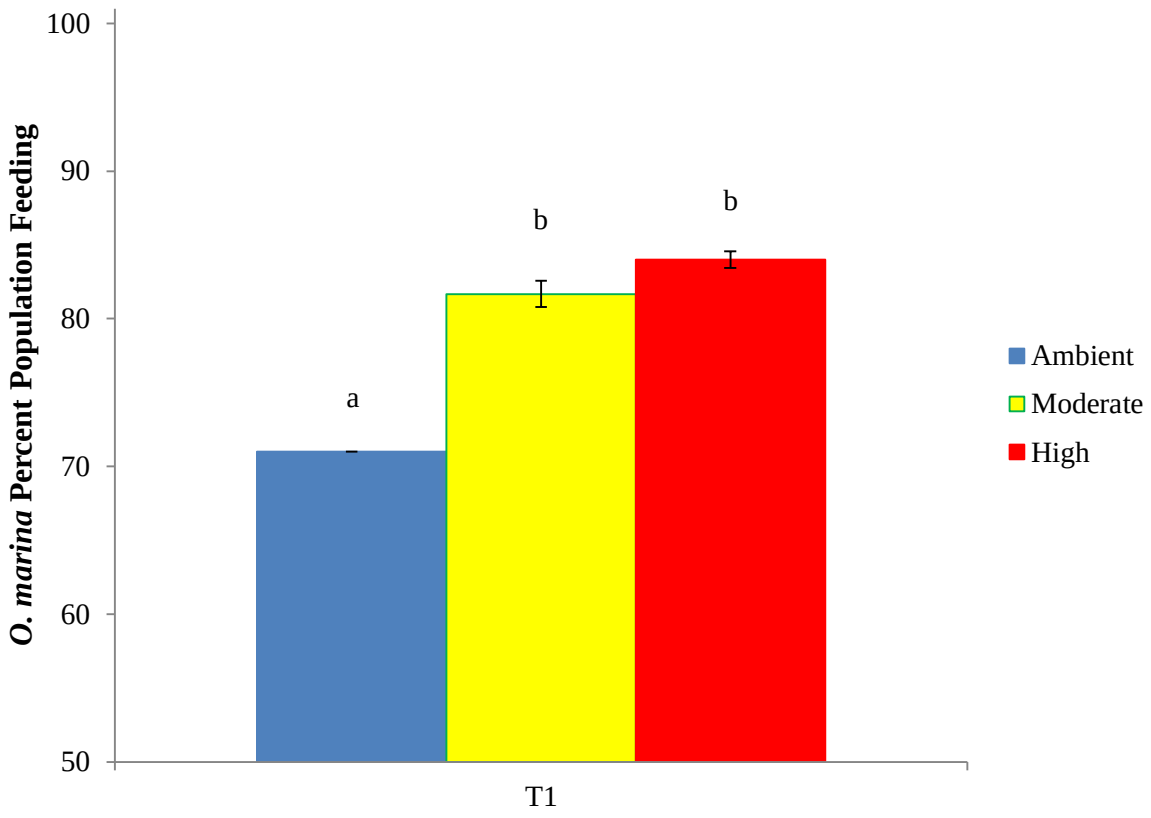


Figure 23. *Oxyrrhis marina* percent population feeding on *E. huxleyi* at time point $T_1$ (30 min). *E. huxleyi* was pre-acclimated to Ambient, Moderate, and High $pCO_2$ treatments. Letters over bars show significant differences across treatments within each experiment; bars with shared letters represent treatments that were not statistically different (Tukey's post hoc analysis). Refer to Table 10 for data and p values. Error bars represent ± 1 SD.

Table 11. Multiple linear regression model eliminated all but a single variable predicting short-term ingestion rates. The regression model used biochemical and physiological predictive variables associated with $pCO_2$ induced changes in *E. huxleyi* during OA1-OA2a/b. For each grazer, cell size was the only predictive factor that explained variation in short-term ingestion rates.

| | Predictive Factors | Regression Equation | $R^2$ | p value |
|---|---|---|---|---|
| *Eutintinnus sp.* | Cell size | $y = (0.016)\ x_1 - 0.868$ | 0.978 | < 0.001 |
| *Favella taraikaensis* | Cell size | $y = (0.004)\ x_1 - 0.452$ | 0.672 | 0.007 |
| *Oxyrrhis marina* | Cell size | $y = (0.021)\ x_1 - 1.010$ | 0.909 | 0.001 |

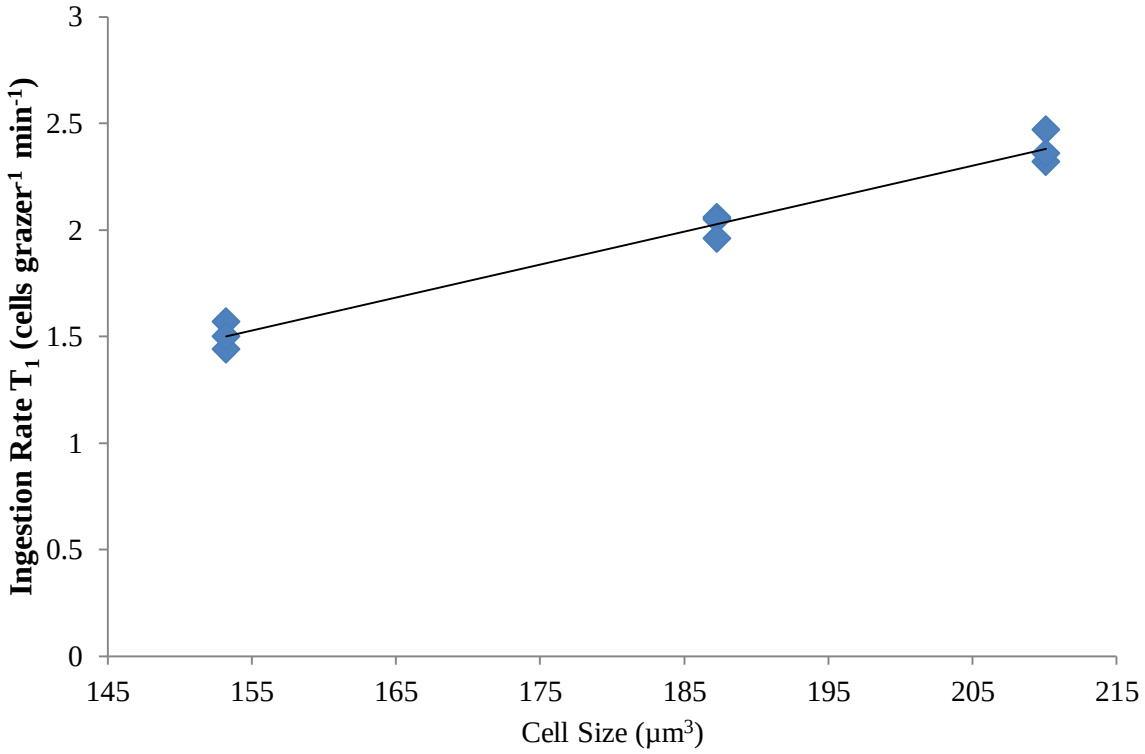


Figure 24. Data points represent triplicate ingestion rates for *Eutintinnus* sp. at $T_1$ plotted against *Emiliania huxleyi* size. Regression line corresponds to the equation predicted by the Multiple Linear Regression Model (Table 11).

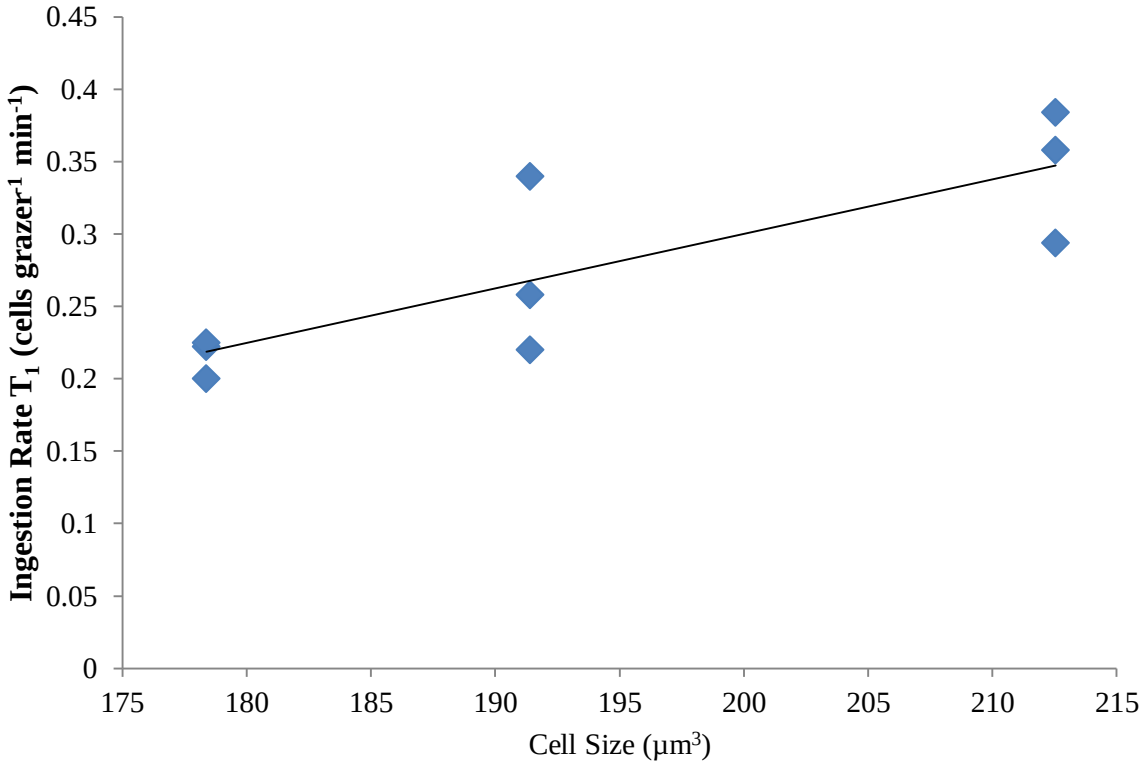


Figure 25. Data points represent triplicate ingestion rates for *Favella taraikaensis* at $T_1$ plotted against *Emiliania huxleyi* size. Regression line corresponds to the equation predicted by the Multiple Linear Regression Model (Table 11).

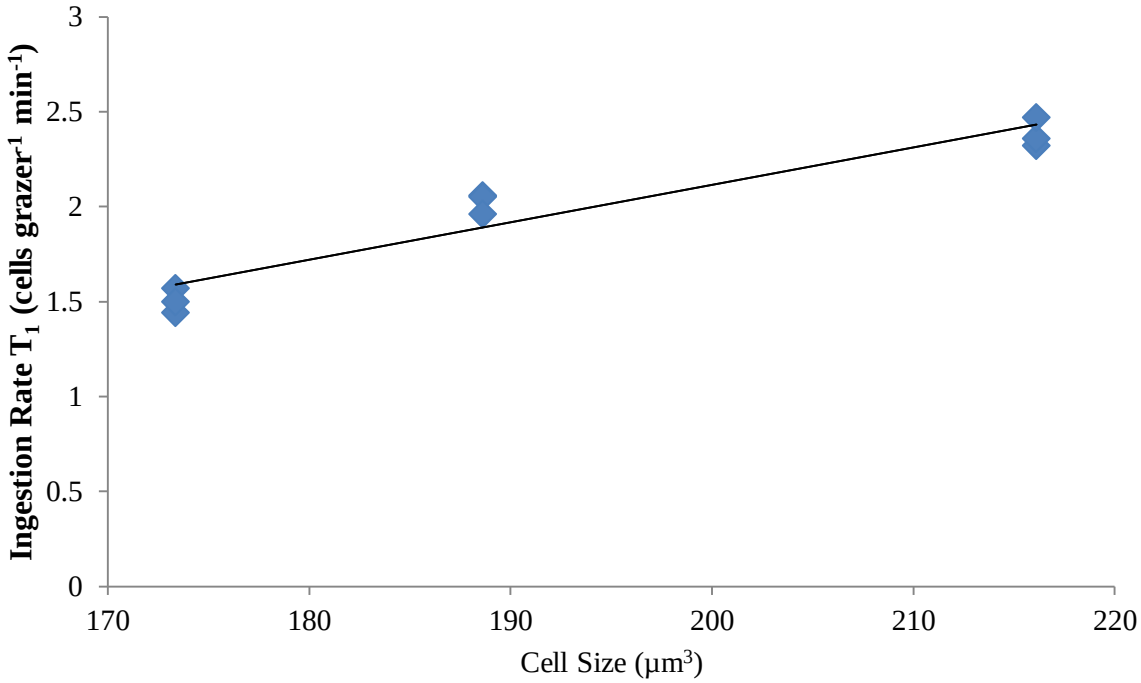


Figure 26. Data points represent triplicate ingestion rates for *Oxyrrhis marina* at $T_1$ plotted against *Emiliania huxleyi* size. Regression line corresponds to the equation predicted by the Multiple Linear Regression Model (Table 11).

# DISCUSSION

## Overview

In this study, I observed that $pCO_2$-induced changes in phytoplankton resulted in increased short-term grazing and the percentage of the microzooplankton population that were feeding for all three of the grazer species explored. Depending on how robust these findings are, several important ecological questions arise: How will the indirect effects of ocean acidification observed in microzooplankton grazing affect marine planktonic food webs, and how prevalent will those changes in feeding be among microzooplankton ocean-wide? Are the observed changes in *E. huxleyi* state under elevated $pCO_2$ consistent with other phytoplankton taxa? If so, what are the global biogeochemical impacts of altered coupling between microzooplankton grazing and their prey? In order to answer these questions, it is necessary to first understand which $pCO_2$ related effects on phytoplankton induced the microzooplankton feeding response observed in this study, and how prevalent those changes might be for phytoplankton and microzooplankton in the future ocean.

## Indirect Effects on Microzooplankton

My data show that microzooplankton grazing is strongly affected by the influence of OA on their prey. In the current study, microzooplankton short-term ingestion rates and percent population feeding increased consistently across all three species feeding on *E. huxleyi* diets grown under elevated $pCO_2$ (Table 7 & 9). *E. huxleyi* grown in the High $pCO_2$ treatment were always grazed 1.5 times faster and by 10- 20% more of the grazer population than *E. huxleyi* grown in the Ambient $pCO_2$ treatment. This finding was consistent on a $cell^{-1}$ and biovolume-normalized basis (Table 7 & 8). More strikingly, the finding was consistent between both ciliates and the dinoflagellate, despite their different feeding strategies. Both microzooplankton functional groups are acutely sensitive to the condition of their prey and can be very selective according to prey cell size (Andersson et al. 1986;

Jonsson 1986; Verity and Villareal 1986; Simek and Chrzanowski 1992; Boenigk et al. 2001; Calbet et al. 2001), food quality (Verity and Villareal 1986; Verity 1988; Anderson and Pondaven 2003; Barofsky et al. 2010), and chemical signatures (Levandowski and Hauser 1978; Meunier et al. 2011; Montagnes et al. 2011), which might account for the consistency found between the different grazer types. Given how sensitive microzooplankton are to changes in their prey, and the observation found here that microzooplankton grazing increased on phytoplankton grown in elevated $pCO_2$, the question remains: what $pCO_2$- induced changes in *E. huxleyi* are causing increased grazing rates in the three microzooplankton grazers used in this study?

The first aspect to explore is how these microzooplankton might be sensitive to $pCO_2$ induced changes in chemical signaling of their phytoplankton prey. Verity (1988) found that certain ciliates were chemically attracted to phytoplankton. The ciliates were able to seek prey hotspots, i.e. locations where prey abundance was high, by detecting chemical cues and altering swimming behavior to remain in the prey hotspots. Further, the physiological state of the prey had a strong influence on the ciliates' grazing behavior. Those phytoplankton cultures that had reached stationary phase were less attractive to the ciliates, which were less likely to remain within hotspots. Dinoflagellate grazing can also be very dependent on prey food quality (Levandowski and Hauser 1978; Meunier et al. 2011). Meunier et al. (2011) found that *O. marina* is able to selectively feed on prey whose C:N and C:P ratio is most complementary to their own cellular stoichiometry in an effort to ingest prey that are rich in nutrients that the grazer may be lacking.

Another aspect to explore is the impact of $pCO_2$ induced changes in prey size on microzooplankton grazing. Many microzooplankton are tightly constrained by the range of prey sizes they can consume (Tillmann 2004). Those constraints are largely based in the grazer's own cell size, morphology, and feeding behavior (Jeong et al. 2010). Organisms that engulf or ingest their prey whole typically have a much smaller range of available prey sizes than those that palium-feed or use a

feeding appendage to latch onto prey cells and siphon out cellular organic matter without engulfment. Jonsson (1986) found that many loricate ciliates selectively feed on a narrow range of particle sizes, with the maximum diameter of the particle between 10% and 40% of the maximum cytostome diameter. Examinations of three contact-feeding nanoflagellates in laboratory experiments revealed that all three grazers preferentially ingested larger cells when given a range of prey sizes (Simek and Chrzanowski 1992). Tillmann (2004) reviewed the available literature on microzooplankton feeding behavior and found that prey cell size and shape are 1$^{st}$ order determinants of prey suitability for microzooplankton, meaning that their prey's size and shape requirements must be met before other factors can influence grazing. Additionally, 2$^{nd}$ order determinants allow microzooplankton to further narrow the window of optimal prey type beyond size and shape. These 2$^{nd}$ order determinants encompass food quality, chemosensory cues, and the physiological state of potential prey. Collectively, these determinants allow microzooplankton to select among a consortium of prey types.

Despite the significant effect of ocean acidification on *E. huxleyi* cell size, many of the additional phytoplankton characteristics that were analyzed in this study didn't change significantly, or the changes were variable over time. Under ocean acidification scenarios, *E. huxleyi* chlorophyll *a*, carbohydrate content, photosynthesis, intrinsic growth rate, particulate organic carbon and inorganic carbon content, and carbon to nitrogen ratios did not change appreciably, but several attributes did have subtle variations and trends that might have affected microzooplankton grazing. To assess which of the variables measured during the characterization experiments was linked with the significant increases in initial grazing rates seen for each microzooplankton grazer, I ran a multiple linear regression model (MLR). The MLR allowed me to determine which phytoplankton traits were responsible for the variance in short-term grazing rates. The model revealed that the variability in the biochemical characteristics measured for *E. huxleyi* did not significantly predict the trends observed in short-term ingestion rates. Instead, the majority of the increase in grazing rate was explained by

cell size after all other variables were removed from the model by stepwise comparison. *E. huxleyi* cell size explains 98% of the increased grazing rate in *Eutintinnus* sp., 67% of the increased grazing in *F. taraikaensis*, and 91% of increased grazing in *O. marina* (Table 10). As the sole predictive factor for the increase in grazing rates between *E. huxleyi* $pCO_2$ treatments, it is clear that prey cell size was a 1st order determinant for grazing in *E. huxleyi* 2668. This is in line with Tillmann's discussion of 1st and 2nd order determinants (2004), and shows that changes in prey cell size might be the most significant mechanism by which ocean acidification affects microzooplankton feeding behavior.

## Ecological Significance

What will be the scope of the microzooplankton grazing response in the future ocean? That depends on the prevalence and magnitude of phytoplankton responses in a high $CO_2$ world. If phytoplankton physiology and biochemistry are substantially altered by ocean acidification, changes in microzooplankton grazing could be widespread. Since microzooplankton consume such a large fraction of phytoplankton production (Landry and Calbet 2004), they are critical to oceanic nutrient cycling and flux of organic matter (Sherr and Sherr 1994, 2002; Strom et al. 1997). The potential impact of altered coupling between microzooplankton and their prey could therefore be important for marine planktonic food webs and biogeochemical cycling.

### Cell Size

This study looked at a single strain of *E. huxleyi* 2668 that showed increased cell size under ocean acidification scenarios without any other prominent changes in the cell. Cell size increased stepwise with elevated $pCO_2$ in all of the experiments for *E. huxleyi* 2668 (Table 4). Lefebvre et al. (2012) also found that *E. huxleyi* (CCMP 371) grows larger under high $pCO_2$, when grown in culture

with $NO_3^-$ without $NH_4^+$. The same stepwise increase was seen during characterization experiments with *Rhodomonas* sp. 755 (Figure A8; Risenhoover unpub data). This parallel response between two very different types of phytoplankton demonstrates that increased cell size, as a primary direct response to elevated $pCO_2$, could be a common response to increased $CO_2$. Cell size is not often assessed or reported for studies exploring ocean acidification effects on phytoplankton, so it is unclear how prevalent cell size changes will be for other types of phytoplankton in the future.

It is clear that for *E. huxleyi* 2668, the change in volume affected grazing in two very different groups of microzooplankton, ciliates and dinoflagellates. Despite the dissimilarity between the two functional groups, all three species of microzooplankton explored in this study showed the same grazing response to *E. huxleyi* grown in ocean acidification conditions, and cell size was the sole predictive factor explaining the variation in grazing rates in all three microzooplankton. Ciliates and heterotrophic dinoflagellates dominate the biomass in microzooplankton communities (Sherr and Sherr 1994; Vargas and Martinez 2009) and represent very different sets of feeding strategies and constraints (Jonsson 1986; Verity and Villareal 1986; Jeong et al. 2010). Both of the loricate ciliates used in this study, *Eutintinnus* sp. and *F. taraikaensis*, are much larger than the *E. huxleyi* cells they are consuming and represent two different size classes of ciliates (length: 80 μm and 150 μm; *Eutintinnus* sp. and *F. taraikaensis* respectively). As stated earlier, loricate ciliates have a very narrow window of optimal prey size (Jonsson 1986; Tillmann 2004; Jeong et al. 2010), because the lorica is a shell-like inflexible outer covering with a fixed geometry. Naked ciliates, those without lorica, are not as size-restricted as their loricate counter-parts. Due of the limitation of the lorica, the maximum predator:prey cell size ratio for loricate ciliates is 8:1 (Hansen et al. 1994), whereas the optimal prey size window occurs when the maximum diameter of the particle is 10% to 40% of the maximum cytostome diameter (Jonsson 1986).

Dinoflagellate grazing is typically much less size restricted, just as it is for naked ciliates (Smetacek 1981; Gifford 1985), because feeding strategies are varied and not limited by lorica (Heinbokel 1978; Jonsson 1986; Verity and Villareal 1986). While the optimal predator:prey size ratio for heterotrophic dinoflagellates approaches 1:1, in laboratory cultures dinoflagellates can grow on prey from 15% to 500% of their own cell size (Hansen 1992; Jakobsen and Hansen 1997; Naustvoll 2000a, 2000b; Tillmann 2004). For all three microzooplankton species, the increase in *E. huxleyi* cell size increased the predator:prey size ratio towards optimal size ratios (Table 12). For *Eutintinnus* sp., the increase in *E. huxleyi* cell size shifts the prey size window from 33% to 36% of the maximum cytostome diameter, while for *F. taraikaensis*, the increase in *E. huxleyi* cell size shifts the window from 15% to 16% (Table 12).

While *E. huxleyi* is not the typical food source for *O. marina* maintenance cultures, even the smallest size of *E. huxleyi* (Ambient) is readily ingested by *O. marina*. This is indicated by the similarity between the predator:prey size ratio of *O. marina*: Ambient *E. huxleyi* and the ratio of *O. marina*: maintenance prey (Table 12). However, the larger High *E. huxleyi* 2668 cells are preferred over smaller cells, and grazing rates are higher on the larger cells (Figure 17) as the High treatment predator:prey size ratio increase for *O. marina*, which selectively feeds on larger cells and prefers prey that are close to a 1:1 predator:prey size ratio (Hansen et al. 1994). Despite the different sensitivity thresholds between ciliates and dinoflagellates, the increase in cell size in *E. huxleyi* under elevated $pCO_2$ observed in this study was sufficient to influence the grazing and percent population feeding rates of both ciliates and dinoflagellate. Increased grazing rates and percent population feeding for all three grazers were caused by the increased availability of cells that were larger and closer to the optimal predator:prey size ratio for each grazer. The increase in cell size of *E. huxleyi* with elevated $pCO_2$ also potentially moves *E. huxleyi* into a window of higher grazing efficiency for the tintinnids.

Table 12. Predator:prey size ratios of *Eutintinnus* sp., *Favella taraikaensis*, and *Oxyrrhis marina* feeding on *E. huxleyi* 2668 grown in Ambient (400 ppmv), and Moderate (750 ppmv), and High (1000 ppmv) treatments. Predator:prey size ratio is estimated using Equivalent Spherical Diameter (ESD) for *E. huxleyi* 2668, the optimal diet species and the dinoflagellate, *O. marina*, according to Hansen et al. 1994. Predator:prey size ratio for the tintinnids, *Eutintinnus* sp., and *F. taraikaensis*, is based on the maximum cystostome diameter. Optimal diets were *Heterocapsa rotundata*, *H. triquetra*, *Duneliella tertiolecta* for *Eutintinnus* sp., *F. taraikaensis*, and *O. marina* respectively.

| | **Optimal Ratio** | **Optimal Diet** | **Ambient** | **Moderate** | **High** |
|---|---|---|---|---|---|
| *Eutintinnus* sp. | **10:1 – 2.5:1** | **2.32:1** | **3.07:1** | **2.87:1** | **2.76:1** |
| *F. taraikaensis* | **10:1 – 2.5:1** | **2.17:1** | **6.57:1** | **6.42:1** | **6.19:1** |
| *O. marina* | **1:1** | **2.26:1** | **2.25:1** | **2.19:1** | **2.09:1** |

Although no significant changes in biochemical or physiological attributes aside from cell size of *E. huxleyi* 2668 were detected in this study, change in cell size is not the only response commonly seen when phytoplankton are exposed to elevated $pCO_2$. Others have found that different strains of *E. huxleyi* and other phytoplankton species respond in a variety of ways to elevated $pCO_2$, including changes in calcification, photosynthesis, growth rates, carbon and nitrogen stoichiometry, chlorophyll *a* and carbohydrate content (Zondervan et al. 2002; Iglesias-Rodriguez et al. 2008; De Bodt et al. 2010; Fiorini et al. 2011; Rokitta and Rost 2012; Lefebvre 2012; Feng et al. 2012; Bach et al. 2013). In these studies, if cell size changed, it was often assumed by the researchers to be a secondary response to an increase in another primary factor. For *E. huxleyi* 2668 and *Rhodomonas* sp. 755, increased cell size appears to be a direct primary response to ocean acidification since it occurred without evidence of change in any of the various other biochemical and physiological attributes that were measured. However, both primary or secondary responses of phytoplankton to ocean acidification can further affect microzooplankton grazing. The following sections will explore some primary and secondary responses to address the full range of potential food web responses to ocean acidification.

## Calcification

As OA increases $CO_2$ concentrations in the surface ocean (Chen 1993), aragonite and calcite saturation states are reduced (Feely et al. 2004). Calcification potentially becomes more energetically costly under such circumstances for calcifying organisms such as *E. huxleyi*, the bloom-forming coccolithophore that was chosen as the model organism for this study. A lower saturation state could lead to decreased calcification in *E. huxleyi* 2668 in the High $CO_2$ treatment (1000 ppmv) (Rokitta and Rost 2012; Lefebvre et al. 2012; Feng et al. 2012).

Calcification was not found to be a major factor determining grazing rates in the present study, since *E. huxleyi* 2668 calcification was not significantly affected by elevated $pCO_2$ in any experiment and the MLR model rejected particulate inorganic carbon (PIC) content per cell, and biovolume-normalized PIC as predictive factors. There was no significant increase or decrease in PIC per cell in any experiment (Figure 4; Table 5). However, the ratio of PIC to particulate organic carbon (POC) decreased in a single experiment, OA2a, due to an increase in POC per cell with no change in PIC per cell (Figure 5; Table 5).

The effect of $pCO_2$ on *E. huxleyi* 2668 in the present study differs from several documented cases in which *E. huxleyi* calcification decreased under acidified conditions. De Bodt et al. (2010) investigated the effect of ocean acidification and warming on calcification and size of *E. huxleyi* AC481. They found that PIC production rates decreased with increasing $pCO_2$, independent of warming conditions. Changes in calcification in this scenario might have been partially due to the choice of culture conditions for the experiments. Since Hopkinson et al. (2010) demonstrate that lowered pH reduces iron availability, not adding trace metals to culture media might leave cells iron-limited, potentially complicating the effects of elevated $CO_2$ on the calcification and growth of *E. huxleyi* in De Bodt et al.'s experiments (2010).

Zondervan et al. (2002) also found decreased PIC per cell and PIC:POC under elevated $pCO_2$ conditions, though their treatment $pCO_2$ levels were achieved using acid/base manipulations of seawater. So the decrease in calcification may have been due in large part to the acid addition during total alkalinity (TA) manipulation without the increase in DIC seen in $CO_2$ driven ocean acidification. Hoppe et al. (2011) compared TA and dissolved inorganic carbon (DIC) manipulations to determine the efficacy of acid/base manipulations. The latter method is accomplished by adding $CO_2$ to the water to manipulate DIC while TA remains constant, and is considered to be the more accurate representation of changing carbonate chemistry in the ocean with climate change. The former method

involves adding acid to lower pH and reduce TA while DIC remains unchanged. This method exaggerates the effects of OA because of the lower saturation states compared to $CO_2$ addition to the same pH. However, Hoppe et al. (2011) were unable to reproduce the variety of responses seen in other studies on the strains of *E. huxleyi* they chose for their study, and did not detect a difference between TA or DIC manipulation despite the disparity in saturation states between the two methods. However, they did find strong evidence to suggest that greater light intensity can modify the response of *E. huxleyi* to ocean acidification by making the cells less sensitive to elevated $pCO_2$ (Hoppe et al. 2011). If calcification is more energetically costly in high $CO_2$, then greater light intensity may allow the cell to produce the extra energy required to maintain calcification without hindering other important cellular processes. In these experiments, *E. huxleyi* 2668 was grown under 250 µmol photons $m^{-2}$ $s^{-1}$, which closely approximates the level of light needed to saturate photosynthesis (Figure 12).

In the 24 experiments reviewed by Meyer and Riebesell (2014), they highlight that calcification decreases with elevated $pCO_2$ across all of the strains of *E. huxleyi* that they examined. Closer comparison of *E. huxleyi* experiments resulting in decreased calcification (Rokitta and Rost 2012; Lefebvre et al. 2012; Feng et al. 2012) to those that resulted in increased calcification (Iglesias-Rodriguez et al. 2008; Fiorini et al. 2011; Bach et al. 2013) supports the hypothesis that ocean acidification effects on calcification are highly moderated and modified by light intensity (Hoppe et al. 2011), as well as being strain-specific. All of these experiments, including this one, have been conducted at light levels that *E. huxleyi* populations could experience in nature. Therefore the variety of calcification responses seen across those experiments illustrate the range of changes that *E. huxleyi* and other coccolithophores might experience in the future ocean.

For those strains of *E. huxleyi* that have reduced calcification in an acidifying ocean, that reduction in calcification could alter grazing rates. Decreased grazing defense could be a product of

lighter calcification in *E. huxleyi*, if microzooplankton are able to ingest cells with fewer or thinner coccoliths more easily. Lighter calcification could therefore result in increased grazing pressure on *E. huxleyi* at the same time that it increases the relative food quality of *E. huxleyi*. As the proportion of organic carbon per cell increases with decreasing calcification, ingestion of *E. huxleyi* becomes more beneficial to microzooplankton grazers compared to heavily calcified cells. Since increased cell size led to higher grazing pressure in this study, and PIC $cell^{-1}$ was unaffected, thinner calcification could have played a role in the increased grazing pressure.

## Photosynthesis and Growth

Phytoplankton food quality may also be affected by ocean acidification through the increased availability of $CO_2$ for photosynthesis. Low-Decarie et al. (2014) theorize that contrary to Liebig's law of the minimum, $CO_2$ can be co-limiting for phytoplankton photosynthesis. They present the argument that due to the low affinity of RuBisCO for $CO_2$, $CO_2$ itself is a rate limiting resource and contributes to the limitation of productivity. Major taxonomic groups differ in their potential to be limited by $pCO_2$ (Low-Decarie et al. 2014; Beardall and Raven 2004, 2013), with cyanobacteria tending to be the least sensitive and chlorophytes potentially as the most sensitive (Low-Decarie et al. 2014). Current ocean conditions are $CO_2$ limiting for *E. huxleyi*, as RuBisCO is less than half-saturated at present day $pCO_2$ (Giordano et al. 2005). With atmospheric $CO_2$ concentrations rising, increasing $pCO_2$ in the surface ocean may relieve $CO_2$ limitations for photosynthesis. Relieving $CO_2$ limitation may alter the growth of *E. huxleyi* and other phytoplankton as photosynthesis increases (Beardall and Raven 2004, 2013; Rokitta and Rost 2012; Bach et al. 2013; Low-Decarie et al. 2014). Rokitta and Rost (2012) found that *E. huxleyi* (RCC 1216) actively downscales light harvesting under ocean acidification, indicating that photosynthesis may become more efficient with no net increase in photosynthesis when there is greater availability of $CO_2$. Additionally, as *E. huxleyi* 1216

photosynthesis became more efficient, POC increased at the expense of PIC production while TOC remained constant. In a similar study exploring a different strain of *E. huxleyi*, Feng et al. (2012) found that photosynthesis in *E. huxleyi* (CCMP 371) was very responsive to both elevated $pCO_2$ and temperature. Photosynthetic efficiency in *E. huxleyi* 371 increased in high $pCO_2$ (750 ppmv) over ambient $pCO_2$ (375 ppmv), and was greater at 24 °C than 20 °C. Increased photosynthetic efficiency was also correlated with decreased calcification in high $pCO_2$ treatments (Feng et al. 2012). In both of these studies, PIC production was significantly correlated with photosynthetic efficiency.

Analysis of photosynthesis for *E. huxleyi* 2668 during OA3 revealed that neither the rate of photosynthesis nor the maximum photosynthetic capacity changed with increasing $pCO_2$ under these conditions (Figures 12 & 13). The chlorophyll *a* (chl *a*) content of the cells was also unaffected by elevated $pCO_2$ (Figure 8). No change in chl *a* combined with the lack of change in photosynthesis in *E. huxleyi* 2668 might be evidence of the use of a carbon concentrating mechanism (CCM). Beardall and Raven (2013) suggest that the presence of a CCM in *E. huxleyi* would be detectable if photosynthesis and growth is not stimulated by elevated $pCO_2$ as $CO_2$ concentrations continue to rise. If the cell experiences decreasing dependence on the CCM as $CO_2$ concentrations increase, energy may be diverted away from maintenance of a CCM and reallocated to other cellular processes (Rokitta and Rost 2012). The increase in *E. huxleyi* 2668 cell size may be a result of decreasing dependence on a CCM. According to Hopkinson et al. (2010) there is ample research to support the hypothesis that down regulation of the CCM allows energy and materials previously devoted to inorganic carbon accumulation to be reallocated to replication, organic carbon accumulation, as well as carbohydrate, lipid, and chlorophyll *a* production. Beardall and Raven (2013) suggest that this would occur because *E. huxleyi*'s CCM is actually a result of the process of calcification, which produces and concentrates internal $CO_2$. Changes in organic carbon accumulation, carbohydrate and lipid storage, and chlorophyll *a* can all translate to changes in food quality in phytoplankton, which

can further influence microzooplankton grazing (Meunier et al. 2011) given their sensitivity to not only prey cell size, but also to chemical cues and prey food quality (Tillmann 2004).

Elevated $pCO_2$ also has a strong influence on phytoplankton communities through stimulation of growth rate and increased carbon accumulation (Yoshimura et al. 2010). Several studies showed that *E. huxleyi* cultures grown under elevated $pCO_2$ experienced decreased intrinsic growth rates (Iglesias-Rodriguez et al. 2008; Hoppe et al. 2011; Borchard and Engel 2012; Van de Waal et al. 2013), while others have noted increased carbon accumulation and increased growth rates as *E. huxleyi* acclimates to increased $CO_2$ availability in longer experiments (>10 days) (Fiorini et al 2010; Lohbeck et al. 2012). According to the relationship described by Goldman et al. (1979), increasing intrinsic growth rate in *Duneliella tertiolecta*, *Monochrysis lutheri,* and *Thalassiosira pseudonana* correlates negatively with cellular C:P and N:P ratios as a function of the culture's nutrient limitation. Further, Reinfelder (2012) found that elevated $pCO_2$ results in increased C:N ratios in two diatoms, *Thalassiosira pseudonana* and *T. weissflogii*, and a prymnesiophyte, *Isochrysis galbana*. Therefore, I expected that increased *E. huxleyi* growth rate could be associated with increased carbon accumulation and C:N ratios under elevated $pCO_2$, since neither nitrogen or phosphorous are limiting in this study.

Though there was a large amount of daily variation in growth across our semi-continuous culturing experiments, there was no significant effect of elevated $pCO_2$ on *E. huxleyi* 2668 growth rate (Table 3). Given the strong relationship between phytoplankton growth rates and chemical composition, it is not surprising that since there was no significant effect of elevated $pCO_2$ on growth rate, there was also no effect on the POC:PON ratio of *E. huxleyi* 2668 in any experiment. Engel et al. (2005) similarly found that POC:PON did not change in elevated $CO_2$ conditions until nitrate concentration was depleted. Since our cultures were always nutrient replete, there was no chance for nitrate limitation to change POC:PON in *E. huxleyi* 2668.

The MLR model revealed that despite some subtle variation in *E. huxleyi* growth rate, photosynthetic efficiency, and C:N ratio, they were not significant predictors of increased grazing rates for these three microzooplankton species. But for those phytoplankton species and strains of *E. huxleyi* where growth rate does change with elevated $pCO_2$, microzooplankton grazing may be affected. If there are widespread increases in growth rates among phytoplankton, then that would result in a higher proportion of cells in early growth stages, since $CO_2$ is a co-limiting resource for many phytoplankton (Giordano et al. 2005). The growth stage of a culture does influence grazing rates in microzooplankton, as cells in late stationary phase are chemically distinguishable from fast growing cells in exponential phase (Barofsky et al. 2010). Microzooplankton grazing, therefore, may be affected in those species that can detect the chemical attributes of newer, faster growing phytoplankton cells and preferentially feed on the younger cells.

## Energy Storage

The cellular concentration of phytoplankton carbohydrate, the primary phytoplankton reductant, has been shown to change in response to elevated $pCO_2$ (Borchard and Engel 2012), possibly due to reallocation of cellular energy budgets. Borchard and Engel (2012) found that *E. huxleyi* (PML B 92/11) cells exposed to 900 μatm $CO_2$ at 14 °C had greater total carbohydrate content $cell^{-1}$ than those cells exposed to 300 or 550 μatm at the same temperature (by almost 2X). Based on their findings I expected to see a similar increase in *E. huxleyi* 2668 carbohydrate content since similar $pCO_2$ concentrations were used in this study. In Borchard and Engel's experiments, *E. huxleyi* increased energy storage in the form of carbohydrate production, which may point toward decreased dependence on CCM maintenance in *E. huxleyi* with elevated $pCO_2$. However, possibly because of large variability within treatments, there was no detectable treatment effect on *E. huxleyi* 2668 total carbohydrate content during OA3, even when normalized to biovolume (Figure 10, 11).

Borchard and Engel (2012) further associated the increased carbohydrate content in *E. huxleyi* B 92/11 with reduced growth rates and increased C:P ratio in cells grown at 900 μatm $CO_2$, which I did not see in *E. huxleyi* 2668. Wynn-Edward et al. (2014) explored the cellular carbohydrate content of several Antarctic phytoplankton in high $CO_2$ conditions, but did not find a consistent trend either. In their study, a prasinophyte, *Pyramimonas gelidicola*, saw a 22% reduction in cellular carbohydrate content in 1000ppmv, while a haptophyte, *Phaeocystis antarctica*, increased cellular carbohydrates by 30%.

It is probable that since no observed change was seen in C:N and growth rate of *E. huxleyi* 2668, the cells were not reallocating energy. Verity (1988) found that ciliates have strong chemosensory responses to differences in food types that represent differing food quality and benefit to the grazer. Similar chemosensory response to food quality was demonstrated in *O. marina*, as the dinoflagellate is very sensitive to changes in food composition (Meunier et al. 2011). Since no change in cellular carbohydrate content was observed, this could not have been a factor affecting microzooplankton grazing on *E. huxleyi* 2668. It is not known how widespread the effect on carbohydrates might be in *E. huxleyi* and other primary producers, since there seem to be a variety of species-specific responses to ocean acidification and energy storage. Since changes in carbohydrate storage are associated with changes in growth and elemental composition (Borchard and Engel 2012), increased carbohydrate content may result in altered chemical signaling to microzooplankton predators (Verity and Villareal 1986; Buskey and Stoecker 1988; Verity 1988; Anderson and Pondaven 2003; Meunier et al. 2011).

**Planktonic Food Web Effects:**

**An *Emiliania huxleyi* bloom**

In a future acidified ocean, higher grazing pressure by microzooplankton would be especially significant for *E. huxleyi*, a coccolithophorid that is responsible for massive, persistent algal blooms in the open ocean and along continental shelves each year ($50 – 250 \times 10^3$ km$^2$). As *E. huxleyi* blooms form and subsequently dies each year, massive amounts of inorganic carbon are exported to the ocean floor in the form of calcium carbonate bound up in coccoliths. Due to the size and scope of these blooms and the potential for carbon export, understanding how elevated $pCO_2$ will affect the balance within the bloom is important for understanding the effects of ocean acidification on a global scale. Diminished bloom persistence under ocean acidification could decrease the efficiency of the ocean as a carbon sink as global atmospheric $CO_2$ concentrations continue to rise.

Grazing pressure and environmental factors oscillate in importance in regulating marine food webs as changes in predation affect the balance between bottom-up and top-down control of phytoplankton blooms (Calbet et al. 2001). Since the microzooplankton in *E. huxleyi* blooms are predominantly ciliates and dinoflagellates (Widdicombe et al. 2002; Strom and Olson 2002), *E. huxleyi* cells are easily within the size range of available prey for the microzooplankton (Buskey 1997). If the *E. huxleyi* cells composing the bloom become larger under elevated $pCO_2$ and are consequently ingested at faster rates by the microzooplankton community (as suggested by this study), then *E. huxleyi* blooms may not persist as long under ocean acidification conditions as they do in the current ocean. Additionally, if reduced grazing is necessary for the formation and persistence of the *E. huxleyi* bloom (Strom and Olson 2002), then increased grazing on larger *E. huxleyi* could stunt the formation and shorten the duration of the bloom.

## APPENDIX

### *Rhodomonas* sp. Characterization

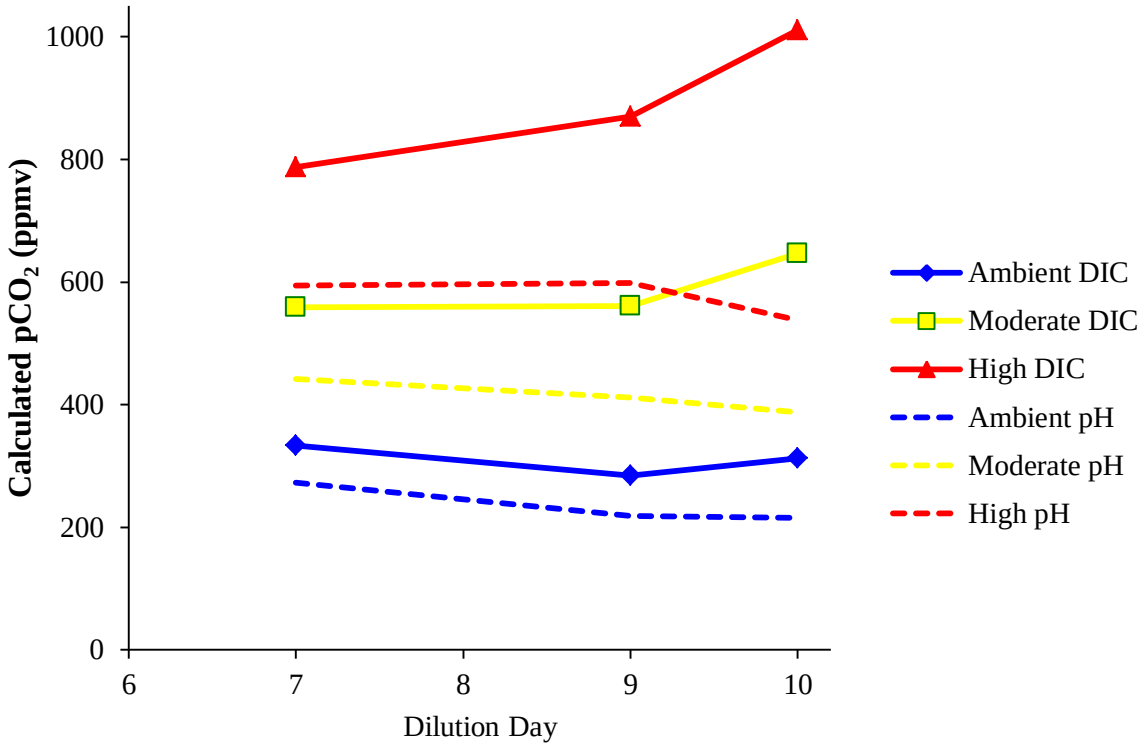


Figure A1. Comparison of $pCO_2$ calculated using DIC vs. spectrophotometric pH for *Rhodomonas* sp. cultures during OA4. The discrepancy between DIC and pH calculated $pCO_2$ led to utilization of a DIC analyzer in ongoing and future experiments. Spectrophotometric pH is believed to be unreliable due to the production of water-soluble pigments produced by *Rhodomonas* sp. that interfere with the m-cresol purple dye used in pH measurements.

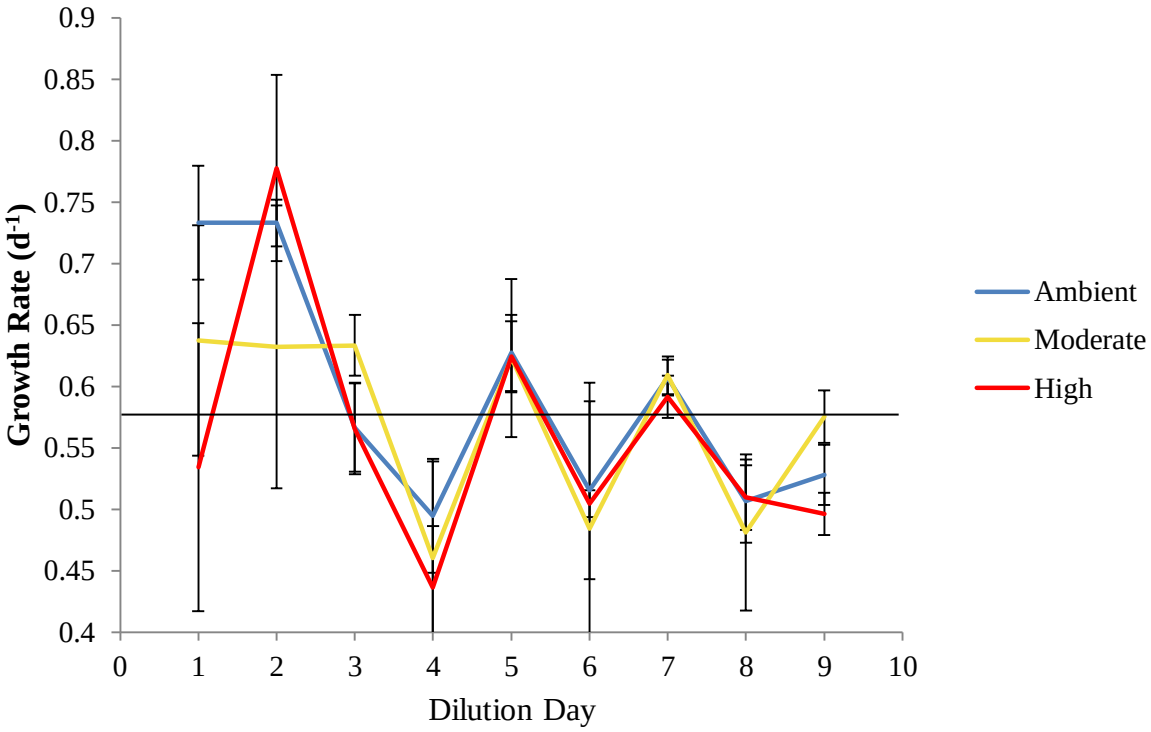


Figure A2. *Rhodomonas* sp. intrinsic growth rate ($d^{-1}$) on each day of semi-continuous experiment OA4. Solid black line represents overall average growth rate for *Rhodomonas* sp. (0.57 ± 0.098 $d^{-1}$). Error bars represent ± 1 SD. There was no statistically significant treatment effect on growth rate.

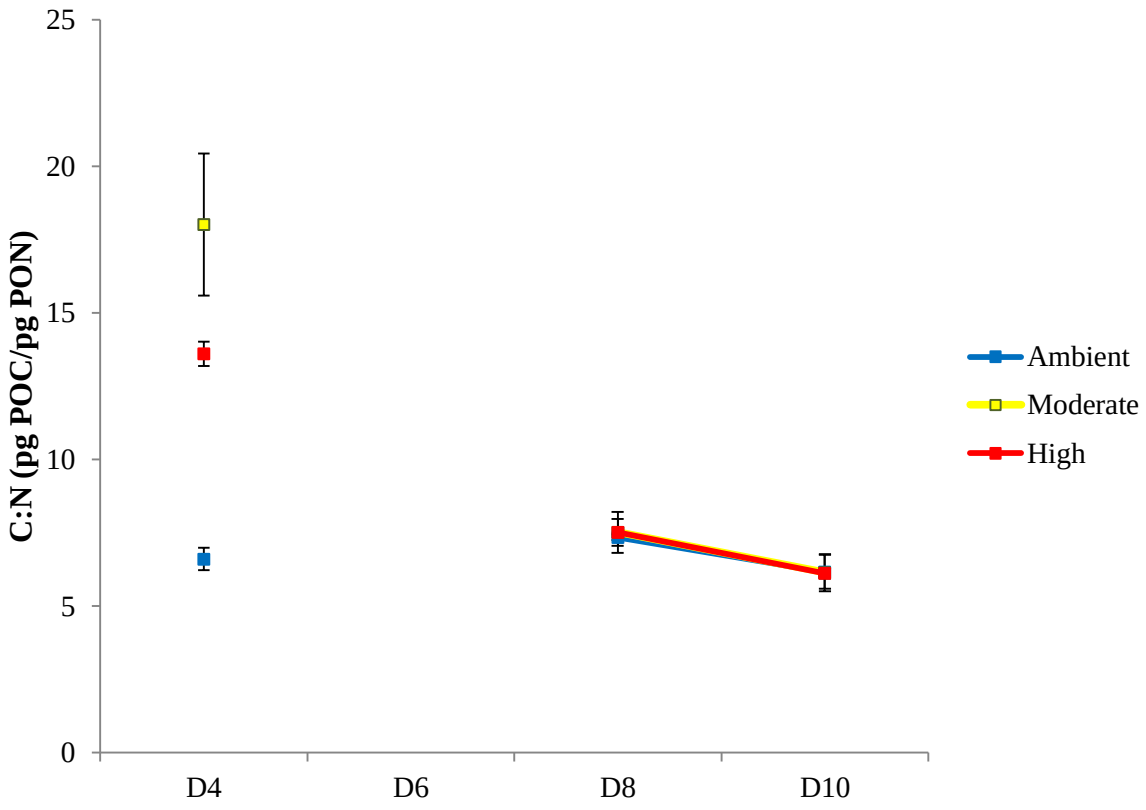


Figure A3. *Rhodomonas* sp. particulate organic carbon to nitrogen ratio (pg POC: pg PON cell$^{-1}$) during semi-continuous experiment OA4. Values were taken from samples obtained on four days of the experiment (Day 4, Day 6, Day 8, and Day 10). Day 4 Ambient: 6.61 ± 0.42 pg POC cell$^{-1}$; Moderate: 18.02 ± 0.39 pg POC cell$^{-1}$; and High: 13.60 ± 2.42 pg POC cell$^{-1}$. Day 6 samples were lost during analysis. Error bars represent ± 1SD.

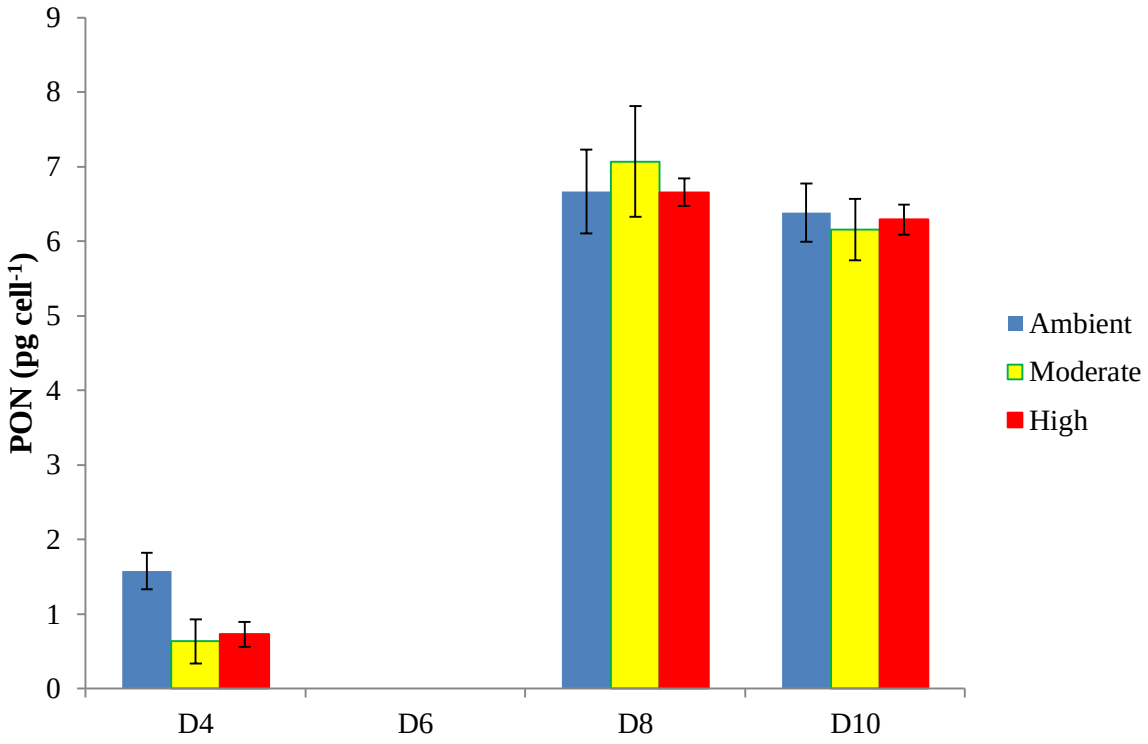


Figure A4. *Rhodomonas* sp.particulate organic nitrogen (pg PON cell$^{-1}$) during semi-continuous experiment OA4. Values were taken from samples obtained on four days of the experiment (Day 4, Day 6, Day 8, and Day 10). Day 4 Ambient: 1.58 ± 0.25 pg PON cell$^{-1}$; Moderate: 0.64 ± 0.30 pg PON cell$^{-1}$; High: 0.73 ± 0.17 pg PON cell$^{-1}$. Day 6 samples were lost during analysis. Error bars represent ± 1SD.

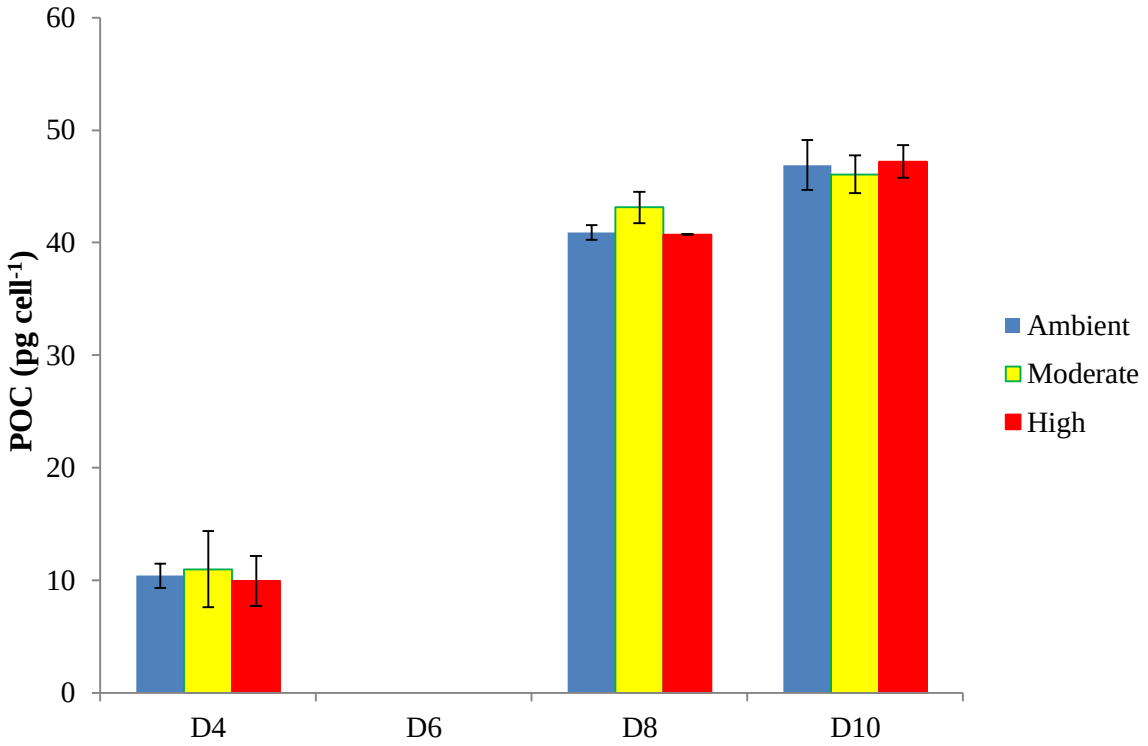


Figure A5. *Rhodomonas* sp. particulate organic carbon per cell (pg POC cell$^{-1}$) during semi-continuous experiment OA4. Values were taken from samples obtained on four days of the experiment (Day 4, Day 6, Day 8, and Day 10). Day 6 samples were lost during analysis. Error bars represent ± 1SD (n = 3).

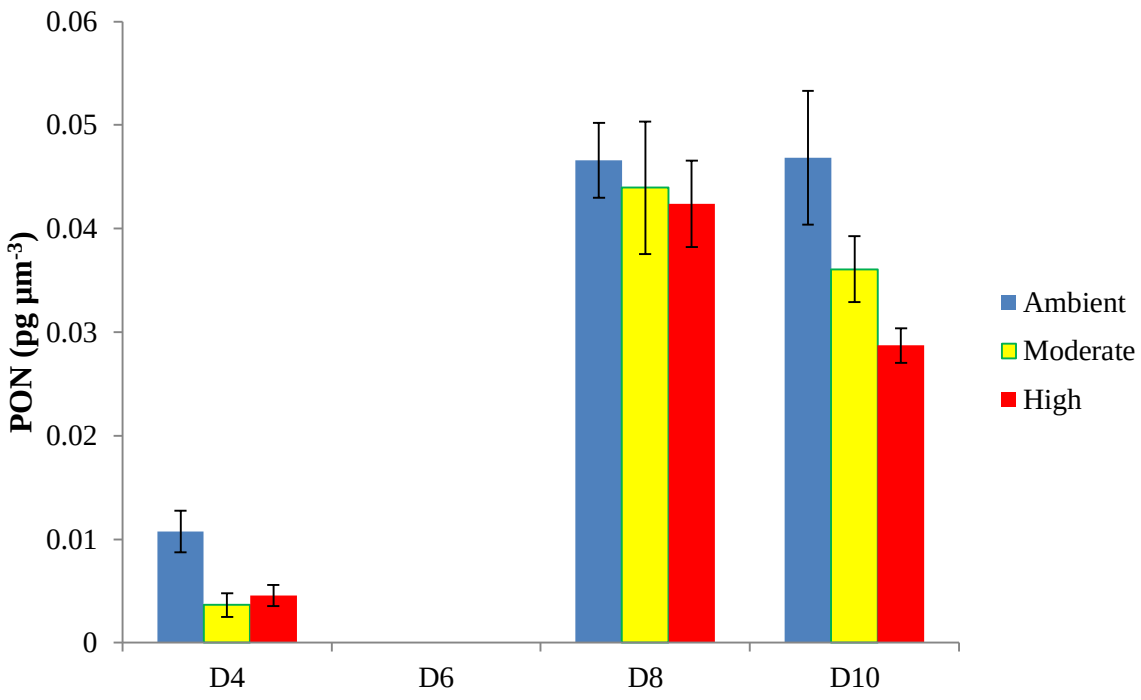


Figure A6. *Rhodomonas* sp particulate organic nitrogen density (pg PON $cell^{-1}\mu m^{-3}$) during semi-continuous experiment OA4. Values were taken from samples obtained on four days of the experiment (Day 4, Day 6, Day 8, and Day 10). Day 6 samples were lost during analysis. Error bars represent ± 1SD.

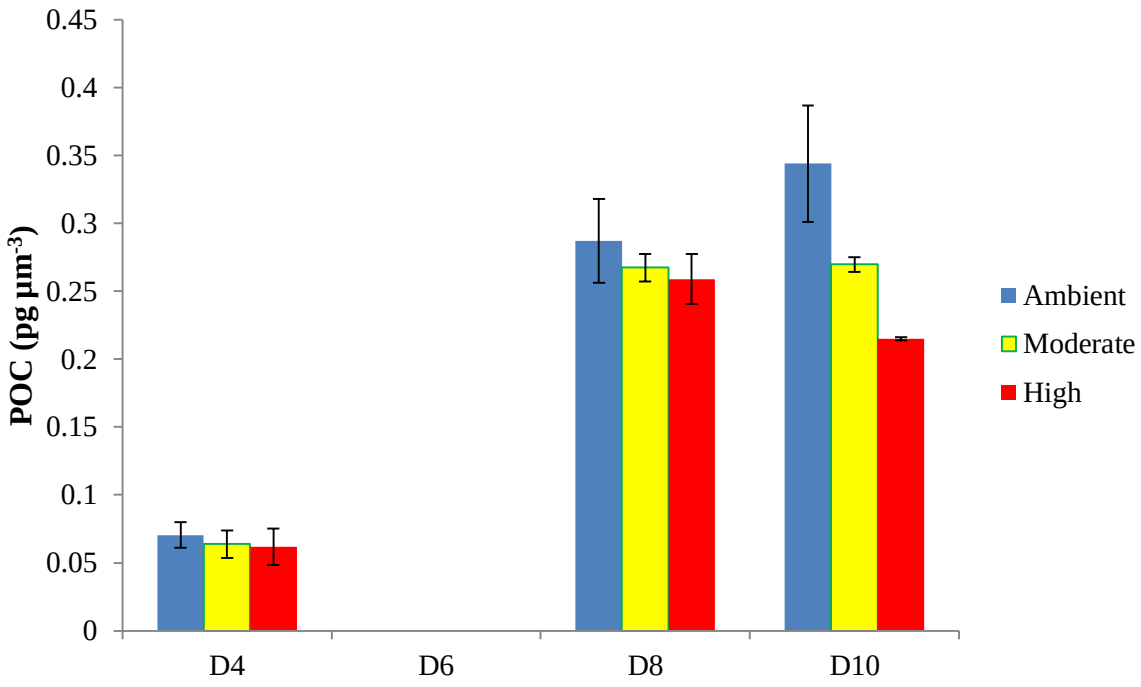


Figure A7. *Rhodomonas* sp. particulate organic carbon density (pg POC $cell^{-1}\mu m^{-3}$) during semi-continuous experiment OA4. Values were taken from samples obtained on four days of the experiment (Day 4, Day 6, Day 8, and Day 10). D6 samples were lost during analysis. Error bars represent ± 1SD.

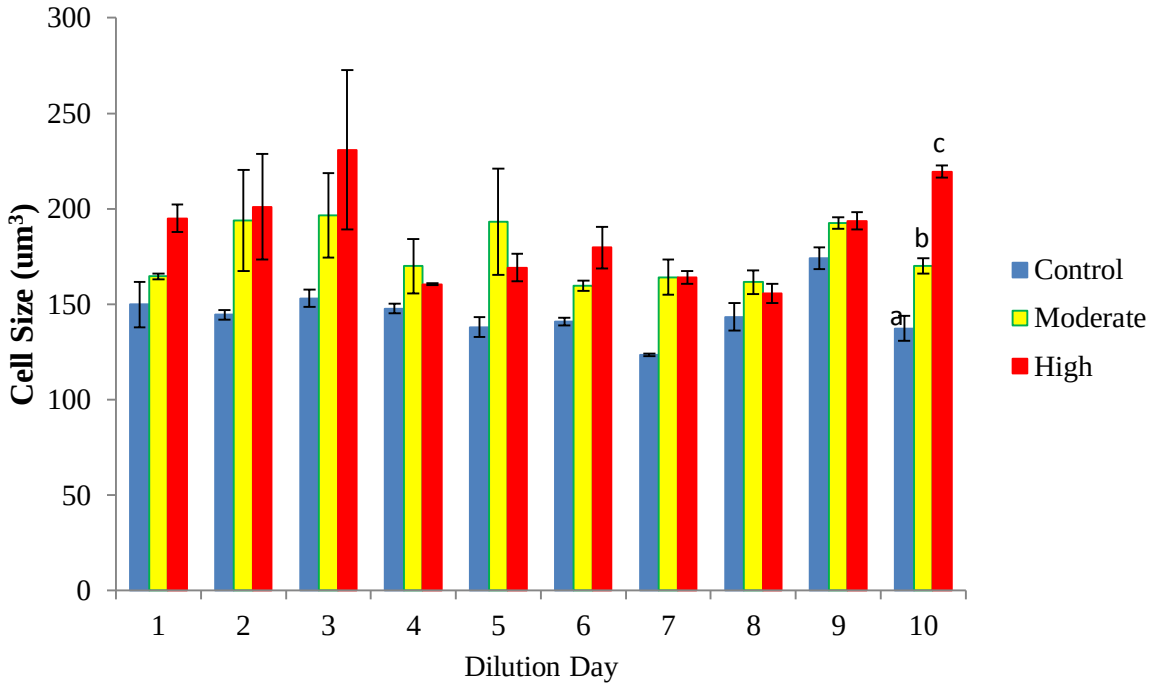


Figure A8. *Rhodomonas* sp. cell size ($\mu m^3$) on each day of semi-continuous experiment OA4. Letters over bars show significant differences across treatments on the final day of semi-continuous culture; bars with shared letters represent treatments that were not statistically different ($p < 0.001$; ANOVA, $\alpha = 0.05$; Tukey's post hoc analysis). Day 10 Ambient: 137.3 ± 11.5 $\mu m^3$; Moderate: 170.9 ± 6.8 $\mu m^3$; and High 219.4 ± 5.6 $\mu m^3$. Error bars represent ± 1 SD.

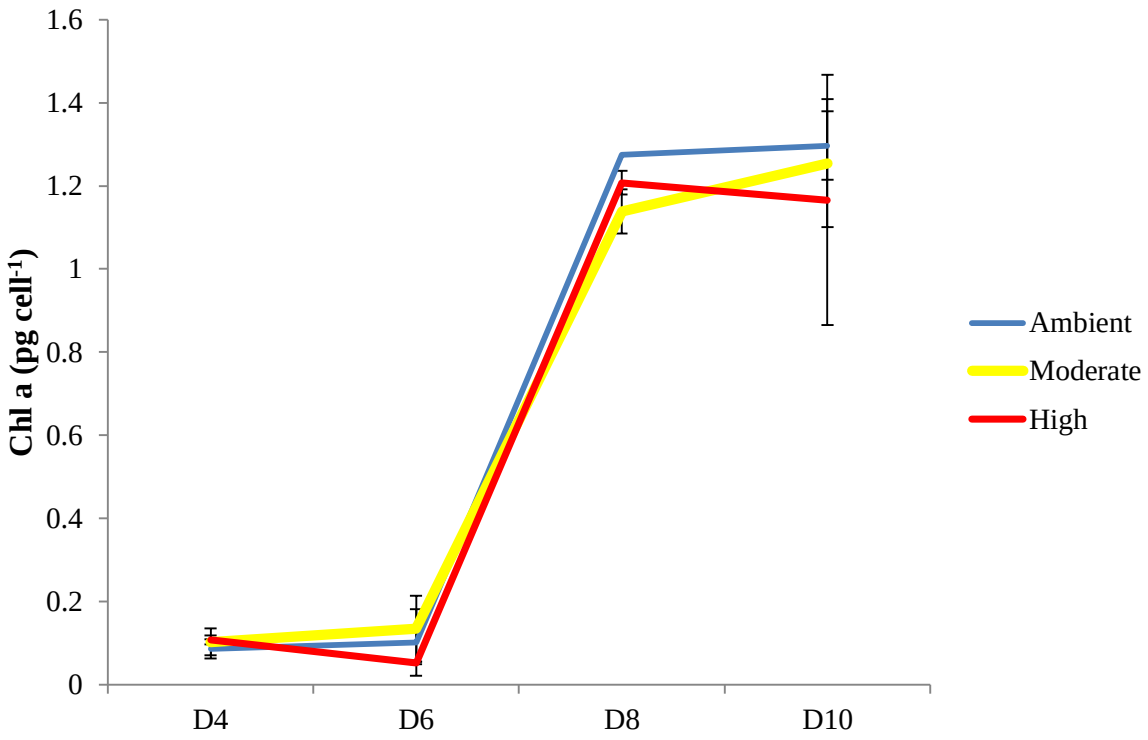


Figure A9. *Rhodomonas* sp. chlorophyll *a* content (pg Chl *a* cell$^{-1}$) during semi-continuous experiment OA4. Values were taken from samples obtained on four days of the experiment (Day 4, Day 6, Day 8, and Day 10). Error bars represent ± 1SD.

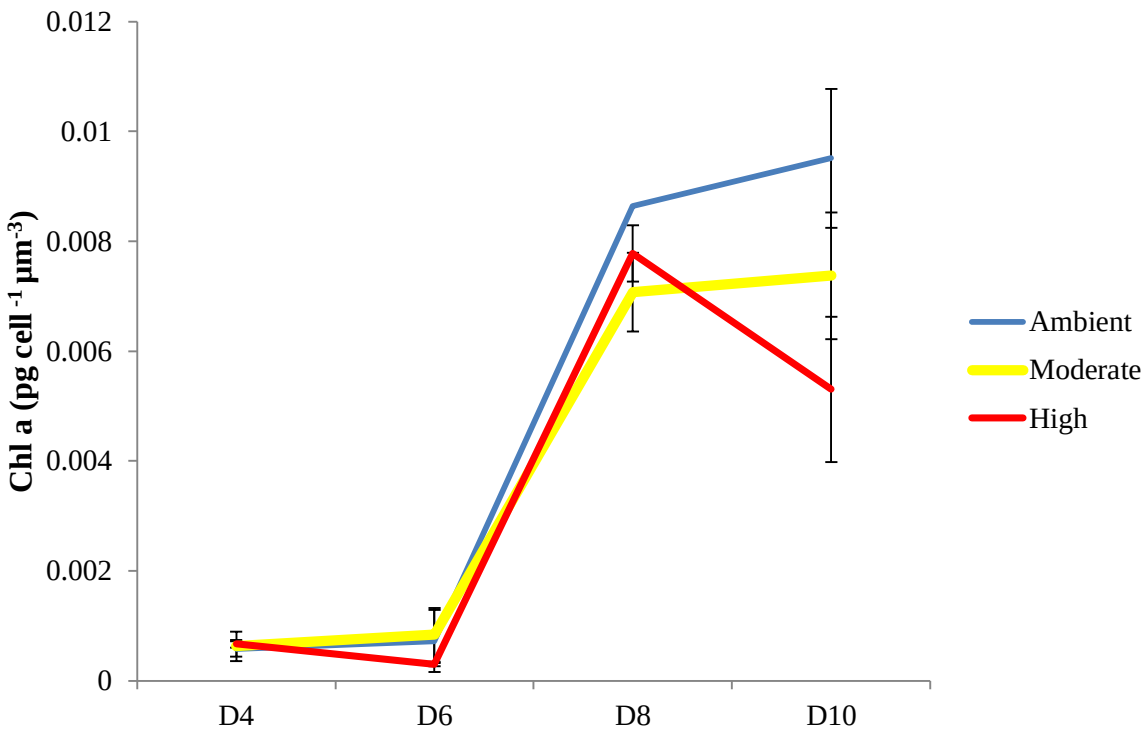


Figure A10. *Rhodomonas* sp. chlorophyll *a* density (pg Chl *a* $\mu m^{-3}$) during semi-continuous experiment OA4. Values were taken from samples obtained on four days of the experiment (Day 4, Day 6, Day 8, and Day 10). Error bars represent ± 1SD.

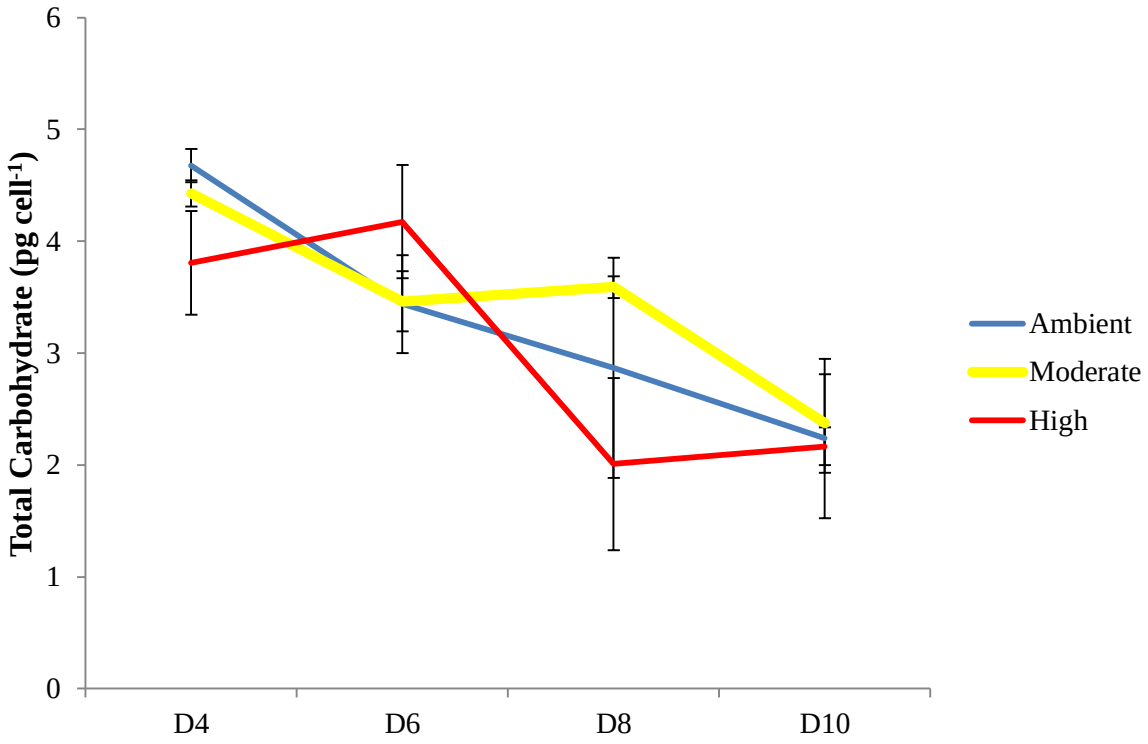


Figure A11. *Rhodomonas* sp. total carbohydrate content (pg fructose equiv. cell$^{-1}$) during semi-continuous experiment OA4. Values were taken from samples obtained on four days of the experiment (Day 4, Day 6, Day 8, and Day 10). Error bars represent ± 1SD.

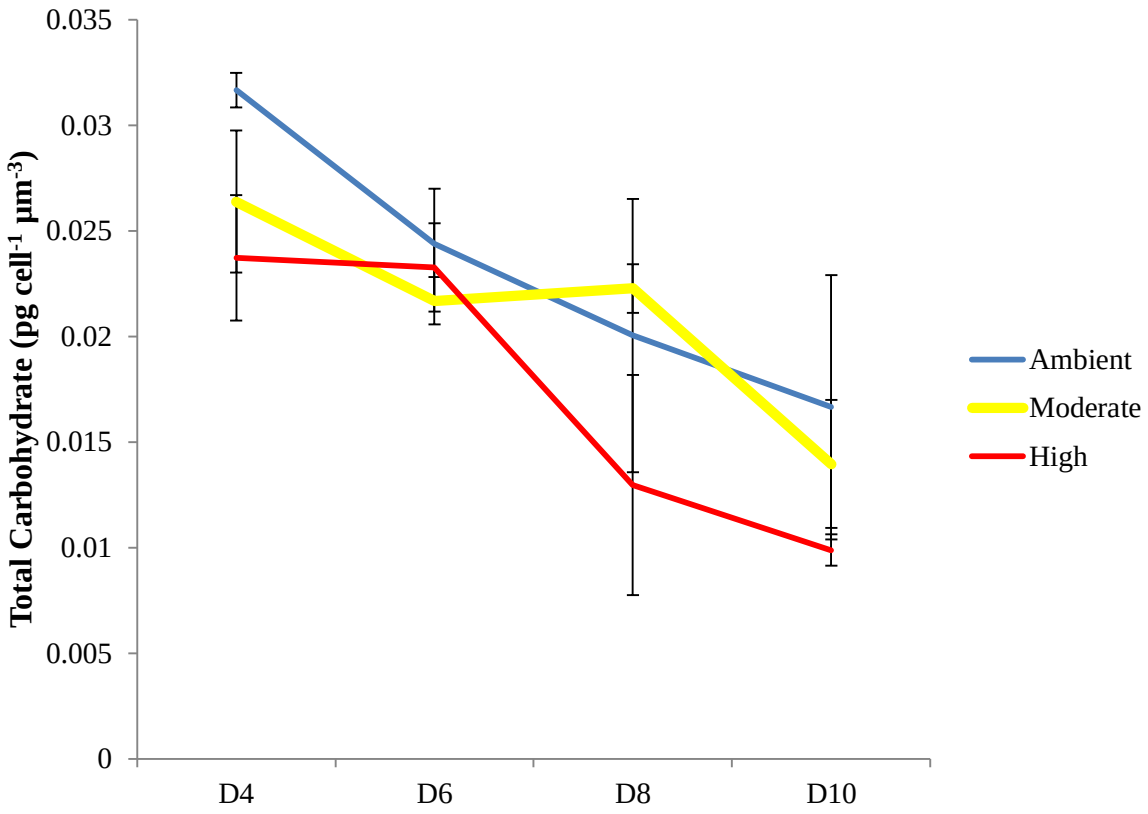


Figure A12. *Rhodomonas* sp. carbohydrate density (pg fructose equiv. $\mu m^{-3}$) during semi-continuous experiment OA4. Values were taken from samples obtained on four days of the experiment (Day 4, Day 6, Day 8, and Day 10). Error bars represent ± 1SD.

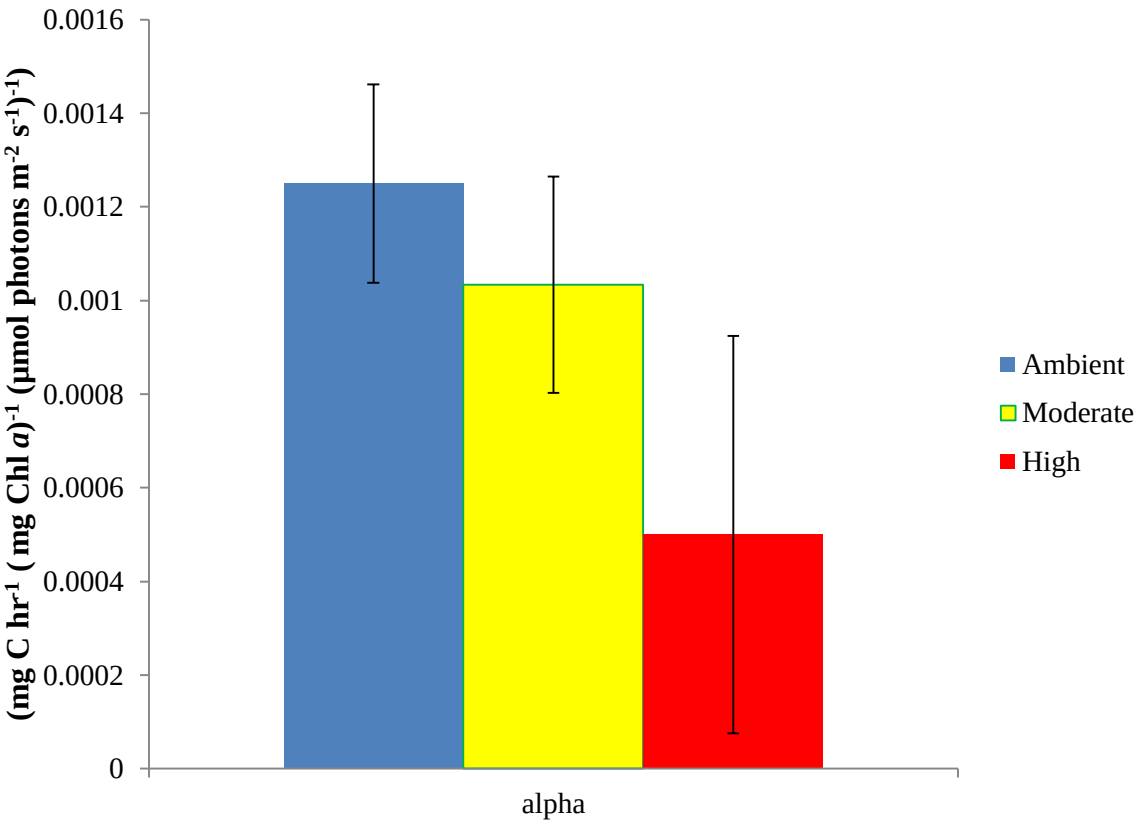


Figure A13. *Rhodomonas* sp. alpha normalized to cellular chlorophyll *a* (mg C $hr^{-1}$ ( mg Chl *a*)$^{-1}$ (µmol photons $m^{-2}$ $s^{-1}$)$^{-1}$) from photosynthesis vs. irradiance response (PI) curves done on the final day of semi-continuous experiment OA4. Error bars represent ± 1SD.

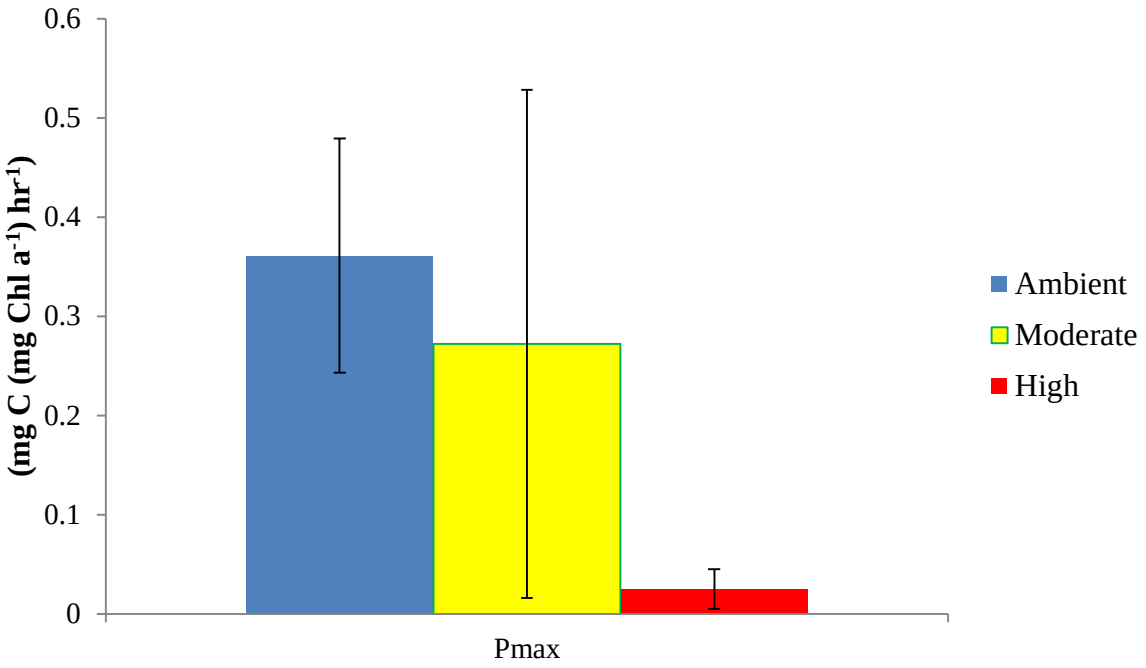


Figure A14. *Rhodomonas* sp. $p_{max}$ normalized to cellular chlorophyll *a* (mg C (mg Chl $a^{-1}$) $hr^{-1}$) from photosynthesis vs. irradiance response (PI) curves done on the final day of semi-continuous experiment OA4. Error bars represent ± 1SD.

## LITERATURE CITED


**Anderson, T.R. and P. Pondaven.** 2003. Non-redfield carbon and nitrogen cycling in the Sargasso Sea: pelagic imbalances and export flux. Deep-Sea Research Part I- Oceanographic Research Papers 50:573-591.

**Andersson, A., U. Larsson, and A. Hagstrom.** 1986. Size-selective grazing by a microflagellate on pelagic bacteria. Marine Ecology Progress Series 33:51-57.

**Arnold, H.E., P. Kerrison, and M. Steinke.** 2012. Interacting effects of ocean acidification and warming on growth and DMS-production in the haptophyte coccolithophore Emiliania huxleyi.

**Bach, L.T., L.C.M. Mackinder, K.G. Schulz, G. Wheeler, D.C. Schroeder, C. Brownlee, and U. Riebesell.** 2013. Dissecting the impact of $CO_2$ and pH on the mechanisms of photosynthesis and calcification in the coccolithophore Emiliania huxleyi. New Phytologist 199:123-134.

**Barofsky, A., P. Simonelli, C. Vidoudez, C. Troedsson, J.C. Nejstgaard, H.H. Jakobsen, and G. Pohnert.** 2010. Growth phase of the diatom Skeletonema marinoi influences the metabolic profile of the cells and the selective feeding of the copepod Calanus spp. Journal of Plankton Research 32:263-272.

**Beardall, J. and J.A. Raven.** 2004. The potential effects of global climate change on microalgal photosynthesis, growth and ecology. Phycologia 43:31-45.

**Beardall, J. and J.A. Raven.** 2013. Calcification and ocean acidification: new insights from the coccolithophore Emiliania huxleyi. New Phytologist: Commentary 199:1-3.

**Beaufort, L., I. Probert, T. deGaridel-Thoron, E.M. Bendif, D. Ruiz-Pino, N. Metzl, C. Goyet, N. Buchet, P. Coupel, M. Grelaud, B. Rost, R.E.M. Rickaby, and C. de Vargas.** 2011. Sensitivity of coccolithophores to carbonate chemistry and ocean acidification. Nature 476:80-83.

**Dickson, A.G., C.L. Sabine, J.R. Christian.** 2007. Guide to best practices for ocean $CO_2$ measurements. PICES Special Publication 3

**Boenigk, J., C. Matz, K. Jurgens, and H. Ardnt.** 2001. The influence of preculture conditions and food quality on the ingestion and digestion of three species of heterotrophic nanoflagellates. Microbial Ecology 42:168-176.

**Borchard, C. and A. Engel.** 2012. Organic matter exudation by Emiliania huxleyi under simulated future ocean conditions. Biogeosciences Discussion 9:1199-1236.

**Boyd, P.W., R. Strzepek, F. Fu, and D.A. Hutchins.** 2010. Environmental control of open-ocean phytoplankton groups: now and in the future. Reviews in Limnology and Oceanography 55:1353-1376.

**Buskey, E.J.** 1997. Behavioral components of feeding selectivity of the heterotrophic dinoflagellate Protoperidinium pellucidum. Marine Ecology Progress Series 153:77-89.

**Buskey, E.J. and D.K. Stoecker.** 1988. Locomotory patterns of the planktonic ciliate Favella sp.: adaptations for remaining within food patches. Bulletin of Marine Science 43:783-796.

**Calbet, A.** 2008. The trophic roles of microzooplankton in marine systems. ICES Journal of Marine Science 65:325-331.

**Calbet, A., M.R. Landry, and S. Nunnery.** 2001. Bacteria-flagellate interactions in the microbial food web of the oligotrophic subtropical North Pacific. Aquatic Microbial Ecology 23:283-292.

**Caldeira, K., and M.E. Wickett.** 2003. Anthropogenic carbon and ocean pH. Nature 425:365.

**Canadell, J.G., C. Le Quere, M.R. Raupach, C.B. Field, E.T. Buitenhuis, P. Ciais, T.J. Conway, N.P. Gillett, R.A. Houghton, and G. Marland.** 2007. Contributions to accelerating atmospheric $CO_2$ growth from economic activity, carbon intensity, and efficiency of natural sinks. PNAS 0702737104.

**Chen, C.T.A.** 1993. The oceanic anthropogenic $CO_2$ sink. Chemosphere 27:1041-1064.

**De Bodt, C., N. Van Oostende, J. Harlay, K. Sabbe, and L. Chou.** 2010. Individual and interacting effects of $pCO_2$ and temperature on Emiliania huxleyi calcification: study of the calcite production, the coccolith morphology and the coccosphere size. Biogeosciences 7:1401:1412

**DuBois, M., K.A. Gilles, J.K. Hamilton, P.A. Rebers, and F. Smith.** 1956. Colorimetric method for determination of sugars and related substances. Analytical Chemistry 28:350-356.

**Engel, A., I. Zondervan, K. Aerts, L. Beaufort, A. Benthien, L. Chou, B. Delille, J.P. Gattuso, J. Harlay, C. Heemann, L. Hoffmann, S. Jacquet, J. Nejstgaard, M.D. Pizay, E. Rochelle-Newall, U. Schneider, A. Terbrueggen, and U. Riebesell.** 2005. Testing the direct effect of $CO_2$ concentration on a bloom of the coccolithophorid Emiliania huxleyi in mesocosm experiments. Limnology and Oceanography 50:493-507.

**Fabry, V.J.** 2008. Marine calcifiers in a high-$CO_2$ ocean. Science 320:1020-1022.

**Feely, R.A., C.L. Sabine, K. Lee, W. Berelson, J. Kleypas, V.J. Fabry, and F.J. Millero.** 2004. Impact of anthropogenic $CO_2$ on the $CaCO_3$ system in the oceans. Science 305:362-366.

**Feng, Y., M.E. Warner, Y. Zhang, J. Sun, F.X. Fu, J.M. Rose, and D.A. Hutchins.** 2012. Interactive effects of increased $pCO_2$, temperature and irradiance on the marine coccolithophore Emiliania huxleyi (Prymnesiophyceae). European Journal of Phycology 43:87-98.

**Fiorini, S., J.J. Middelburg, and J.P. Gattuso.** 2011. Testing the effects of elevated $pCO_2$ on coccolithophores (Prymnesiophyceae): comparisons between haploid and diploid life stages. Journal of Phycology 47:1281-1291.

**Frada, M.J., K.D. Bidle, I. Probert, and C. de Vargas.** 2012. In situ survey of life cycle phases of the coccolithophore Emiliania huxleyi (Haptophyta). Environmental Microbiology 14:1558-1569.

**Giordano, M., J. Beardall, and J.A. Raven.** 2005. $CO_2$ concentrating mechanisms in algae: mechanisms, environmental modulation, and evolution. Annual Review of Plant Biology 56:99-131.

**Gifford, D.J.** 1985. Laboratory culture of marine planktonic oligotrophs (Ciliophora, Oligotricha). Marine Ecology Progress Series 23:257-267.

**Goldman, J.C, J.J. McCarthy, and D.G. Peavey.** 1979. Growth rate influence on the chemical composition of phytoplankton in oceanic waters. Nature 279:210-215.

**Hansen, P.J.** 1992. Prey size selection, feeding rates and growth dynamics of heterotrophic dinoflagellates with special emphasis on Gyrodinium spirale. Marine Biology 114:327-334.

**Hansen, B., P.K. Bjornsen, and P.J. Hansen.** 1994. The size ratio between planktonic predators and their prey. Limnology and Oceanography 39:395-403.

**Haugan, P.M. and H. Drange.** 1996. Effects of $CO_2$ on the ocean environment. Energy Conversion and Management 37:1019-1022.

**Heinbokel, J.F.** 1978. Studies on the functional role of tintinnids in the southern California Bight I: grazing and growth rates in laboratory cultures. Marine Biology 47:177-189.

**Hopkinson, B.M., Y. Xu, D. Shi, P.J. McGinn, and F.M.M. Morel.** 2010. The effect of $CO_2$ on the photosynthetic physiology of phytoplankton in the Gulf of Alaska. Limnology and Oceanography 55:2011-2024.

**Hoppe, C.J.M., G. Langer, and B. Rost.** 2011. Emiliania huxleyi shows identical responses to elevated $pCO_2$ in TA and DIC manipulations. Journal of Experimental Marine Biology and Ecology 406:54-62.

**Iglesias-Rodriguez, M.D., P.R. Halloran, R.E.M. Rickaby, I.R. Hall, E. Colmenero-Hidalgo, J.R. Gittins, D.R.H. Green, T. Tyrrell, S.J. Gibbs, P. von Dassow, E. Rehm, E.V. Armbrust, and K.P. Boessenkool.** 2008. Phytoplankton classification in a high-$CO_2$ world. Science 320:336-340.

**IPCC.** 2007. Fourth assessment report of the intergovernmental panel on climate change. Cambridge University Press, Cambridge.

**Jakobsen, H.H., and P.J. Hansen.** 1997. Prey size selection, grazing and growth response of the small heterotrophic dinoflagellate Gymnodinium sp. and the ciliate Balanion comatum- a comparative study. Marine Ecology Progress Series 158:75-86.

**Jeong, H.J., Y.D. Yoo, J.S. Kim, K.A. Seong, N.S. Kang, and T.H. Kim.** 2010. Growth, feeding and ecological roles of the mixotrophic and heterotrophic dinoflagellates in marine planktonic food webs. Ocean Science Journal 45:65-91.

**Jin, P., K. Gao, V.E. Villafane, D.A. Campbell, and E.W. Helbling.** 2013. Ocean acidification alters the photosynthetic responses of a coccolithophorid to fluctuating ultraviolet and visible radiation. Plant Physiology 162:2084-2094.

**Jonsson, P.R.** 1986. Particle size selection, feeding rates and growth dynamics of marine planktonic oligotroph ciliates (Ciliophora: Oligotrichina). Marine Ecology Progress Series 33:265-277.

**Kroeker, K.J., R.L. Kordas, R.N. Crim, and G.G. Singh.** 2010. Meta-analysis reveals negative yet variable effects of ocean acidification on marine organisms. Ecology Letters 13:1419-1434.

**Landry, M.R. and R.P. Hassett.** 1982. Estimating the grazing impact of marine microzooplankton. Marine Biology 67:283-288.

**Landry, M.R. and A. Calbet.** 2004. Microzooplankton production in the oceans. Journal of Marine Science 61:501-507.

**Le Quere, C., M.R. Raupach, J. G. Canadell, G. Marland, L. Bopp, P. Ciais, T.J. Conway, S.C. Doney, R.A. Feely, P. Foster, P. Friedlingstein, K. Gurney, R.A. Houghton, J.I. House, C. Huntingford, P.E. Levy, M.R. Lomas, J. Majkut, N. Metzl, J.P. Ometto, G.P. Peters, I.C. Prentice, J.T. Randerson, S.W. Running, J.L. Sarmiento, U. Schuster, S. Sitch, T. Takahashi, N. Viovy, G.R. van der Werf, and F.I. Woodward.** 2009. Trends in the sources and sinks of carbon dioxide. Nature Geoscience 2:831-836.

**Lefebvre, S.C., I. Benner, J.H. Stillman, A.E. Parker, M.K. Drake, P.E. Rossignol, K.M. Okimura, T. Komada, and E.J. Carpenter.** 2012. Nitrogen source and $pCO_2$ synergistically affect carbon allocation, growth, and morphology of the coccolithophore Emiliania huxleyi: potential implications of ocean acidification for the carbon cycle. Global Change Biology 18:493-503.

**Levandowski, M. and D.C.R. Hauser.** 1978. Chemosensory responses of swimming algae and protozoa. International Review of Cytology 53:145-210.

**Lohbeck, K.T., U. Riebesell, S. Collins, and T.B.H. Reusch.** 2012. Functional genetic divergence in high $CO_2$ adapted Emiliani huxleyi populations. Evolution doi:10.1111/j.1558-5646.2012.01812.x

**Low-Decarie, E., G.F. Fussmann, and G. Bell.** 2014. Aquatic primary production in a high $CO_2$ world. Trends in Ecology and Evolution 29:223-232.

**Menden-Deuer, S., and E.J. Lessard.** 2000. Carbon to volume relationships for dinoflagellates, diatoms, and other protest plankton. Limnology and Oceanography 45:569-579.

**Meunier, C.L., F.M. Hantzsche, A.O. Cunha-Dupont, J. Haafke, B. Oppermann, A.M. Malzahn, and M. Boersma.** 2011. Intraspecific selectivity, compensatory feeding and flexible homeostasis in the phagotrophic flagellate Oxyrrhis marina: three ways to handle food quality fluctuations. Hydrobiologia DOI 10.1007/s10750-011-0900-4

**Meyer, J. and U. Riebesell.** 2014. Responses of coccolithophores to ocean acidification: a meta-analysis. Biogeosciences Discussions 11:14857-14887.

**Millero, F.J., J.Z. Zhang, K. Lee, and D.M. Campbell.** 1993. Titration alkalinity of seawater. Marine Chemistry 44:153-165.

**Montagnes, D.J.S., C.D. Lowe, L. Martin, P.C. Watts, N. Downes-Tettmar, Z. Yang, E.C. Roberts, and K. Davidson.** 2011. Oxyrrhis marina growth, sex and reproduction. Journal of Plankton Research 33:615-627.

**Moore, T.S., M.D. Dowell, B.A. Franz.** 2012. Detection of coccolithophore blooms in ocean color satellite imagery: a generalized approach for use with multiple sensors. Remote Sensing of Environment 117:249-263.

**Naustvoll, L.J.** 2000a. Prey-size spectra and food preferences in thecate heterotrophic dinoflagellates. Phycologia 39:187-198

**Naustvoll, L.J.** 2000b. Prey size spectra in naked heterotrophic dinoflagellates. Phycologia 39:448-455.

**Olson, M.B. and S.L. Strom.** 2002. Phytoplankton growth, microzooplankton herbivory and community structure in this southeast Bering Sea: insight into the formation and temporal persistence of an Emiliania huxleyi bloom. Deep Sea Research II 49:5969-5990.

**Orr, J.C., V.J. Fabry, O. Aumont, L. Bopp, S.C. Doney, R.A. Feely, A. Gnanadesikan, N. Gruber, A. Ishida, F. Joos, R.M. Key, K. Lindsay, E. Maier-Reimer, R. Matear, P. Monfray, A. Mouchet, R. G. Najjar, G.K. Plattner, K.B. Rodgers, C.L. Sabine, J.L. Sarmiento, R. Schlitzer, R. D. Slater, I.J. Totterdell, M.F. Weirig, Y. Yamanaka, and A. Yool.** 2005. Anthropogenic ocean acidification over the twenty-first century and its impact on calcifying organisms. Nature 437:681-686.

**Parsons, T.R., Y. Maita, and C.M. Lalli.** 1984. A manual of chemical and biological methods for seawater analysis. Pergamon, Oxford.

**Pierrot, D.E., E. Lewis, D.W.R. Wallace.** 2006. MS Excel program developed for $CO_2$ system calculations. Oak Ridge National Laboratory, Carbon Dioxide Information Analysis Center, 105, US Department of Energy, Oak Ridge.

**Riebesell, U., K.G. Schulz, R.G.J. Bellerby, M. Botros, P. Fritsche, M. Meyerhofer, C. Neill, G. Nondal, A. Oschlies, J. Wohlers, and E. Zollner.** 2007. Enhanced biological carbon consumption in a high $CO_2$ ocean. Nature Letters vol. 450: 545-548.

**Reinfelder, J.R.** 2011. Carbon concentrating mechanisms in eukaryotic marine phytoplankton. Annual Review of Marine Science 3:291-315.

**Reinfelder, J.R.** 2012. Carbon dioxide regulation of nitrogen and phosphorus in four species of marine phytoplankton. Marine Ecology Progress Series 466:57-67.

**Rokitta, S.D. and B. Rost.** 2012. Effects of $CO_2$ and their modulation by light in the life-cycle stages of the coccolithophore Emiliania huxleyi. Limnology and Oceanography 57:607-618.

**Sabine, C.L., R.A. Feely, N. Gruber, R.M. Key, K. Lee, J.L. Bullister, R. Wanninkhof, C.S. Wong, D.W.R. Wallas, B. Tilbrook, F.J. Millero, T.H. Peng, A. Kozyr, T. Ono, and A.F. Rios.** 2004. The oceanic sink for anthropogenic $CO_2$. Science 305:367-371.

**Sherr, B.F., E. B. Sherr, and J. McDaniel.** 1992. Effect of protistan grazing on the frequency of dividing cells in bacterioplankton assemblages. Applied and Environmental Microbiology 58:2381-2385.

**Sherr, E.B. and B.F. Sherr.** 1994. Bacterivory and herbivory: key roles of phagotrophic protists in pelagic food webs. Microbial Ecology 28:223-235.

**Sherr, E.B. and B.F. Sherr.** 2002. Significance of predation by protists in aquatic microbial food webs. Antonie van Leeuwenhoek 81:293-308.

**Sherr, E.B. and B.F. Sherr.** 2007. Heterotrophic dinoflagellates: a significant component of microzooplankton biomass and major grazers of diatoms in the sea. Marine Ecology Progress Series 352:187-197.

**Sieburth, J.M., V. Smetacek, and J. Lenz.** 1978. Pelagic ecosystem structure: heterotrophic compartments of the plankton and their relationship to plankton size fractions. Limnology and Oceanography 23:1256-1263.

**Simek, K. and T.H. Chrzanowski.** 1992. Direct and indirect evidence of size-selective grazing on pelagic bacteria by freshwater nanoflagellates. Applied and Environmental Microbiology 58:3715-3720.

**Smetacek, V.** 1981. The annual cycle of protozooplankton in the Kiel Bight. Marine Biology 63:1-11.

**Steeman Nielsen, E.** 1952. The use of radio-active carbon (14C) for measuring organic production in the sea. J. Cons. Perm. Int. Explor. Mer 18:117-140.

**Strom, S.L., R. Benner, S. Ziegler, and M.J. Dagg.** 1997. Planktonic grazers are a potentially important source of marine dissolved organic carbon. Limnology and Oceanography 42:1364-1374.

**Tillmann, U.** 2004. Interactions between planktonic microalgae and protozoan grazers. Journal of Eukaryotic Microbiology 51:156-168.

**Van de Waal D.B., U. John, P. Ziveri, G.J. Reichart, M. Hoins, A. Sluijs, and B. Rost.** 2013. Ocean acidification reduces growth and calcification in a marine dinoflagellate. PLoS ONE 8:e65987.

**Vargas, C.A. and R.O. Martinez.** 2009. Grazing impact of natural populations of ciliates and dinoflagellates in a river-influenced continental shelf

**Verity, P.G.** 1988. Chemosensory behavior in marine planktonic ciliates. Bulletin of Marine Science 43:772-782.

**Verity, P.G. and T.A. Villareal.** 1986. The relative food value of diatoms, dinoflagellates, flagellates and cyanobacteria for tintinnid ciliates. Archiv fur Protistenkunde 131:71-84.

**Widdicombe, C.E., S.D. Archer, P.H. Burkill, and Widdicombe, S.** 2002. Diversity and structure of the microzooplankton community during a coccolithophore bloom in the stratified northern North Sea. Deep Sea Research II 49:2887-2903.

**Wuori, T.** 2012. The effects of elevated $pCO_2$ on the physiology of Emiliania huxleyi. Master's Thesis, Western Washington University, Bellingham, WA.

**Wynn-Edwards, C., R. King, A. Davidson, S. Wright, P.D. Nichols, S. Wotherspoon, S. Kawaguchi, and P. Virtue.** 2014. Species-specific variations in the nutritional quality of Southern Ocean phytoplankton in response to elevated $pCO_2$. Water 6:1840-1859.

**Yoshimura, T., J. Nishioka, K. Suzuki, H. Hattori, H. Kiyosawa, and Y.W. Watanabe.** 2010. Impacts of elevated $CO_2$ on organic carbon dynamics in nutrient depleted Okhotsk Sea surface waters. Journal of Experimental Marine Biology and Ecology 395:191-198.

**Zondervan, I., B. Rost, and U. Riebesell.** 2002. Effect of $CO_2$ concentration on the PIC/POC ratio in the coccolithophore Emiliania huxleyi grown under light-limiting conditions and different daylengths. Journal of Experimental Marine Biology and Ecology 272:55-70.